Lakehead University

Planning for Battery Electric Buses Charging in Transit System

by

Ehsan Sobhani

A thesis submitted in partial fulfillment for the degree of Master

in the
Computer Science

July 2024

Declaration of Authorship

I, Ehsan Sobhani, declare that this thesis titled 'Planning for Battery Electric Buses Charging in Transit System' and the work presented in it are my own. I confirm that:

- This work was done wholly or mainly while in candidature for a research degree at this University.
- Where any part of this thesis has previously been submitted for a degree or any other qualification at this University or any other institution, this has been clearly stated.
- Where I have consulted the published work of others, this is always clearly attributed.
- Where I have quoted from the work of others, the source is always given. Except for such quotations, this thesis is entirely my own work.
- I have acknowledged all main sources of help.
- Where the thesis is based on work done by myself jointly with others, I have made clear exactly what was done by others and what I have contributed myself.

Signed: ____

Date: ____

Lakehead University

Abstract

Faculty Name
Computer Science

Master of Science

by Ehsan Sobhani

With the growing focus on sustainable transportation, Battery Electric Buses (BEBs) have emerged as a viable solution. BEBs have received significant recognition as an environmentally conscious and sustainable means of transportation. In many cases, transitioning from a conventional diesel-fueled transit system to a fully electric one is essential. Designing an effective strategy, which encompasses placing charging sites and implementing proper charging mechanisms, is crucial to ensuring efficient and consistent charging of BEBs in an electrified public transit system. However, the challenge intensifies when the transit planner aims to maintain a consistent daily service timetable.

The research endeavours to tackle this challenge by formulating efficient charging strategies and methodologies for infrastructure planning. This thesis outlines a four-step approach for transit system planners to attain optimal solutions, encompassing worst-case energy consumption calculation, off-service charging site placement, off-service (overnight) charging mechanism, on-route charging planning, and finding the number required BEBs and integration of them to fully electric transit system. Four methods are designed for use in planning: the Constrained Greedy Clustering (CGC) algorithm, the Priority Charging Mechanism (PCM), the Constraint Affinity Clustering Algorithm (CACA), and timetable tuning. A case study based on a real-world Thunder Bay, ON transit system validates the proposed methodologies and assesses their effectiveness in improving the overall performance of the BEB fleet. Results demonstrate significant improvements in operational efficiency, cost reduction, and environmental sustainability by implementing the proposed charging infrastructure optimization strategies.

The findings of this research contribute to the advancement of sustainable transportation by providing practical insights and solutions to the challenges associated with BEB charging infrastructure design and optimization.

Acknowledgements

I am appreciative of the support of my supervisor, Dr. Abdulsalam Yassine. This thesis and research would not have been possible without his exceptional support. I am grateful for his constructive suggestions, patient instruction, and enthusiastic encouragement, especially during the pandemic.

I thank Lakehead University and the Department of Computer Science for providing scholarships and awards as financial support. I am also thankful for the lab space and online remote services, which help improve my productivity.

I am also grateful to my lab mates. Their welcome gave me a wonderful research time. Discussing the newest techniques and their research directions gives me new insight.

Contents

List of Figures

List of Tables

Abbreviations

AI	**A**rtificial **I**ntelligence
BEB	**B**attery **E**lectric **B**us
BFGS	**B**royden-**F**letcher-**G**oldfarb-**S**hanno
CACA	**C**onstraint **A**ffinity **C**lustering **A**lgorithm
CAPEX	**C**apital **E**xpenditure
CGC	**C**onstrained **G**reedy **C**lustering
COBYLA	**C**onstrained **O**ptimization **B**y **L**inear **A**pproximations
DBI	**D**avies-**B**ouldin **I**ndex
EVs	**E**lectric **V**ehicles
LCM	**L**east **C**ommon **M**ultiple
MILP	**M**ixed-**I**nteger **L**inear **P**rogramming
MINP	**M**ixed-**I**nteger **N**onlinear **P**rogramming
OM	**O**pportunity **M**atrix
OPEX	**O**perating **E**xpenditure
PCM	**P**riority **C**harging **M**echanism
SLSQP	**S**equential **L**east **S**quares **Q**uadratic **P**rogramming
SM	**S**imilarity **M**atrix
SS	**S**ilhouette **S**core
TOU	**T**ime-**O**f-**U**se
TPDI	**T**emporal **P**resence **D**ispersion **I**ndex
WCSS	**W**ithin-**C**luster **S**um of **S**quares
WSS	**W**eighted **S**ilhouette **S**core

Symbols

symbol	name	unit
$\mathbf{B} = \{\mathrm{b}_1, \mathrm{b}_2, \ldots, \mathrm{b}_\mathrm{n}\}$	The set of transit system BEBs	
$\mathbf{E^b} = \{\mathrm{e}_{\mathrm{b}_1}, \mathrm{e}_{\mathrm{b}_2}, \ldots, \mathrm{e}_{\mathrm{b}_\mathrm{n}}\}$	The set of transit system BEBs required energy to fulfil activity blocks	
b_n	A transit system BEB	
$\mathrm{e}_{\mathrm{b}_\mathrm{n}}$	A transit BEB block's worst-case energy consumption to fulfill activity block bl_n	kWh
$\mathbf{BL} = \{\mathrm{bl}_1, \mathrm{bl}_2, \ldots, \mathrm{bl}_\mathrm{n}\}$	The set of transit system daily activity blocks	
bl_n	A transit system activity block	
$\mathrm{e}_{\mathrm{bl}_\mathrm{n}}$	A transit system activity block's worst-case energy consumption	kWh
$\mathbf{E^{bl}} = \{\mathrm{e}_{\mathrm{bl}_1}, \mathrm{e}_{\mathrm{bl}_2}, \ldots, \mathrm{e}_{\mathrm{bl}_\mathrm{n}}\}$	The set of transit system activity blocks' worst-case energy consumption	kWh
$\mathbf{S} = \{\mathrm{s}_1, \mathrm{s}_2, \ldots, \mathrm{s}_\mathrm{m}\}$	The set of transit system services	
$\mathbf{T^d} = \{\mathrm{t}^\mathrm{d}_{\mathrm{bl}_1}, \mathrm{t}^\mathrm{d}_{\mathrm{bl}_2}, \ldots, \mathrm{t}^\mathrm{d}_{\mathrm{bl}_\mathrm{n}}\}$	The set of BEBs' departure times from the depot	minute
$\mathbf{T^a} = \{\mathrm{t}^\mathrm{a}_{\mathrm{bl}_1}, \mathrm{t}^\mathrm{a}_{\mathrm{bl}_2}, \ldots, \mathrm{t}^\mathrm{a}_{\mathrm{bl}_\mathrm{n}}\}$	BEBs' arrival times to depot	minute
$\mathbf{T^s} = \{\mathrm{t}^\mathrm{s}_{\mathrm{s}_1}, \mathrm{t}^\mathrm{s}_{\mathrm{s}_2}, \ldots, \mathrm{t}^\mathrm{s}_{\mathrm{s}_\mathrm{m}}\}$	The set of transit system's daily services starting times	minute
$\mathrm{t}^\mathrm{e}_{\mathrm{s}_\mathrm{m}}$	A transit system service starting time	minute
$\mathbf{T^e} = \{\mathrm{t}^\mathrm{e}_{\mathrm{s}_1}, \mathrm{t}^\mathrm{e}_{\mathrm{s}_2}, \ldots, \mathrm{t}^\mathrm{e}_{\mathrm{s}_\mathrm{m}}\}$	The transit system's daily services starting times	minute
$\mathbf{R} = \{1, 2, \ldots, \mathrm{r}\}$	The set of transit system's routes (lines)	

l_r^1, l_r^2	The transit network route's distance[1]	km
$\mathbf{L} = \{l_1^1, l_1^2, l_2^1, l_2^2 \ldots, l_r^1, l_r^2\}$	The Set of the transit system routes' distances	km
$e_{s_m}^s$	A service's worst-case energy consumption	kWh
$\mathbf{E^s} = \{e_{s_1}^s, e_{s_2}^s, \ldots, e_{s_m}^s\}$	The set of transit system services' worst-case energy consumption	kWh
E_w	The transit system's daily worst-case energy consumption	kWh
β	BEB worst-case energy consumption rate	kWh/km
t_q	A transit system's terminal	
$\mathbf{T} = \{t_1, t_2, \ldots, t_q\}$	The set of transit system's terminals	
d_q	Dispatching terminal	
$\mathbf{D} = \{d_1, d_2, \ldots, d_q\}$	The set of transit system's dispatching terminals	
w_q	The d_q dispatching rate	
$\mathbf{W} = \{w_1, w_2, \ldots, w_q\}$	The set of dispatching rates associated with transit network's dispatching terminals	
P_f	The power grid available power at charging site	kW
P_c	Charger power	kW
γ	The CGC algorithm's hyper-parameters [2]	
p_{bl_n}	Required power for charging BEB to fulfill activity block bl_n	kW
$\mathbf{P^{bl}} = \{p_{bl_1}, p_{bl_2}, \ldots, p_{bl_n}\}$	The set of required powers for charging BEBs to meet the daily activity blocks of the transit system	kW
$pr_n = \frac{e_{bl_n}}{T_{se}}$	A charging priority assigned to BEB by the charging system before starting the charging sessions	
$\mathbf{PR} = \{pr_1, pr_2, \ldots, pr_n\}$	The set of charging priorities assigned to transit system BEBs by the	
$\mathbf{N_s}$	The number of charging sessions	

[1]superscripts 1 represent the transit network routes' initial terminals to their ending terminals lengths, and superscripts 2 represent the transit network routes' ending terminals to their initial terminals lengths (they might have different distances)

[2]Set by the transit planner to specify the effective variance amount in the clustering criteria

$\mathrm{T_{se}}$	The charging session time	
$\mathrm{E_t^a}$	Amount of energy that each on-route charging terminal should provide to assigned activity blocks	kWh
$\mathrm{si_t}$	A terminal service index	
$\mathbf{SI} = \{\mathrm{si_1}, \mathrm{si_2}, \ldots, \mathrm{si_t}\}$	The set of transit system terminals' service indexes	
$\mathrm{t_n^{ch}}$	On-route charging terminal	
$\mathbf{T_{ch}} = \{\mathrm{t_1^{ch}}, \mathrm{t_2^{ch}}, \ldots, \mathrm{t_n^{ch}}\}$	The set of transit on-route charging terminals	
$\mathbf{PN_n} = \{\mathrm{t_1}, \mathrm{t_2}, \ldots, \mathrm{t_t}\}$	The set of terminals (nodes) associated with activity block n	
$\mathcal{T}$	The Set of all BEBs presence times at the charging terminal	

This thesis is dedicated to my loving family, whose unwavering support and encouragement have been the cornerstone of my academic journey. To my parents, whose sacrifices and belief in my potential have inspired me to reach for the stars. Your love has been my strength.

I also dedicate this work to my esteemed mentors and professors, whose guidance and expertise have shaped my academic pursuits and enriched my understanding of the subject matter. Your mentorship has been invaluable in shaping this thesis.

Finally, I express my deepest gratitude to all whose names may not be mentioned but whose contributions have left an indelible mark on this work. Your insights, feedback, and support have been instrumental in completing this thesis.

Thank you all for being part of this journey.

Chapter 1

Introduction

1.1 Introduction

Recently, battery electric buses (BEBs) have gained significant attention as a sustainable and environmentally friendly transportation solution [46]. However, BEBs face the challenge of a limited power supply, necessitating recharging when their battery energy is depleted. There are two main methods for recharging the battery. i) Charging during the bus route (known as on-route charging or opportunity/boost charging) and ii) recharging when the bus is not in service (off-service charging) [18, 65]. On-route charging involves recharging BEBs' batteries while operating, typically at designated charging points along their routes [19]. These charging sites can be installed at bus stops, terminals, or depots to quickly top up the battery's charge [5]. This method is particularly useful for extending the range of BEBs and ensuring continuous service without requiring long breaks for recharging. Off-service charging refers to recharging BEB batteries when the buses are not in regular service, such as overnight or during scheduled breaks. This approach is commonly used to ensure that BEBs have sufficient power to complete their routes and minimize disruption to service during peak operational hours.

The high capital costs associated with BEBs pose a significant barrier to market penetration. Consequently, several studies have conducted cost-benefit analyses of BEBs, considering both capital and operating costs. For example, in [76], researchers found that despite the high initial capital investment, the lower fuel costs of BEBs made them competitive with diesel buses.

Various strategies have been proposed to address demand charges associated with BEBs. Gallo et al. [22] suggests methods such as enhancing EB efficiency, utilizing energy transfer technology, employing time-of-use pricing, or temporarily suspending demand charges. You et al. [74] propose a battery-switching strategy where depleted batteries are replaced with charged ones at battery-switching stations, minimizing electricity costs and battery degradation.

In [29], fast chargers, in combination with Electric Shock chargers, are used to pinpoint the ideal charging station locations. The study employed a simulation method to examine the relationship between battery capacity and the charging capability of fast-charging stations. In [59], a method is employed to investigate the connection between battery capacity and the charging capability of fast-charging sites.

Past studies addressing the setup of BEB fleets have typically utilized optimization models that need to be more user-friendly for transit system operators. These models rely on specific assumptions, parameters, and constraints that can present challenges concerning BEB fleets. These models provide charging opportunities based on these inputs, but if any of these factors change during operation, the optimized solutions may become invalid. Consequently, numerous external factors can disrupt the model's functionality, making it less practical for operators. Additionally, these models can encounter computational difficulties when dealing with extensive transit systems featuring multiple terminals and depots. Furthermore, most researchers have concentrated on on-route charging strategies dependent on unpredictable delays in service schedules [69, 73].

Urban transit system planning considers numerous factors in its design, including population density, land use, traffic patterns, demographics, accessibility, environmental considerations, economic development, safety and security, technological advances, and stakeholder engagement [9, 10, 35, 40, 80]. By integrating these considerations, planners can develop transit systems that are efficient, accessible, sustainable, and responsive to the needs of urban communities. Transit systems are often designed for urban areas with specific characteristics tailored to the population's needs and environment. With the transition to electrification, it is crucial to maintain the fundamental characteristics of the existing transit system and adhere to key planning priorities, which may take precedence over optimizing electric power consumption and its impact on the grid. More comprehensive planning is needed for BEBs charging within the electrification of diesel-fueled transit systems while maintaining unchanged daily schedule services. This comprehensive planning map should guide the system planner, starting from an initial point and sequentially selecting charging approaches to achieve the best strategy to minimize infrastructure and operating costs. The planning map should outline practical charging mechanisms for each chosen strategy and ultimately provide the locations of charging sites, chargers' characteristics, the minimum number of chargers at each site, the number of required BEBs in a fully electric transit system, and propose schedule tuning to minimize Capital Expenditure (CAPEX) and Operating Expenditure (OPEX).

Developing a robust charging strategy encompassing off-service and on-route charging approaches or adding extra BEBs can solve the uncertainties of relying solely on one charging method. By considering multiple charging approaches, we can explore the most effective infrastructure and operating cost while maintaining the transit timetable services established by transit system planners for diesel-fueled transit systems. This approach allows flexibility and efficiency in managing electric bus fleets without altering inherited transit schedules.

The proposed map begins by pinpointing worst-case energy consumption estimation for daily schedules as the starting point. It then endeavours to meet the estimated energy needs through various charging approaches sequentially, starting with the one that incurs lower infrastructure and operating costs (overnight charging) and progressing towards a more expensive approach (adding extra BEBS). As Figure 1.1 shows energy serves as the foundation of this comprehensive map, acting as the bridge between the diesel-fueled transit system and the battery-electric-powered transit system, operating on the exact service schedules.

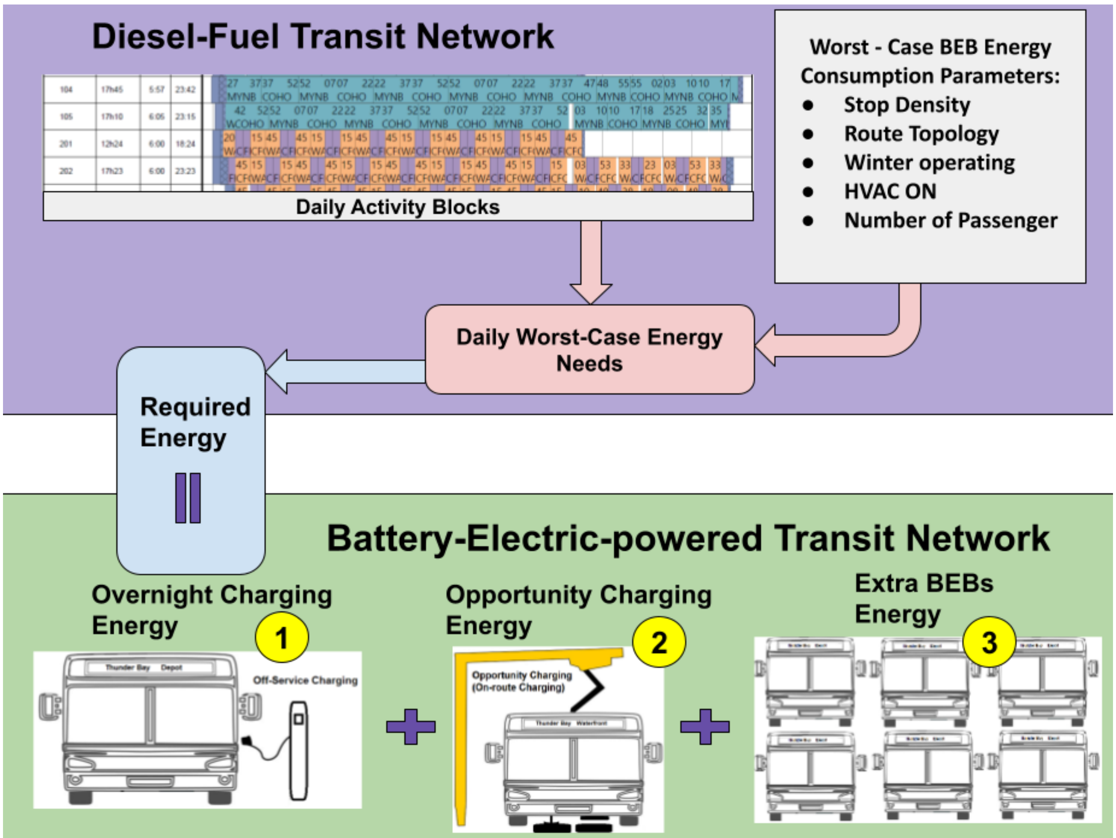

FIGURE 1.1: Overall view of electrification of transit system

1.2 Technical Challenges

Electrifying transit systems faces numerous challenges, including:

1. Strategic placement of charging sites presents a challenge for transit planners, particularly concerning power grid considerations. Efficient placement can reduce energy consumption for BEBs, minimizing operational costs and aiding load balancing across the power grid. Moreover, when repurposing diesel bus depots and garages for electrified systems to mitigate infrastructure costs, considering newly calculated placement locations could be beneficial for locating charging sites from depots and garages, particularly in large-scale transit systems.

2. Off-service charging should occur during hours with minimum electricity cost, avoiding overloads or disruptions in electricity supply by ensuring that the combined power demand from charging BEBs does not exceed the power grid's capacity (power grid constraints) while determining the minimum number of charging piles in charging sites can significantly reduce CAPEX, an essential consideration for transit system planners when migrating from a diesel-fueled system to an electrified one. Unified charging processes for BEBs off-service (overnight) are essential for minimizing charging malfunctions and optimizing resource utilization in charging sites (depots or garages). Designing the proper charging model to ensure that all BEBs receive the maximum possible charge despite pile malfunctions is challenging for planners. This approach also enables planners to automate the charging process, reducing OPEX and malfunctions while eliminating the need for manual intervention.

3. Due to the limited travelling distances of BEBs compared to diesel buses, planners often require more BEBs to fulfill transit daily services. However, BEBs, regardless of size and battery technology, tend to be expensive [38]. Therefore, one of the main challenges for planners is finding the minimum number of BEBs and efficiently assigning them to transit daily services. In essence, efficiently assigning BEBs to fulfill transit daily services minimizes the overall number of BEBs required for operation.

4. Implementing on-route charging presents challenges, irrespective of the BEB battery's capacity. It often requires the installation of costly fast-charging infrastructure [19]. Adhering to bus service schedules by relying on the time intervals between services for recharging creates a strong connection between charging times and service schedules. Relying heavily on service schedules has a detrimental impact on charging schedules, which are inherently inflexible and critically essential. Therefore,

the challenges are specifying the minimum transit terminals for on-route charging to satisfy all working BEBs on-route charging. Moreover, allocating on-route chargers efficiently to BEBs ensures BEBs have the most opportunities for charging in pre-defined timetable schedules. In large-scale transit systems, selecting only one charging approach can be challenging due to varying power grid constraints, charging sites' locations, and routes' topologies. Incorporating both off-service and on-route charging introduces complexity to the planning process. This complexity stems from coordinating charging schedules, determining ideal infrastructure placement, and managing operational logistics to ensure seamless integration while minimizing service disruptions. Moreover, factors like battery capacity, charging times, and route variations further complicate decision-making for transit planners. Therefore, achieving a balance between these charging approaches is essential for effectively managing the electrification of transit systems.

1.3 Research Approach

We aim to divide the charging planning into sub-problems and propose practical solutions. Based on the transit system characteristics, planners can select the most suitable charging strategy and apply the corresponding methods to migrate to an electric transit system. In addressing the challenges of planning BEB charging within the transit system, our approach involves thoroughly analyzing the existing diesel-fueled transit system designed to meet the urban public commuting demands. This analysis aims to estimate the worst-case daily energy consumption of the diesel-fueled transit system. Doing so gives us insight into the most demanding scenarios planners encounter during the BEBs charging planning process. Understanding these worst-case scenarios is essential for devising effective strategies to optimize BEB charging infrastructure and ensure reliable service delivery within the transit system. Subsequently, we endeavour to address the energy requirements in various ways, ranging from cost-effective off-service charging to more expensive solutions such as on-route (opportunity) charging and adding extra BEBs, respectively, considering charging infrastructure and energy costs.

This study uses energy as the common denominator between diesel-fueled and battery-electric-powered transit systems. We start our analysis from the perspective of diesel-fueled transit system activities, where we can see the worst-case daily BEBs energy consumption. After that, we plan to supply the required energy efficiently. Firstly, we attempted to procure energy through off-service (overnight) charging, the most cost-effective approach due to the lower electricity rates during nighttime hours as depicted in Figure 4.5 (bars in orange colour). The endeavour yielded two methods: the Constrained Greedy

Clustering (CGC) for ideal placement of off-service charging sites to comply with power grid constraints, and The Priority Charging Mechanism (PCM) is designed explicitly for off-service charging to ensure that all BEBs are charged simultaneously, thereby guaranteeing efficient charging performance even in the event of charger malfunctions by distributing the malfunction effect between all charging BEBs.

Driven by the challenge of determining the minimum number of on-route charging terminals, their most effective locations, and their allocation to BEBs, we developed the On-route Charging strategy. This strategy utilizes inherited service schedules from the diesel-fueled transit system and allocates chargers to BEBs, ensuring energy balance among all chargers. Moreover, we proposed the service schedule tuning method to maximize the BEBs charging opportunities. It's worth mentioning that the proposed planning strategy can be used either independently or as a complementary component with off-service charging. Transit system planners facing limitations with off-service charging can employ this approach independently.

In cases where neither off-service nor on-route charging can fully supply the daily energy needs of the transit system, transit system planners are compelled to add extra BEBs to meet the scheduled services. We propose a planning approach to determine the minimum number of BEBs required for a fully electric transit system and to assign these BEBs in a way that minimizes energy consumption while fulfilling service requirements. The outcome is the Constrained Affinity Clustering Algorithm (CACA), which clusters the distances travelled by BEBs to fulfill transit system activity blocks. This clustering efficiently enables us to utilize shared BEBs to fulfill the services belonging to each cluster.

1.4 Contributions

The following are the contributions of the thesis.

1. To address challenge one, this thesis introduces the CGC algorithm, an approach designed to determine the most effective charging placement. The algorithm uses clustering techniques to minimize energy consumption and optimize charging load distribution in transit systems. This improves the placement of charging sites for off-service charging in transit systems, aiming to reduce energy consumption and balance the load among the charging sites. Further, this thesis introduces an intelligent overnight charging mechanism called PCM, specifically designed to charge BEBs simultaneously using the minimum number of chargers. This approach directly addresses challenges three and four. The goal is to minimize infrastructure

costs while effectively distributing the impact of charging malfunctions among all BEBs being charged, thereby mitigating the effects of such malfunctions.

2. To address challenge two, a comprehensive assessment of daily energy requirements is carried out under various scenarios, yielding findings contributing to solving subsequent challenges. This thesis suggests a planning approach (CACA) to calculate the minimum number of BEBs needed in a transit system by distributing them among the activity blocks in the transit system, tackling challenge three. The CACA algorithm ensures efficient allocation of BEBs to activity blocks, minimizing shared BEB travel distances.

3. To address challenge four, the thesis presented a comprehensive three-step planning approach to determine the minimum number of on-route charging terminals necessary within a transit system. Emphasizing effective allocation, it addresses the strategic assignment of transit system activity blocks to the identified charging terminals, optimizing the charging opportunities for BEBs. Furthermore, the approach aims to balance the distribution of supplied energy among the charging terminals, ensuring efficient utilization of resources across the transit network. The thesis proposes a planning mechanism, Figure 1.1, for transit planners aiming to utilize multiple charging approaches while minimizing total costs efficiently. This mechanism involves three prioritized steps, allowing planners to skip each step individually and use the others in the design process. By providing this flexible approach, planners can adapt their strategies based on their specific needs and constraints, ultimately achieving cost-effective electrification of the diesel-fueled transit system.

4. To address challenge four, which stems from inheriting the service timetable from a diesel-fueled transit system, maximizing the charging opportunities for each BEB requires them to be at the charging terminal at intervals that maximize temporal separation from other BEBs at the same charging terminal. The thesis proposes a timetable tuning method to achieve maximum temporal dispersion and minimize synchronicity without altering the activity blocks' service rate. This method enhances BEB charging opportunities by tuning the timing of transit system activity blocks slightly forward or backward.

1.5 Publications

E. Sobhani, A. Yassine and A. Ameli, "Maximizing On-Route BEB Charging Opportunity through Temporal Dispersion in Inherited Transit Timetables" IEEE Transactions on Intelligent Transportation Systems, 2024.

E. Sobhani, A. Yassine and A. Ameli, S. Riahinia "Placement of Charging Sites for Off-Service Battery Electric Bus in Transit Systems," 2024 IEEE Energy Conference (ENERGYCON), 2024.

E. Sobhani, A. Yassine and A. Ameli, S. Riahinia "Optimal Planning for Off-Service Charging of Electric Public Transit Networks," 2024 IEEE Smart Cities Futures Summit (2024 IEEE SCF), 2024.

E. Sobhani, A. Yassine and A. Ameli, S. Riahinia "Intelligent Overnight Charging Mechanism for Battery Electric Buses in a Transit Network," 2024 International Joint Conference on Computer Science and Software Engineering (TIMES-iCON2024), 2024.

E. Sobhani, A. Yassine and A. Ameli, S. Riahinia "Optimal Planning for On-Route Charging of Battery Electric Buses in Public Transit Networks," 2024 IEEE Smart Cities Futures Summit (2024 IEEE SCF), 2024.

1.6 Organization

This thesis is organized as follows:

- Chapter 1: Introduction - This chapter provides a comprehensive overview of the thesis, giving insight into its various aspects and components.
- Chapter 2: Background, Related Work - This chapter describes migrating diesel-fueled to battery electric-power buses. This chapter also presents a summary of relevant published works. This chapter also presents a summary of relevant published works.
- Chapter 3: Estimation of Required Energy for the Transit System - This chapter introduces the methodology for estimating the daily energy requirements of a battery-electric-powered transit system.
- Chapter 4: Planning for Off-Service Charging - This chapter introduces an algorithm for strategically placing charging sites within a transit system to minimize energy consumption and ensure a uniform distribution of charging loads across all chargers. Additionally, it presents an off-service (overnight) charging mechanism, prioritizing the simultaneous charging of all BEBs while minimizing the impact of charging malfunctions. Furthermore, it introduces the CACA algorithm, which effectively plans off-service charging for fully electrified public transit systems, determining the number of BEBs and efficiently assigning them to activity blocks.

- Chapter 5: Planning for opportunity charging - This chapter introduces effective planning for on-route charging BEBs. It emphasizes optimizing the number of charging terminals and strategically allocating them to BEBs to maximize charging opportunities while ensuring balanced energy distribution among the charging terminals. This chapter presents a method for adjusting the inherited timetable from diesel-fueled transit systems without affecting the service rate to maximize BEBs' opportunity to charge.

- Chapter 6: Conclusion and Research Directions - This chapter presents the conclusions drawn from the analysis of the results obtained in this study. Additionally, it proposes potential avenues for future research and provides an overview of the current limitations.

Chapter 2

Background and Related Work

This chapter provides an overview of the background and related work pertinent to planning BEB charging in transit networks. It includes an analysis of the body of research on approaches, technologies, and literature pertinent to the effective installation of charging infrastructure and the enhancement of BEB charging tactics in transit networks.

2.1 Background

In recent years, a critical global effort to address climate change has focused on reducing emissions. With the transportation sector contributing 20% of global CO_2 emissions in 2020 and 75% of those emissions from motor vehicles [13], it is essential to implement decarbonization and sustainability measures in this sector. Policymakers have long recognized public transportation as crucial for promoting environmentally friendly mobility [16, 21]. One widely adopted strategy worldwide is electrifying public buses [48, 67]. BEBs have garnered significant attention due to their unique advantages: they are quieter, more reliable, energy-efficient, and emit no tailpipe emissions [68]. Many countries, including China [17], the United States [20], Korea [11], and various European countries [12], have conducted BEB demonstration projects. By May 2020, China had deployed over 420,000 electric buses, constituting 60% of its transit fleet and nearly 99% of the world's total [32]. The US e-bus market has experienced a 66% increase since 2021 [61]. Despite the recent increase in electric bus adoption, there is still a long journey ahead before BEBs widely replace traditional buses.

Two significant challenges to making transit buses electric are planning where and when to charge BEBs [28, 39]. Batteries currently store less energy than diesel ones. According to [25, 44, 59], BEBs need big batteries to charge slowly overnight at depots or medium-sized ones to charge periodically at fast-charging stations along the route. Fast-charging systems for BEBs, unlike slow ones, have several benefits. A bus with a smaller battery is lighter, can carry more passengers, and costs less for batteries [24]. Many electric bus projects worldwide use fast-charging systems. However, switching to them poses serious challenges. While they save money upfront, agencies must carefully place fast-charging stations to keep the transit system running smoothly. Fast charging can be costly without an intelligent charging plan due to high power demand charges and expensive electricity during busy times [30, 56]. Demand charges, also known as demand fees, are usually billed monthly and start when there is a sudden spike in power usage during the billing period [1].

2.1.1 Brief Overview of BEB Charging Technologies

Charging infrastructure technologies for BEBs encompass a variety of options tailored to different operational needs.

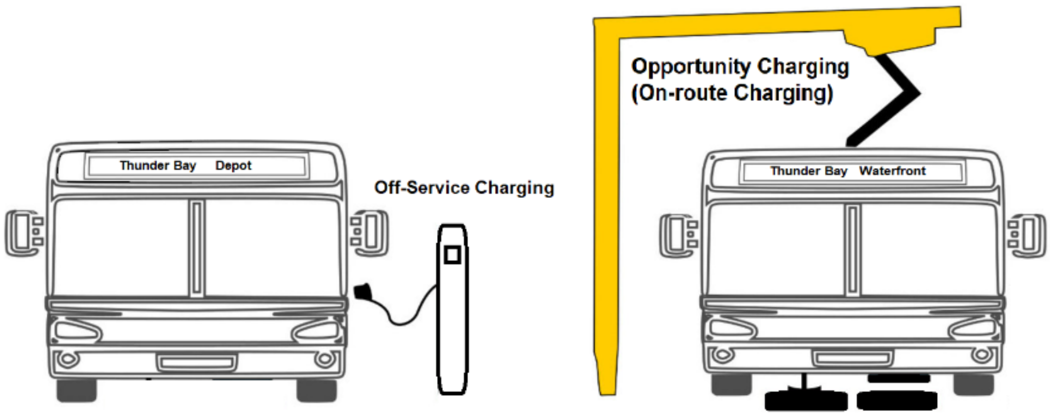

FIGURE 2.1: BEB off-service and on-route charging

Off-service charging sites (Plug-In Charging): Charging sites a familiar and straightforward plug-in for charging BEBs, the same as used for electric vehicles. They are typically utilized for overnight charging at bus depots or designated charging locations, allowing BEBs to start their routes with a full charge each day. One of the main advantages of plug-in stations is their ease of installation and operation, making them a convenient choice for transit operators. However, they also have limitations, such as the need for BEBs to connect to the charging point using a charging cable. This process can be time-consuming and labour-intensive, especially for large fleets. Additionally, plug-in sites generally offer slower charging speeds than other technologies, resulting in longer charging times and potential scheduling challenges for transit networks [62].

On-route charging (Opportunity charging, Pantograph Charging): Charging sites offer a more advanced charging solution for BEBs, allowing for rapid charging during layovers or dwell times. These systems utilize overhead pantographs mounted on the BEB and the charging infrastructure, enabling high-power charging with reduced charging times. Pantograph systems can be integrated into existing infrastructure along bus routes or main terminals, minimizing the need for additional infrastructure modifications. However, they also come with challenges, including higher initial installation costs, compatibility issues with different BEB models and charging infrastructure standards. Despite these challenges, pantograph charging systems are gaining popularity in transit networks seeking to minimize service disruptions and improve operational efficiency [55, 62].

Inductive charging Charging: Technology represents a cutting-edge approach to BEB charging, offering the convenience of wireless charging without needing physical connections. This technology is well-suited for dynamic charging scenarios, such as in-motion charging on electrified roadways or stationary charging at bus stops. Inductive charging pads can be embedded in the road surface, minimizing visual impact and offering a seamless charging experience for BEBs. However, inductive charging also has limitations, including lower charging efficiency than direct connection methods and higher initial installation costs due to specialized infrastructure requirements. Additionally, compatibility issues with current BEB models and infrastructure standards may limit the adoption of inductive charging technology in transit networks. Despite these challenges, ongoing advancements in inductive charging technology hold promise for the future of BEB charging infrastructure.

Battery swapping is the least utilized method for on-route charging. It entails the automated removal of depleted or low-SOC batteries and their replacement with fully charged ones. Efficient management of the recharging process at these stations can help minimize electricity costs. However, challenges include the potential financial implications of acquiring additional batteries and ensuring battery swaps are conducted without causing damage [36].

Advancements in BEB charging technology and infrastructure are ongoing, with research focusing on areas such as ultra-fast charging, vehicle-to-grid (V2G) integration, and dynamic charging solutions. These innovations aim to improve further the efficiency, reliability, and sustainability of BEB operations within transit networks.

2.1.2 Brief Overview of the BEB Charging Planning

Charging infrastructure must be strategically deployed to support BEB operations within the transit network. This may involve installing charging stations at bus depots for overnight charging, along bus routes for on-route charging, or at terminus stations for rapid charging during layover periods. Infrastructure deployment should consider route coverage, energy demand, BEB fleet size, and charging infrastructure interoperability. Charging infrastructure should be integrated with energy management systems to optimize charging schedules, balance energy consumption, and minimize operational costs. Intelligent charging algorithms can prioritize charging based on energy demand, grid capacity, and renewable energy availability. Efficient BEB charging planning contributes to the sustainability of public transit systems by maximizing the utilization of renewable energy sources and minimizing grid impacts. This aligns with goals such as achieving carbon neutrality and promoting clean energy transitions in urban transportation systems.

Adoption and successful operation of electric public transportation systems depend on effective planning for BEB charging in transit networks. According to [15], switching to electric buses has several advantages for the economy, society, and environment. These advantages include decreased greenhouse gas emissions, better air quality, and a reduced dependency on fossil fuels. Nevertheless, deploying the charging infrastructure, energy management plans, and operational optimization must be carefully considered to integrate BEBs successfully into transit networks.

The importance of efficient BEB charging planning is underscored by its impact on several key factors. Ensuring reliable and consistent charging infrastructure availability is essential for maintaining the operational reliability of BEB fleets. Effective planning helps prevent downtime due to insufficient charging capacity or equipment malfunctions. Ideal placement of charging infrastructure and strategic scheduling of charging sessions can help minimize infrastructure costs and energy expenses associated with BEB operation [45]. Efficient charging planning involves strategically managing when and how BEBs are charged within a transit network. By optimizing charging schedules and infrastructure utilization, it becomes possible to minimize peak demand charges. These charges occur when electricity usage spikes during periods of high demand, such as during peak hours [26]. Transit operators can reduce the strain on the electrical grid by spreading out charging sessions, avoiding simultaneous high-demand periods, and avoiding costly peak-demand charges [30]. By optimizing the utilization of renewable energy sources and minimizing grid impacts, efficient BEB charging planning contributes to the long-term sustainability of public transit services. This aligns with achieving carbon neutrality and promoting clean energy transitions in urban transportation systems [51].

Ensuring that BEBs are charged on time is crucial for maintaining reliable service availability and punctual performance in public transit systems. When BEBs are correctly charged, they can adhere to their schedules, minimizing delays and providing passengers with a dependable transportation experience. This reliability contributes significantly to passenger satisfaction, as travellers can trust that the buses will arrive on time and complete their routes efficiently. When public transit services consistently meet passengers' needs for punctuality and reliability, they are more likely to choose public transportation as their preferred mode of travel. Therefore, timely charging of BEBs is vital in enhancing overall passenger satisfaction and ensuring public transit systems' continued success and viability [42].

2.2 Literature Review

This literature review thoroughly examines the adoption and utilization of BEBs, focusing on charging infrastructure planning and scheduling strategies, namely off-service and on-route charging. While off-service charging remains the primary method, it has received less attention than opportunity charging. Studies aim to minimize energy costs and alleviate peak loads, which are crucial concerns for public transit planners, with grid constraints being an important consideration, particularly during simultaneous charging at depots. Recent research emphasizes opportunity charging, categorized into two groups: optimizing charging schedules based on predetermined BEB-to-trip assignments and joint optimization considering both assignment and charging schedules. For fixed BEB-to-trip assignments, the objective is to minimize en-route charging costs while ensuring successful trip completion without energy depletion. Table 2.1 compares different research studies based on their models and approaches. The primary objective is to minimize energy costs or reduce peak loads, which are significant concerns for public transit planners. Grid constraints are also considered, especially when multiple BEBs charge simultaneously at the depot. Many studies focus on developing heuristic algorithms to solve the off-service charging scheduling problem because this problem is often formulated as a Mixed-Integer Linear Programming (MILP) or Mixed-Integer Nonlinear Programming (MINP), which can be challenging to solve efficiently, particularly for large-scale scenarios.

[72] proposes a collaborative optimization model for electric bus line scheduling with multiple on-route charging modes, showcasing cost reduction and enhanced utilization rates for buses and drivers while considering the impact of bus line length on charging mode selection. The model effectively reduces costs, improves utilization rates, and minimizes the number of buses and drivers, with bus line length playing a significant role in charging mode selection. [57] introduces a new framework for analyzing off-service charging strategies for electric buses, emphasizing intelligent algorithms' cost-saving potential and the benefits of participating in ancillary services markets. It employs a comprehensive methodology to assess charging costs and grid load impacts, exemplified through a case study of three depots in the Netherlands, outlining the research design and

mathematical models utilized. [63] proposes a Real-Time Smart Optimization algorithm, utilizing a genetic algorithm to optimize BEB depot charging schedules, emphasizing the need for intelligent charging algorithms and potential future enhancements. A framework for analyzing BEB on-route charging strategies is introduced in [7], highlighting the cost-saving potential of smart charging algorithms and the benefits of participating in ancillary services markets. Through a detailed methodology incorporating diverse factors, it evaluates charging impacts on costs and grid load, exemplified by a case study of Dutch bus depots. [23] delves into the transition to electric buses in public transit; it introduces an extended vehicle time-window scheduling model tailored to multi-depot BEB transit systems, optimizing charging cost and waiting time. [33] introduces two off-service charging scheduling algorithms for large bus depots to reduce peak load, tested using actual data from the Alsterdorf depot, with one algorithm targeting peak demand and the other aiming to flatten average load. Validation is done using a Bus Depot Simulator, scheduling jobs, calculating intervals, and organizing buses to minimize peak demand.

[34] tackles the multi-depot on-route BEBs scheduling problem, emphasizing BEB-depot constraints and partial recharging policies, employing a mixed-integer programming model and a branch-and-price heuristic algorithm to optimize operational costs effectively. Key findings showcase the effectiveness of the branch-and-price algorithm in producing high-quality solutions, demonstrating cost reduction potential through increased battery capacity and charging rate. [4] explores electrifying public transportation with plug-in charging and proposes a coordinated charging algorithm for BEBs depots, integrating energy storage and photovoltaic systems to maximize profit and minimize grid impact. The methodology involves mathematical modelling, simulations on the SkyBus fleet, and assessing PEB charging impact in Auckland, NZ, with a proposed scheduling algorithm for profit optimization and grid stability enhancement. [71] addresses the multi-objective electric vehicle scheduling problem, integrating time-of-use pricing and peak load risk, showcasing cost reduction and peak load management effectiveness. [78] addresses BEBs charging scheduling problem by considering nonlinear charging profiles and battery degradation effects, aiming to minimize costs for peak-hour bus services while determining bus-to-trip assignments and charging schedules. It proposes mixed-integer programming models and valid inequalities to solve the problem efficiently. It demonstrates its application through a case study on Singapore's No.171 bus route, offering insights for public transport operators. [3] explores the managerial benefits of adding electric buses alongside diesel vehicles in fleets, proposing a novel MIP formulation for Electric Vehicle Scheduling Problems. [6] presents a vehicle scheduling method for electric buses, emphasizing idle recharge times to enhance scheduling robustness amidst stochastic volatilities in trip travel time and energy consumption. It underscores the significance of integrating recharging

behaviours, limited driving range, and stochastic factors into scheduling strategies, advocating against continuous trips and promoting collaborative optimization of scheduling and charging plans.

[43] explores the challenge of efficiently scheduling electric vehicles (EVs) with limited range and charging constraints, proposing mathematical formulations and solution methods based on the deficit function theory and an equivalent bi-objective integer programming model to minimize the total number of EVs and battery chargers. The study validates the effectiveness of these models and methods through numerical examples and a real-life case study in Singapore, indicating their potential for solving large-scale battery-electric transit vehicle scheduling problems. [31] proposes a method to optimize overnight charging for electric bus fleets, aiming to minimize battery aging costs while considering variable temperatures and operational conditions. Simulation results demonstrate a substantial reduction in battery capacity loss over ten years compared to conventional charging strategies, addressing concerns regarding battery longevity and operational costs in increasing electrified transit in urban public transport. [58] proposed a MILP for effective electric and hybrid/non-electric bus scheduling, emphasizing careful modelling of mixed-fleet conditions. The methodology offers potential for decision support systems transitioning to greener transport, utilizing an overlapping approach to enhance optimally over complex decomposition schemes. [41] presents a formulation for the multi-depot vehicle scheduling problem with multi-vehicle types, including EBs, addressing range and refuelling constraints. It introduces a novel approach to generate feasible time-space-energy and time-space networks, formulating the problem as an Integer linear programming to minimize total system cost while considering emissions and proposing a simplified formulation for computational efficiency. Applied to Hong Kong's bus services, it analyzes fleet size, operational and passenger costs, emissions, and implications of government subsidies, Low-Emission-Zone scheduling, and safe driving ratios for bus refuelling. [79] explores the Electric Bus Charging Facility Planning problem, focusing on heterogeneous BEB fleets in urban transit networks. It aims to optimize charger deployment at terminals and depots to meet daily charging demand while minimizing costs, considering uncertainties in BEB travel time and battery degradation. A two-stage stochastic programming model is formulated, and heuristic methods are proposed to solve large-scale instances. Experiments on fictitious and real-world BEB transit networks in Singapore evaluate model and algorithm performance, providing managerial insights for enhancing BEB transit system efficiency.

In [70], a directed graph models the available charge times for BEBs, which periodically return to the station for passenger pickup and battery recharging. A Constrained Network Flow MILP problem is formulated to optimize charger scheduling and determine the necessary number of chargers to maintain battery state of charge thresholds. This study

TABLE 2.1: BEB Charging Litterateurs Overview

Authors	Method	Year	Objective	Algorithm
Jahic et al. [33]	Off-service	2019	Min peak load	Simulaion
Gkiotsalitis et al. [23]	Off-service	2023	Min OPEX	MILP
Brinkel et al. [7]	Off-service	2023	peak-shaving	Optimization
Verbrugge et al. [63]	Off-service	2022	Min OPEX	Genetic Algorithm
Rafique et al. [57]	Off-service	2022	Min OPEX and Penalty	MILP
Xie et al. [72]	On-route	2023	Min OPEX	NL Optimization
Jiang et al. [34]	On-route	2022	Min OPEX	MILP and Heuristic
Arif et al. [4]	Off-service	2020	Max profit	MILP
Wu et al. [71]	On-route	2022	Vehicle scheduling & Min OPEX	LP and Heuristic
Zhang et al. [78]	On-route	2022	Min OPEX	Branch and Price
Alvo et al. [3]	Off-service	2021	Min BEBs	Benders Decomposition
Bie et al. [6]	On-route	2021	Min OPEX and CAPEX	MINL and NCP
Liu et al. [43]	On-route	2020	Vehicle scheduling & Min OPEX	ILP
Houbbadi et al. [31]	Off-service	2019	Min aging cost	Gradient-based Optimisation
Rinaldi et al. [58]	On-route	2020	Min OPEX	ILP
Li et al. [41]	On-route	2019	Min OPEX ,Emission Cost and Passenger Cost	MILP
Zhou et al. [79]	On-route	2023	Min (CAPEX), Num of chargers and their types	reinforcement learning method and a surrogate-based optimization
Whitaker et al. [70]	Both	2023	Min TCO	MILP
Zhou et al. [77]	On-route	2020	vehicle scheduling and chargers scheduling	simulated annealing and greedy dynamic selection

demonstrates the effectiveness of the proposed method in generating the best charging plans. The approach considers costs and accommodates fixed and variable charger numbers. This study views the problem independently without considering the current diesel-fueled transit system. It causes the solution to be less practical.

The paper [77] introduces a Multi-objective Bi-level programming model to optimize both vehicle scheduling and charging schedule of a mixed bus fleet operating from a single depot. The upper level of the model minimizes operating costs and carbon emissions while considering constraints such as connecting times between trips and the limited driving range of electric buses. The lower level focuses on charging scheduling to minimize charging costs while meeting the constraints of charging time and driving distance limitations. An integrated heuristic algorithm is proposed to solve the model, utilizing an iterative neighbourhood search algorithm based on simulated annealing for vehicle scheduling and a greedy dynamic selection strategy for charging scheduling. A case study based on a mixed bus fleet in Beijing demonstrates the effectiveness of the proposed model and solution algorithm. the paper does not consider transit system planning parameters such as travel demand for vehicle scheduling.

In summary, current research predominantly focuses on deterministic optimization for BEB charging facility planning and charging strategy, assuming known input parameters and constraints with certainty. This approach aims to find the best solution that maximizes or minimizes an objective function while satisfying all constraints, and it is suitable when uncertainties are absent or accurately quantified. Therefore, the solutions heavily rely on the input data, leaving planners needing insight into the process behind reaching these solutions. Therefore, if there is a slight change in any input, we must perform the entire optimization again, which could yield a completely different solution from the previous one. Most research treats the BEB transit system as an entirely new problem to solve. However, transit system planning involves a complex interplay of parameters, such as route configurations, scheduling, passenger demand patterns, and infrastructure capabilities. Therefore, viewing BEB transit system planning as dependent on the current diesel-fueled transit system is crucial. The goal should be to maintain the existing route structures, timetables, driver assignments, and operational shifts as much as possible during the migration to a battery-electric transit system.

Previous studies on BEB on-route charging scheduling have focused on minimizing energy costs by considering time-of-use tariffs, existing timetables, and charger power. However, there remains to be a significant gap in the literature regarding adapting and tuning existing timetables for a smooth transition to electric buses. This gap is crucial as it involves optimizing the scheduling to reduce synchronization issues and ensure equitable charging opportunities for all BEBs at the terminal. The current approaches often overlook the need to adjust bus schedules to accommodate the specific requirements of electric buses, such as varying charging times. Consequently, there needs to be more strategies that address the equal distribution of charging opportunities among all buses without changing the service rates defined by transit system planners, potentially leading to inefficiencies and increased waiting times at charging stations. Addressing this gap would involve developing scheduling algorithms that minimize the required chargers at each charging terminal, which lowers infrastructure and operating costs (minimizing power demand), and optimizing the operational timetable to balance the charging demand across all BEBs. This approach would maximize the charging infrastructure utilization and enhance the overall efficiency of BEB operations.

The expectation for BEB transit systems to utilize a combination of various charging technologies arises from several factors. Different regions or transit networks may possess diverse infrastructure capabilities and constraints. Incorporating a mix of charging technologies provides flexibility to adapt to existing infrastructure and accommodate future expansions. Operational efficiency is paramount in BEB transit networks. Different charging technologies offer varying charging speeds, costs, and energy efficiency. By integrating these technologies, BEB transit systems can optimize charging processes to minimize operational costs and maximize efficiency. BEBs may operate on routes with varying distances and schedules, necessitating different charging solutions to meet their range requirements. Utilizing a combination of charging technologies allows greater flexibility in addressing range limitations and optimizing charging schedules. Despite these anticipated benefits, only a few studies have explored integrating different charging technologies in BEB transit networks. This could be attributed to factors such as the complexity of coordinating multiple technologies, limited availability of data on their performance and interoperability, and the relative novelty of BEB technology in many regions. Hence, further research is needed to investigate how to effectively coordinate and integrate diverse charging technologies in BEB transit networks to realize their full potential.

Chapter 3

Estimation of Daily Required Energy for the Transit System

3.1 Introduction

As we transition from diesel to electric buses, we must recognize that transit planning primarily focuses on providing efficient, reliable, and accessible public transportation services that meet the community's needs. While electrification is a crucial step towards reducing our environmental footprint, it's not the only factor to consider.

A comprehensive transit plan must consider factors beyond electrification, such as:

- Population density and land use patterns influence the demand for public transportation.
- Employment centers, educational institutions, and healthcare facilities that rely on public transportation services.
- Accessibility and mobility needs, including those of people with disabilities.
- Traffic congestion and parking issues that public transportation can mitigate.
- Environmental impact and sustainability goals.
- Funding and budgeting constraints affecting the feasibility of electric bus adoption.

Given these priorities, it's essential to recognize that the transition to electric buses will not necessarily require changes to timetables and routes. The primary focus should be ensuring that the new electric buses can seamlessly integrate into the existing public transportation system without disrupting the community's services.

By prioritizing the community's needs and focusing on the bigger picture, we can ensure that the transition to electric buses succeeds while minimizing disruptions to the public transportation services people rely on. It's time to put the community's needs first and prioritize the factors that truly matter in transit planning.

As daily worst-case transit system energy consumption is the foundation of transit system electrification planning, we utilize the data-driven model application to estimate the BEB worst-case energy consumption for the transit system. This estimation is based on the exact timetable of the diesel-fueled transit system. Subsequently, we use the estimated amount for daily worst-case energy consumption estimation, which provides the foundation for further planning. The energy consumption of BEB is influenced by a complex web of factors, including the bus itself, its operation, its route, and external conditions. This complexity makes it difficult to accurately predict how much energy these buses use. In this section, we calculate the worst-case energy consumption for each transit network route, considering its characteristics, such as stop densities and topology. For the next step, we utilize the calculated energy consumption for each route to determine the total energy consumption of the city of Thunder Bay's transit system.

3.1.1 Preliminaries

We define the terminology and assumptions used in the context of a transit system as follows:

- A service refers to a trip along a route, either starting from the starting terminal and concluding at the ending terminal or vice versa.
- All fleet BEBs have specific schedules for their service times.
- Every BEB in the fleet departs from the depot at the start of the workday and returns to the depot after completing its assigned services.
- Transit route or transit line typically refers to a specific path or track followed by BEBs travelling between terminals. As the distances travelled for departure and return services' paths may vary, they are defined separately, with route length denoted by superscripts 1 (for departure service path) and 2 (for return service path).
- The worst-case energy consumption, caused by weather conditions, number of stops along the route, number of passengers and driving habits, is α per kilometre.
- The transit system has one depot for all BEBs to stay overnight. A large fleet-size transit system might have more than one depot.

- One BEB serves each activity block shown in figure 3.1. That means the number of the working fleet BEBs equals the number of activity blocks shown in Figures 1, 2, and 3.

The set of BEBs in the transit system is presented by $\mathbf{B} = \{b_1, b_2, \ldots, b_n\}$. $\mathbf{BL} = \{bl_1, bl_2, \ldots, bl_n\}$ denotes the set of transit system's daily activity blocks. The services within each activity block are denoted as $\{s_j, s_k, \ldots, s_r\}$ and $\mathbf{S} = \{s_1, s_2, \ldots, s_m\}$ be the set of all daily performed services within the transit system. Each block bl_n in $\mathbf{BL}$ comprises the daily services assigned to one BEB. The BEBs' departure times from and arrival times to the transit system depot are presented by $\mathbf{T^d} = \{t^d_{bl_1}, t^d_{bl_2}, \ldots, t^d_{bl_n}\}$ and $\mathbf{T^a} = \{t^a_{bl_1}, t^a_{bl_2}, \ldots, t^a_{bl_n}\}$ respectively. The service $s_m \in S$ consists of the tuple $< r, l^1_r | l^2_r, t^s_{s_m}, t^e_{s_m}, e_{s_n} >$ which is defined as follows.
The set $\mathbf{T^s} = \{t^s_{s_1}, t^s_{s_2}, \ldots, t^s_{s_m}\}$ represents the transit system's daily services starting times, where $\forall s_n \in \mathbf{S}$, and the set $\mathbf{T^e} = \{t^e_{s_1}, t^e_{s_2}, \ldots, t^e_{s_m}\}$ represents the transit system's daily services ending times, where $\forall s_n \in \mathbf{S}$.
Definition (Service Routes): The set of transit system's routes (lines) within the transit network.

$$\mathbf{R} = \{1, 2, \ldots, r\}, \quad \forall r \in R \tag{3.1}$$

Definition (Departure/Return service routes' Lengths-L): Set of distances from the transit network routes' initial terminals to their ending terminals (superscript 1) or from the transit network routes' ending terminals to their initial terminals (superscript 2).

$$\mathbf{L} = \{l^1_1, l^2_1, l^1_2, l^2_2 \ldots, l^1_r, l^2_r\}, \quad \forall r \in R \tag{3.2}$$

Definition (Service-Routes' Energy Consumption-E): Set of transit system services' worst-case energy consumption:

$$\mathbf{E^s} = \{e^s_{s_1}, e^s_{s_2}, \ldots, e^s_{s_m}\}, \quad \forall s_m \in \mathbf{S} \tag{3.3}$$

A service's worst-case energy consumption is given by:

$$e^s_{s_m} = \beta \times l^i_j, \quad i \in \{1, 2\}, j \in \mathbf{R} \tag{3.4}$$

Figure 3.1 shows the transit system's activity block.

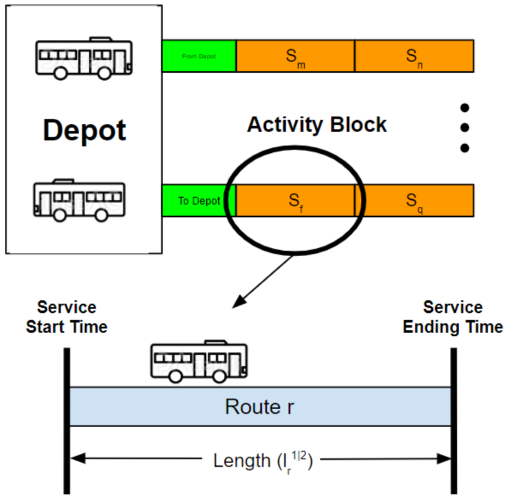

FIGURE 3.1: Transit system activity block

The required energy to perform each activity block in the activity blocks set **BL**, given in Equation (5.1), equals the total energy requirement to perform the assigned activity block's services, as represented in Equation (5.2).

$$\mathbf{E^{bl}} = \{\mathrm{e_{bl_1}}, \mathrm{e_{bl_2}}, \ldots, \mathrm{e_{bl_n}}\}, \quad \forall \mathrm{bl_n} \in \mathbf{BL} \tag{3.5}$$

$$\mathrm{e_{bl_n}} = \mathrm{e^{s}_{s_i}} + \ldots + \mathrm{e^{s}_{s_j}}, \quad \forall \mathrm{e^{s}_{s_j}}, \ldots, \mathrm{e^{s}_{s_j}} \in \mathbf{E^{s}} \tag{3.6}$$

As the activity blocks encompass all necessary services within a working day, the transit system's daily worst-case energy requirement, denoted as $\mathrm{E_w}$, is the sum of all required energy for each activity block. This is expressed as:

$$\mathrm{E_w} = \mathrm{e_{bl_1}} + \ldots + \mathrm{e_{bl_n}}, \quad \forall \mathrm{e_{bl_1}}, \ldots, \mathrm{e_{bl_n}} \in \mathbf{E^{bl}} \tag{3.7}$$

3.1.2 BEB worst-Case Energy Consumption Estimation for Each Route of City of Thunder Bay Transit Network

In this section, we calculate the city of Thunder Bay's daily worst-case energy consumption using the approach outlined in the previous section. Therefore, we must determine each route service's energy consumption rate (β). For calculating β, we utilized the BEB energy consumption simulator, depicted in Figure 3.2, which was developed by McMaster University, BEB Simulator. It is designed based on a published paper titled "Machine learning prediction models for battery-electric bus energy consumption in transit" [2].

The simulator parameters which are taken into account are:

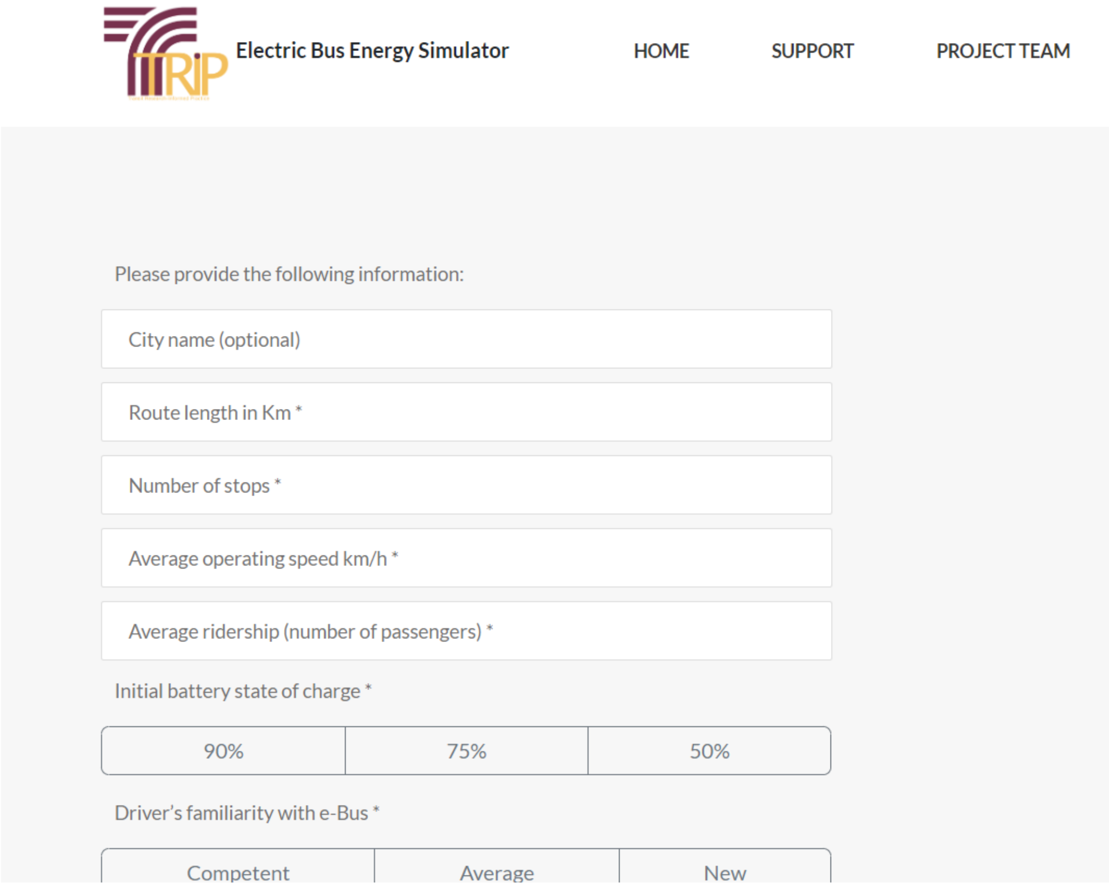

Figure 3.2: Screenshot of BEB energy consumption estimator application

- The route length is measured in kilometres, and each route may have a different length in two directions. Therefore, we assume different lengths for each direction of the route.
- Number of stops, we assume fifty percent of the total transit route's stops as worst-case stops.
- Average BEB speed km/h during the service route.
- Number of passengers in BEB during the service route.
- Initial battery state of the charge (SOC)
- Driver's familiarity with BEBs can be set into three states: competent, average, and new.
- BEB battery capacity can be set into 150, 300, 450, and 600 kWh.
- Electrical HVAC can be ON and OFF.
- Working season can be summer, fall, winter, and spring.

- Route topology grade can be set into Mostly Rolling Grade, Mostly downgrade, Mostly upergrade, Extreme downgrade, and Extreme upergrade, for detailed information, see Appendix A.

To calculate the worst-case energy consumption rate (β) for each transit line (route), we made the following assumptions: the average BEB speed is 20 km/h, the average number of passengers is 25, the initial battery state of charge is 50%, the driver's familiarity with BEB is competent, the BEB battery capacity is 600 kWh, the operation time is winter, Electric HVAC is ON, and the number of stops is one-third of the total line (route) stops. The topology grade %, the total number of stops, and the length for each route are presented in Table 3.1.

Table 3.1: Thunder Bay's transit network Lines (Routes) Parameters and Energy Consumption Rate

Route (Line)	Direction	Topology Grade %	Rolling grade	Number of Stops	Length	Energy Rate kWh/Km
1	Cowan to Mary NB	-0.22	(-1%-1%)	30	22.755	2.08
1	Mary NB to Cowan	0.24	(-1%-1%)	17	21.022	1.99
2	Waterfront to Confederation	-0.01	(-1%-1%)	10	10.16	2.02
2	Confederation to Waterfront	0.01	(-1%-1%)	11	12.569	2
3C	Waterfront to Catlegreen	0.89	(-1%-1%)	11	7.491	2.07
3C	Castkegeen to Waterfront	-0.85	(-1%-1%)	10	7.898	2.05
3J	Waterfront to Sherwood	0.88	(-1%-1%)	10	9.007	2.03
3J	Sherwood to Waterfront	-0.88	(-1%-1%)	7	5.459	2.05
3M	Waterfront to City hall	0.01	(-1%-1%)	8	8.199	2.01
3M	City hall to Waterfront	-0.01	(-1%-1%)	8	7.193	2.03

Continued on next page

Table 3.1 – continued from previous page

Route (Line)	Direction	Topology Grade %	Rolling grade	Number of Stops	Length	Energy Rate kWh/Km
4	Loop	0	(-1%-1%)	18	23.862	1.98
5	Confederation to Brown	0.1	(-1%-1%)	8	5.34	2.08
5	Brown to Confederation	-0.1	(-1%-1%)	6	4.984	2.04
6	Loop	0	(-1%-1%)	11	23.826	1.94
7	Waterfront to Shunia	0.5	(-1%-1%)	12	7.921	2.08
7	Shunia to Waterfront	-0.5	(-1%-1%)	8	5.174	2.09
8	Intercity to City hall	0.02	(-1%-1%)	14	15.391	2
8	City hall to Intercity	-0.02	(-1%-1%)	14	13.942	2.02
9	Waterfront to Intercity	0.02	(-1%-1%)	11	14.635	1.99
9	intercity to Waterfront	-0.02	(-1%-1%)	12	13.943	2
10	Confederation to City hall	0	(-1%-1%)	9	7.838	2.04
10	City hall to Confederation	0	(-1%-1%)	9	8.196	2.03
11	Waterfront to Winsdor	0.86	(-1%-1%)	8	5.058	2.09
11	Winsdor to Waterfront	-0.86	(-1%-1%)	8	5.708	2.07
12	Loop	0	(-1%-1%)	10	9.751	2.02
13	Waterfront to Dawson	-0.87	(-1%-1%)	7	7.048	2.01
13	Dawson to Waterfront	0.87	(-1%-1%)	10	9.970	2.01
14	City hall to Airport	0.07	(-1%-1%)	9	10.157	2

Continued on next page

Table 3.1 – continued from previous page

Route (Line)	Direction	Topology Grade %	Rolling grade	Number of Stops	Length	Energy Rate kWh/Km
14	Airport to City hall	-0.07	(-1%-1%)	5	6.315	1.99
16	Confederation to City hall	0	(-1%-1%)	4	4.165	2
16	City hall to Confederation	0	(-1%-1%)	4	4.165	2

We can calculate the daily worst-case energy consumption amount by obtaining the β value for all Thunder Bay's transit network lines (routes). The daily working activity consists of 33 activities, shown in Figures 1, 2, and 3, activity blocks containing scheduled services.

With the worst-case energy consumption rate determined for all lines (routes) and their corresponding lengths, we can calculate the daily worst-case energy consumption for the entire transit system. Figure 3.3 illustrates the estimation of daily worst-case energy consumption for all activity blocks within the Thunder Bay transit system. Consequently, the total estimated daily worst-case required energy amounts to 17,612 kWh.

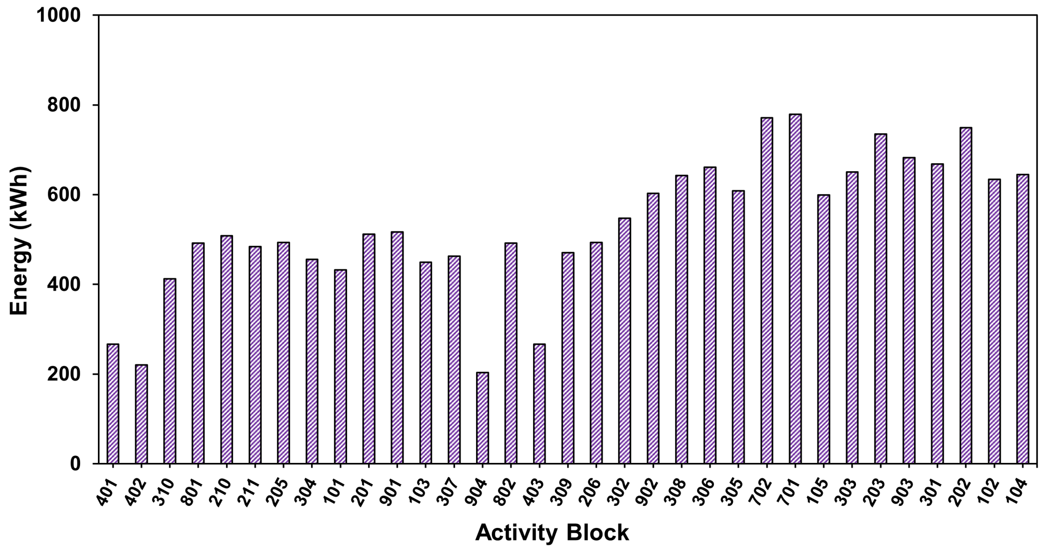

FIGURE 3.3: Estimated daily worst-case energy consumption for the Thunder Bay transit system's activity blocks

In summary, we utilized the BEB energy consumption estimator, developed through a data-driven approach, to determine the worst-case energy consumption rate for transit system lines (routes). Using this rate, along with the lengths of each route and their corresponding service schedules (activity blocks), we estimated the daily worst-case energy consumption for the entire transit system, specifically for the city of Thunder Bay. The total estimated daily worst-case required energy is 17,612 kWh.

Chapter 4

Planning for Off-service Charging

4.1 Introduction

Off-service charging planning is crucial for electrifying transit systems. It involves strategically scheduling the charging of BEBs during off-peak hours, typically overnight, when the electricity demand is lower. This approach helps minimize disruptions to transit operations while ensuring that BEBs are adequately charged to meet their daily service requirements.

By implementing optimized off-service charging plans, transit agencies can achieve several benefits. They can maximize fleet availability by ensuring that BEBs are fully charged and ready for service during peak operating hours, thereby minimizing downtime and improving service reliability. Additionally, they can realize cost savings by optimizing charging infrastructure and leveraging off-peak electricity rates to reduce operational costs associated with BEB charging. Efficient off-service charging planning also enables grid integration by balancing the demand for electricity from BEB charging with the capacity of the local power grid. This helps avoid overloads and ensures grid stability, contributing to a more reliable and sustainable transit system overall. The primary objective of off-service charging planning is to optimize charging infrastructure utilization and minimize operational costs while meeting the energy demands of the transit fleet. Optimization entails determining the minimum number and location of charging sites, scheduling the charging sessions to coincide with periods of low electricity demand, and considering factors such as battery capacity, route schedules, and depot capacities.

This chapter proposes the CGC model for strategically placing off-service charging sites. The aim is to balance the demand for electricity from BEB charging with the capacity of the local power grid, thereby avoiding overloads and ensuring grid stability. The proposed algorithm is evaluated by the placement of charging sites for two different capacities of the local power grid. The chapter introduces a charging mechanism for BEBs during off-service overnight charging in the second phase. The last part of the chapter discusses the transition from diesel buses to fully electrified ones, utilizing the off-service charging approach. This allows transit planners to calculate the required BEBs and assign them to fulfill the diesel-fueled transit system's activity blocks by the proposed CACA algorithm.

4.2 Brief Introduction to Clustering

Clustering is a fundamental technique in unsupervised learning that is used to group similar data points. The goal is to partition a set of data points into clusters, where points within the same cluster are more similar than those in other clusters. Various clustering algorithms exist, each with its approach to defining similarity and grouping data points. Some standard clustering algorithms include K-means, hierarchical clustering, and DBSCAN.

4.2.1 Agglomerate Clustering

Agglomerative clustering is a hierarchical clustering technique used to group similar data points. Agglomerative clustering indeed follows a bottom-up approach. It begins by considering each data point as an individual cluster and iteratively merges the closest pairs of clusters until all points belong to a single cluster. This process is driven by similarity measures, merging clusters based on proximity or similarity. The result is a hierarchical clustering structure where the final, single cluster encompasses all data points. Linkage, a crucial aspect of this process, determines how the similarity between clusters is measured and influences which clusters are merged at each step. There are several standard linkage methods used in hierarchical agglomerative clustering:

- **Single Linkage (Nearest Linkage):** This method calculates the distance between the closest points in two clusters and considers that distance as the distance between the clusters. Single linkage tends to produce elongated clusters and is sensitive to noise and outliers. It is computationally efficient but can suffer from the chaining effect, where clusters are merged based on just one or a few close points.
- **Complete Linkage (Farthest Linkage):** Complete linkage calculates the distance between the farthest points in two clusters and uses that distance to measure dissimilarity between the clusters. This method tends to produce compact, spherical clusters and is less sensitive to noise than a single linkage. However, it can need

help with elongated clusters and is computationally more expensive than single linkage due to the need to consider all pairwise distances.

- **Average Linkage:** Average linkage computes the average distance between all pairs of points in the two clusters being merged. This method balances the strengths of single and complete linkage and is more robust to noise. It tends to produce clusters of more uniform sizes and shapes, making it a popular choice in many applications.

$$\mathrm{d}(\mathrm{C_i}, \mathrm{C_j}) = \frac{1}{|\mathrm{C_i}||\mathrm{C_j}|} \sum_{\mathrm{x} \in \mathrm{C_i}} \sum_{\mathrm{y} \in \mathrm{C_j}} \mathrm{d}(\mathrm{x}, \mathrm{y}) \tag{4.1}$$

  Where $\mathrm{C_i}$ and $\mathrm{C_j}$ are two clusters. $|\mathrm{C_i}|$ and $|\mathrm{C_j}|$ are the number of data points in clusters $\mathrm{C_i}$ and $\mathrm{C_j}$, respectively. $\mathrm{d}(\mathrm{x}, \mathrm{y})$ is the distance between data points x and y, which is used as similarity metric.

  The average linkage criterion computes the average distance between all pairs of data points in clusters $\mathrm{C_i}$ and $\mathrm{C_j}$. This formula calculates the distance between clusters $\mathrm{C_i}$ and $\mathrm{C_j}$, which is then used in the agglomerative clustering process to determine which clusters to merge at each step.

- **Centroid Linkage:** Centroid linkage calculates the distance between the merged clusters' centroids (mean points). This method often produces clusters of approximately equal size and is less sensitive to outliers. It is computationally efficient and can handle high-dimensional data well.

- **Ward's Linkage:** Ward's linkage aims to minimize the increase in variance when merging clusters. It tends to produce clusters with relatively equal sizes and compact shapes. While computationally more intensive than other linkage methods, Ward's linkage is proper when the goal is to identify compact, homogeneous clusters. Given two clusters A and B, the distance $\mathrm{d}(\mathrm{A}, \mathrm{B})$ in Ward's method can be represented as:

$$\mathrm{d}(\mathrm{A}, \mathrm{B}) = \frac{|\mathrm{A}||\mathrm{B}|}{|\mathrm{A}| + |\mathrm{B}|} \|\mu_{\mathrm{A}} - \mu_{\mathrm{B}}\|^2 \tag{4.2}$$

  where:

  - $|\mathrm{A}|$ and $|\mathrm{B}|$ are the sizes of clusters A and B respectively.
  - μ_{A} and μ_{B} are the centroids of clusters A and B.
  - $|\mu_{\mathrm{A}} - \mu_{\mathrm{B}}\|^2$ is the squared Euclidean distance between the centroids of clusters A and B.

The choice of linkage method significantly impacts the resulting clusters' characteristics, including their shapes, sizes, and overall structure. Selecting a linkage method that aligns with the data's characteristics and the desired clustering outcome is essential.

4.2.2 Evaluation Metrics

When evaluating clustering algorithms and benchmarking their performance, several metrics can be used to assess the quality of the clustering results. Here are some commonly used metrics:

- **Silhouette Score (SS):** This metric measures how similar an object is to its cluster compared to others. It ranges from -1 to 1, where a high value indicates that the object is well-matched to its cluster and poorly matched to neighbouring clusters. The SS for a data point i is defined as:

$$\mathrm{SS(i)} = \frac{\mathrm{b(i) - a(i)}}{\max\{\mathrm{a(i), b(i)}\}} \tag{4.3}$$

  where a(i) is the average distance between i and all other points in the same cluster (i.e., the intra-cluster distance), and b(i) is the minimum average distance from i to all points in any other cluster (i.e., the nearest-cluster distance).

  The SS for the entire dataset is the mean SS of all data points:

$$\mathrm{SS} = \frac{1}{\mathrm{n}} \sum_{\mathrm{i=1}}^{\mathrm{n}} \mathrm{s(i)} \tag{4.4}$$

  where n is the number of data points.

- **Weighted Silhouette Score (WSS):** We consider each data point's weight to compute a WSS.

$$\mathrm{WSS} = \frac{\sum_{\mathrm{i=1}}^{\mathrm{N}} \mathrm{w(i) \cdot s(i)}}{\sum_{\mathrm{i=1}}^{\mathrm{N}} \mathrm{w(i)}} \tag{4.5}$$

  where N is the number of data points, w(i) is the weight of data point i, and s(i) is the SS of data point i.

- **Davies-Bouldin Index (DBI):** This index computes the average similarity between each cluster and its most similar cluster, where lower values indicate better clustering.

$$\mathrm{DBI} = \frac{1}{\mathrm{k}} \sum_{\mathrm{i=1}}^{\mathrm{k}} \max_{\mathrm{j \neq i}} \left(\frac{\mathrm{avg(R_i) + avg(R_j)}}{\mathrm{d(C_i, C_j)}} \right) \tag{4.6}$$

  where k is the number of clusters, $\mathrm{R_i}$ is the intra-cluster distances for cluster i, $\mathrm{d(C_i, C_j)}$ is the distance between the centroids of clusters i and j, and $\mathrm{avg(R_i)}$ is the average intra-cluster distance for cluster i.

4.3 Placement of Off-service Charging Sites by CGC Method

A BEB maintains a consistent energy consumption rate of β kWh/km. It has a battery with the capacity of α kWh with Ω percent of charge available. We assume that all variables affecting BEB energy consumption, such as consumption rate and route length, remain constant. Therefore, BEBs assigned to fulfill an activity block's charging needs should consistently need charging at a specific constant terminal along the assigned activity block path that the BEB will travel during the working day. This specific terminal is referred to as the block's dispatching terminal.

T is a set representing the transit network's terminals.

$$\mathbf{T} = \{\mathrm{t}_1, \mathrm{t}_2, \ldots, \mathrm{t}_\mathrm{q}\} \tag{4.7}$$

Definition (Dispatching Terminals-D): The set of the transit network's terminals where BEBs are sent for charging:

$$\mathbf{D} = \{\mathrm{d}_1, \mathrm{d}_2, \ldots, \mathrm{d}_\mathrm{q}\}, \quad \forall \mathrm{q} \in \mathbf{T},\ \&\ \ |\mathbf{D}| < |\mathbf{T}| \tag{4.8}$$

Definition (Dispatching Rates(weights)-W): Set of dispatching rates associated with transit network's dispatching terminals:

$$\mathbf{W} = \{\mathrm{w}_1, \mathrm{w}_2, \ldots, \mathrm{w}_\mathrm{q}\}, \quad \forall \mathrm{q} \in \mathbf{T} \tag{4.9}$$

4.3.1 CGC Method

This section introduces the CGC method, which utilizes Agglomerative clustering [64] to perform clustering for ideal charging sites' placements. Agglomerative clustering offers several advantages due to its hierarchical, proximity-based, and flexible nature. Its hierarchical nature naturally creates clusters at different levels of granularity in data grouping, facilitating decisions on charging site placements. Additionally, it is proximity-based, allowing for the identification of close dispatching terminal clusters, which minimizes travel distances for electric buses to and from charging sites.

Let **D** be the set of all BEB dispatching terminals as defined in (4.8). We initialize individual clusters for each dispatching terminal:

$$\mathrm{C} = \{\mathrm{C}_1, \mathrm{C}_2, \ldots, \mathrm{C}_n\}, \quad \mathrm{n} = |\mathrm{D}| \tag{4.10}$$

Each cluster initially contains only one dispatching terminal. Denote by $\mathbf{d_{ij}}$ to be the distance between clusters $\mathrm{C_i}$ and $\mathrm{C_j}$, and $\mathrm{w_i}$ and $\mathrm{w_j}$ to be the weight associated with clusters $\mathrm{C_i}$ and $\mathrm{C_j}$ respectively. The objective function is to minimize the weighted sum of distances while satisfying the constraints as follows:

$$\text{Minimize } Z = \sum_{\mathrm{C_i} \in \mathbf{C}} \sum_{\mathrm{C_j} \in \mathbf{C}} \mathrm{d_{ij}} \cdot \mathrm{x_{ij}} \cdot \mathrm{w_i} \cdot \mathrm{w_j} \tag{4.11}$$

Subject to the following constraints:

- Binary Decision Variables: $\mathrm{x_{ij}}$ takes binary values, indicating whether terminals $\mathrm{C_i}$ and $\mathrm{C_j}$ are clustered together.

$$\mathrm{x_{ij}} \in \{0, 1\}, \quad \mathrm{C_i}, \mathrm{C_j} \in \mathbf{C}, \tag{4.12}$$

- Cluster Size Constraint: Each new cluster should contain exactly two clusters.
- Maximum weight Clustering Constraint (4.14): The total weight of both clusters merged at a location should not exceed K. Let $\mathrm{P_f}$ represent the available power at the local grid, and $\mathrm{P_c}$ represent the charger power. The number of BEBs k that can be charged simultaneously is determined by dividing the available feeder power by the charger power.

$$\mathrm{K} = \frac{\mathrm{P_f}}{\mathrm{P_c}} \tag{4.13}$$

$$\mathrm{w_i} + \mathrm{w_j} \leq \mathrm{K}, \quad \mathrm{C_i}, \mathrm{C_j} \in \mathbf{C}, \quad \mathrm{w_i}, \mathrm{w_j} \in \mathbf{W} \tag{4.14}$$

- Symmetry Constraint (4.15): If clusters $\mathrm{C_i}$ and $\mathrm{C_j}$ are grouped together, it implies that $\mathrm{C_j}$ and $\mathrm{C_i}$ are also grouped together.

$$\mathrm{x_{ij}} = \mathrm{x_{ji}}, \quad \forall \mathrm{C_i}, \mathrm{C_j} \in \mathbf{C} \tag{4.15}$$

- Cluster selection constraint: This constraint ensures the selection of the cluster with the maximum weight among all clusters in set $\mathbf{G}$ that have a distance to the selected cluster i less than γ times the variance $(\gamma \cdot \mathrm{Var}(i))$ (see Equation 4.17). It restricts the total number of clusters with distances to cluster i less than its variance $\mathrm{Var}(i)$ to be within the variance value for cluster $\mathrm{C_i}$. This selection criterion includes all clusters that satisfy the distance condition based on the variance.

The objective function aims to minimize the weighted sum of distances by determining which two clusters should be merged together while considering the constraint on the maximum total weight of two clusters K(4.13) that can be grouped at a single location.

$$\mathbf{G} = \{\mathrm{C_i}, \ldots, \mathrm{C_k}\}, \quad \forall \mathrm{C_k} \in \mathbf{C} \tag{4.16}$$

Let $\mathrm{d_{ij}}$ represent the distance from cluster i to cluster j, and Var(i) is the variance of distances from cluster i to all other clusters. distance between two clusters' centroids is considered as the distance between two clusters' centroids.

$$\mathrm{x_{ij}} = 1, \quad \forall \mathrm{j} \in \mathbf{C} \text{ where } \mathrm{w_j} + \mathrm{w_i} \leq \mathrm{k} \quad \& \quad \mathrm{d_{ij}} \leq \gamma \cdot \mathrm{Var}(i) \tag{4.17}$$

4.3.2 Algorithm Design

The approach consists of three algorithms: the distance calculator algorithm, which calculates the distance between two clusters, the clustering algorithm, and The CGC algorithm, The higher-level algorithm 3 utilizes algorithm 2 iteratively to merge clusters based on their weights and distances while adhering to specific constraints. This process continues until no more clusters can be merged.

Algorithm 1 (Constraint Greedy Clustering): The algorithm takes as input a set of dispatching terminals D and a set of terminal dispatching rates W; its purpose is to find clusters of terminals that meet certain constraints. At the beginning of lines 1-4, the algorithm Initializes empty sets to store the new clusters, old clusters, and their dispatching rates (weights). (Each terminal in D is initially considered a cluster by itself.) From lines 5-7, a while loop calls Algorithm 2 (described in the next section) to update new clusters and their weights. the loop continues as long as the number of new clusters is the same as the number of old clusters. The algorithm terminates when it is no longer possible to merge any additional clusters.

Algorithm 1 Two Clusters Distance Calculation

Require: Two Clusters $\mathrm{C_1}$, $\mathrm{C_2}$
Ensure: The distance between clusters $\mathrm{C_1}$ and $\mathrm{C_2}$ is $\mathrm{d(C_1, C_2)}$
1: $\mathrm{C_1} = \frac{1}{|\mathrm{C_1}|}\sum_{\mathrm{x}\in\mathrm{C_1}} \mathrm{x}$, $\mathrm{c_2} = \frac{1}{|\mathrm{C_2}|}\sum_{\mathrm{x}\in\mathrm{C_2}} \mathrm{x}$. ▷ Compute the centroid of each cluster
2: $\mathrm{d_{12}} = \|\mathrm{c_1} - \mathrm{c_2}\|$. ▷ Calculate the distance between centroids

---

Algorithm 2 (Clustering Phase): It takes as input the current clusters $\mathrm{C_{old}}$, the current clusters' weights $\mathrm{W_{old}}$, and clustering constraints (4.12) and (4.14). At the beginning of lines 1-3, the Algorithm Initializes empty sets to store clusters' distances, new clusters, and new weights. From lines 4-28, the algorithm starts clustering current

Algorithm 2 Clustering

Require: Clusters $\mathrm{C_{old}}$, weights $\mathrm{W_{old}}$, Clustering Constraints
Ensure: Clusters set $\mathrm{C_{new}}$

1: $\mathrm{dist} \leftarrow \{\}$
2: $\mathrm{C_{new}} \leftarrow \{\}$
3: $\mathrm{W_{new}} \leftarrow \{\}$
4: **while** $\mathrm{C_{old}}$ is not empty **do**
5: $\quad \mathrm{Z} \leftarrow \{\}$
6: $\quad \mathrm{G} \leftarrow \{\}$
7: $\quad$ Select $\mathrm{C_1}$ from $\mathrm{C_{old}}$ such that $w_1 = \min_{W \in W_{old}} (w)$
8: $\quad \mathrm{C_{old}} \leftarrow \mathrm{C_{old}} \setminus \{\mathrm{C_1}\}$ ▷ Remove $\mathrm{C_1}$ from $\mathrm{C_{old}}$
9: $\quad$ **for all** $\mathrm{C} \in \mathrm{C_{old}}$ **do**
10: $\quad\quad \mathrm{d(C_1, C)\}} \leftarrow$ Call Algorithm $3(\mathrm{C_1, C})$
11: $\quad\quad \mathrm{dis} \leftarrow \mathrm{dis} \cup \{\mathrm{d(C_1, C)}\}$
12: $\quad$ **end for**
13: $\quad\quad \mu = \beta \cdot \mathrm{Variance(dis)}$
14: $\quad\quad \mathrm{G} = \{\mathrm{C} \in \mathrm{C_{old}} \,|\, d(\mathrm{C_1, C}) < \mu\}$
15: $\quad\quad$ **for all** $\mathrm{C_2} \in \mathrm{G}$ **do**
$\quad\quad \mathrm{C_2} = \arg\max_{\mathrm{C_2 \in G}} \mathrm{weight(C_2)}$
16: $\quad\quad\quad$ **if** $\mathrm{W_{C_1} + W_{C_2} \leq k}$ **then**
17: $\quad\quad\quad\quad \mathrm{Z} \leftarrow \{\mathrm{C_1, C_2}\}$
18: $\quad\quad\quad\quad \mathrm{C_{new}} \leftarrow \mathrm{C_{new}} \cup \{\mathrm{Z}\}$
19: $\quad\quad\quad\quad \mathrm{W_C^{new}} = \mathrm{W_{C_1} + W_{C_2}}$
20: $\quad\quad\quad\quad \mathrm{W_{new}} \leftarrow \mathrm{W_{new}} \cup \{\mathrm{W_C^{new}}\}$
21: $\quad\quad\quad\quad$ Break;
22: $\quad\quad\quad$ **end if**
23: $\quad\quad$ **end for**
24: $\quad\quad$ **if** Z is empty **then** ▷ No new merge
25: $\quad\quad\quad \mathrm{Z} \leftarrow \{\mathrm{C_1}\}$ ▷ Create a new cluster containing only $\mathrm{C_1}$
26: $\quad\quad\quad \mathrm{C_{new}} \leftarrow \mathrm{C_{new}} \cup \{\mathrm{Z}\}$
27: $\quad\quad\quad \mathrm{W_{new}} \leftarrow \mathrm{W_{new}} \cup \{\mathrm{W_{C_1}}\}$
28: $\quad\quad$ **end if**
29: $\quad$ **end while**

clusters in ascending order in their weights. Then, it solves the optimization problem in (4.11) and returns the new clusters back to the algorithm 3. The output clusters will be used for the next clustering step. from lines 7-8 inside the while loop, the algorithm selects a cluster $\mathrm{C_1}$ from $\mathrm{C_{old}}$ with the minimum weight w1. and removes $\mathrm{C_1}$ from $\mathrm{C_{old}}$. From lines 9-14, the algorithm selects the closest cluster $\mathrm{C_2}$ to $\mathrm{C_1}$ for merging. from lines 15-23, the algorithm merges the clusters $\mathrm{C_2}$ to $\mathrm{C_1}$ if it complies with the maximum allowed weight for the newly created cluster mentioned at (4.14). from lines 15-23, the algorithm finds no clusters that could be merged with $\mathrm{C_1}$, then it simply creates a new cluster containing only $\mathrm{C_1}$ and adds it to $\mathrm{C_{new}}$.

Algorithm 3 (Two cluster distance calculator): Line 1 calculates the centroids of two clusters, then line 2 calculates the distance between these centroids, which is

Algorithm 3 Constraint Greedy Clustering

Require: Set of dispatching terminals D, Set of terminal dispatching rates W
Ensure: Clusters set C
$\mathrm{C_{new}} \leftarrow \{\}$
$\mathrm{W_{new}} \leftarrow \{\}$
$\mathrm{C_{old}} \leftarrow$ [d] for d in D
$\mathrm{W_{old}} \leftarrow$ [w] for w in W
while $|\mathrm{C_{new}}| \neq |\mathrm{C_{old}}|$ **do** ▷ Checking the number of clusters in the previous and new steps.
    $\mathrm{C_{new}}, \mathrm{W_{new}} \leftarrow$ Call Algorithm 2$(\mathrm{C_{old}}, \mathrm{W_{old}})$
end while

considered the distance between two clusters.

4.3.3 Model Evaluation

We started by identifying the dispatching terminals in the Thunder Bay transit network to evaluate the system model. Thunder Bay transit network comprises seventeen routes (lines) with fourteen terminals. Thirty-three buses fulfill the daily transit system's activity blocks. We identified the dispatching terminals for each activity block based on BEBs with a battery capacity of 325 kWh. Clustering algorithms group data points based on their similarities. K-means [66] is a clustering-based model. Therefore, we assess the performance of the CGC algorithm by comparing its results to K-means clustering results, serving as a benchmark for clustering performance. We then ran practical experiments using K-means and CGC algorithms on the Thunder Bay dispatching terminals.

We utilize the Silhouette score [60], weighted Silhouette score, and Davies Bouldin Score [14] as our clustering metrics. The Silhouette Coefficient, or the silhouette score, is a metric used to measure the clustering quality. It produces a value between -1 and 1, with 1 indicating well-separated and distinct clusters. Since terminal weights are associated with dispatching rates linked to distances travelled, we enhanced the Silhouette Score. This enhancement involved calculating weighted distances instead of simple distances between terminals and clusters, creating the weighted Silhouette Score. Additionally, we employed the standard deviation of clusters' weights to assess the evenness of weight distribution within the clusters. Consequently, a lower standard deviation signifies a higher degree of uniformity. The Davies Bouldin Score is 0.5 for K-means and 1 for CGC. The Davies Bouldin Score is a clustering metric used to assess the quality of clusters produced by clustering algorithms. It measures the compactness and separation between clusters, with lower scores indicating better-defined and well-separated clusters.

4.3.4 Constrained Greedy Clustering Experiment

We applied the CGC method to the Thunder Bay transit network's terminals to create groupings of the transit network's dispatching terminals while considering dispatching rates and specific constraints. We configured the algorithm with a hyperparameter, $\gamma = 0.5$, to identify the closest clusters, and we established $K = 15$ to indicate the maximum number of buses capable of simultaneous charging. Figure 4.1 depicts the steps of clustering, and Figure 4.1e shows the output clusters. Table 4.1 shows the dispatching terminals' locations, associated dispatching rates, and the clusters to which they belong. Table 4.2 shows the proposed charging sites' locations according to the CGC model. Table 4.3 presents CGC characteristics.

TABLE 4.1: Clustered Dispatching Terminals by CGC Model

Dispatching Terminal	Dispatching Rate	Latitude	Longitude	Cluster
Waterfront Terminal (1121)	9	48.43579	-89.21709	3
Shuniah & Erie (1337)	3	48.45814	-89.21461	4
Cowan & Hodder (1150)	8	48.47868	-89.18251	4
Sherwood & Valley (1418)	3	48.45223	-89.27195	3
Intercity Shopping Centre (1006)	7	48.40344	-89.24327	2
City Hall Terminal (1019)	2	48.38246	-89.2458	2
Confederation College (1231)	6	48.40297	-89.26967	1
Brown & Frederica (1269)	2	48.36553	-89.28146	1
Thunder Bay Airport(1522)	4	48.37245	-89.3112	1

TABLE 4.2: Charging Sites' Locations

Charging Site	Latitude	Longitude	Address
4	48.47326	-89.19126	459 Richard St
3	48.44098	-89.23375	74 Duke St
2	48.39868	-89.24429	SilverCity Thunder Bay Cinemas
1	48.38635	-89.28999	551 Riverview Dr W

4.3.5 K-means Experiment

K-means requires the number of clusters as input. To determine this, we utilized the elbow method [47] to find the appropriate number of clusters, the elbow method aims to find the suitable number of clusters by plotting the Within-Cluster Sum of Squares (WCSS)[1] against the number of clusters and looks for an "elbow" point where the rate of decrease sharply slows, which was determined to be four, Figure 4.2b. Subsequently, we applied K-means clustering to the dispatching terminals, using the four clusters identified through the elbow method. The resulting clusters are visualized in Figure 4.2a, and Table 4.5 presents the characteristics of the K-means clustering.

[1]WCSS measures the sum of the squared distances between each point in a cluster and the centroid of that cluster. It quantifies the compactness of the clusters; lower WCSS values indicate more compact clusters.

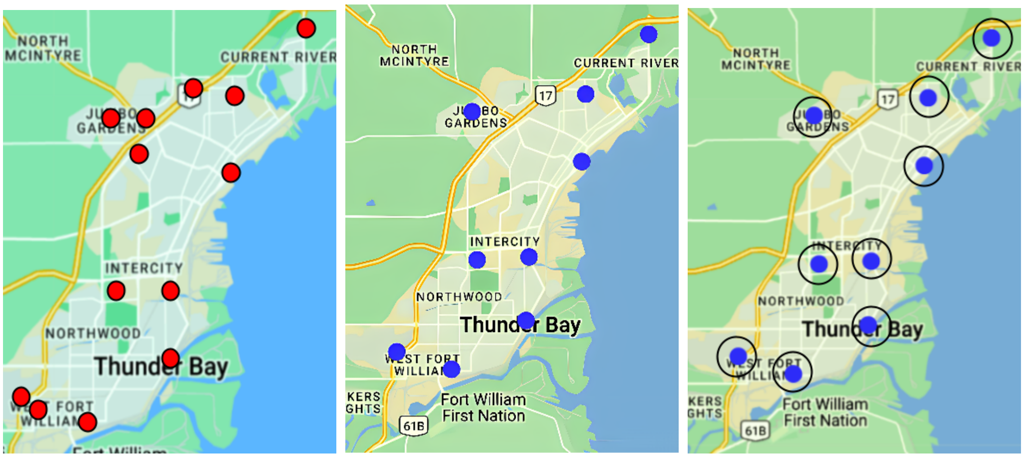

(a) City of Thunder Bay's transit network terminals (b) Dispatching terminals (c) CGC initial step

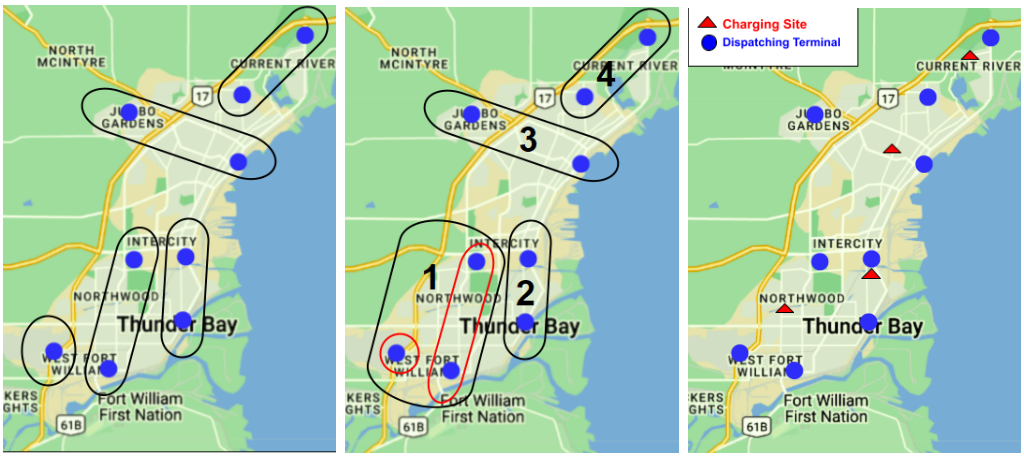

(d) First merging step (e) Second merging step (f) Charging sites at clusters centroid

FIGURE 4.1: The steps' results of the CGC algorithm on dispatching terminals

TABLE 4.3: Characteristics of CGC

Metric	Value
Silhouette Score	0.1
Weighted Silhouette Score	0.74
Davies Bouldin Score	1
Clusters' weights Mean	11
Clusters' weights Standard Deviation	1.4

TABLE 4.4: Clustered Dispatching Terminals by k-means Method

Dispatching Terminal	Dispatching Rate	Latitude	Longitude	Cluster
Waterfront Terminal (1121)	9	48.43579	-89.21709	3
Shuniah & Erie (1337)	3	48.45814	-89.21461	4
Cowan & Hodder (1150)	8	48.47868	-89.18251	4
Sherwood & Valley (1418)	3	48.45223	-89.27195	4
Intercity Shopping Centre (1006)	7	48.40344	-89.24327	2
City Hall Terminal (1019)	2	48.38246	-89.2458	2
Confederation College (1231)	6	48.40297	-89.26967	2
Brown & Frederica (1269)	2	48.36553	-89.28146	1
Thunder Bay Airport(1522)	4	48.37245	-89.3112	1

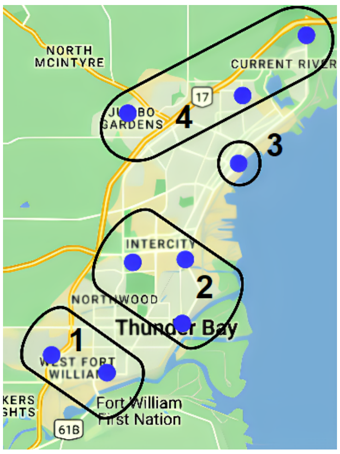

(a) Clustered dispatching terminals by K-means

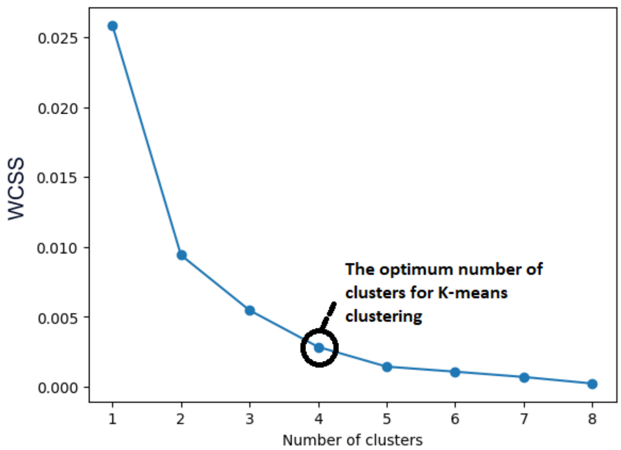

(b) Elbow diagram

FIGURE 4.2: K-means clustering and the elbow method results

4.3.6 Results Analysis and Discussion

Table 4.3 and Table 4.5 display the Silhouette scores for CGC and the K-means clustering algorithms. The K-means Silhouette score is 0.4, while the CGC algorithm score is 0.1. The results show that K-means clustering outperforms the CGC method, as indicated by the Silhouette score and the Davies Bouldin Index. The higher Silhouette score of K-means indicates that it generates well-defined clusters with distinct boundaries, regardless of the dispatching terminal weights. The weighted Silhouette score for K-means and CGC algorithm are 0.76 and 0.74, respectively. The weighted Silhouette Scores for both the K-means and CGC algorithms are close. This indicates that the CGC algorithm performs closely to K-means when considering terminal weights (dispatching rate). Moreover, the lower Davies Bouldin Index for K-means indicates that it achieves a better balance between the compactness of individual clusters and the separation between them, resulting in more effective cluster separation. Clusters' weights Standard Deviation is 4.2 for K-means and 1.4 for CGC. CGC excels in maintaining consistency and uniformity among cluster weights. This is reflected in its lower standard deviation for cluster weights, suggesting that its clusters exhibit less variability in weight distribution. Given our primary objective of adhering to power grid constraints, the uniformity observed in the CGC method becomes valuable. Uniform clusters' weights benefit consistent resource distribution, aligning with our power grid needs.

While clustering aims to minimize the travelled distance by BEBs for charging, the results demonstrate that slight compromises in clustering may not necessarily result in a significant increase in energy consumption (travelled distance). Instead, optimizing the clustering to distribute the charging load among sites promotes stability and reduces fluctuation impacts on the power grid.

Table 4.5: Characteristics of the K-means Clustering

Metric	Value
Silhouette Score	0.4
Weighted Silhouette Score	0.76
Davies Bouldin Score	0.5
Clusters' weights Mean	11
Clusters' weights Standard Deviation	4.2

In summary, comparing CGC and K-means clustering showed that a slight compromise between their clustering efficiencies could result in effective charging load balancing. The uniformity in clusters' weights (dispatching rate) aligns with our specific requirements for power grid constraints, achieving uniform power distribution among the charging sites. Ultimately, ideal placing off-service charging sites improves the overall system performance. Additionally, CGC is a flexible method that considers any constraint in each merging step. This flexibility enriches the transit system planner, who can define and apply localized constraints related to the particular area separately.

It is worth mentioning that when selecting the location for the charging site and the planner decides to utilize the current infrastructures, the proximity to charging site placements is a crucial factor. Choosing a depot or garage as a charging site, which is close to identified charging site placements, is advantageous as it eliminates the need to construct new buildings. Therefore, the nearest depot or garage to the location of the charging site placement is considered the best choice to minimize additional construction efforts.

4.4 Off-service Charging Scheduling

4.4.1 Introduction

The overnight electricity rate typically offers lower costs compared to daytime rates, making overnight charging the most cost-effective solution for fulfilling the daily energy requirements of an electrified transit system. To effectively model overnight charging, we analyzed the transit system's energy consumption from the chapter 3. Such an analysis provides valuable insights for transit system infrastructure planners, including energy consumption levels within the system, their impact on the power distribution grid, the minimum number of chargers required, and determining the minimum charger power needed to meet charging time constraints. This section introduces an intelligent overnight charging mechanism, the Priority Charging Mechanism (PCM), which charges BEBs simultaneously using the minimum number of chargers to minimize infrastructure costs. The model's effectiveness is evaluated using accurate transit system data from Thunder Bay.

4.4.2 SYSTEM MODEL

This section introduces a mechanism to determine the minimum number of chargers and their power for overnight charging within a fully electric public transit system in the City of Thunder Bay. Figures 1, 2, and 3 show the Thunder Bay City transit system activity blocks. The proposed mechanism extracts daily service data from the diesel-fueled transit system activity blocks and calculates the worst-case energy consumption for the BEBs assigned to the activity blocks. This worst-case energy consumption is the foundation for planning the migration from diesel-fueled to electric-powered transit fleets.

4.4.2.1 Preliminaries

Before introducing the mathematical model, we outline the following assumptions:

- A service refers to a trip along a route, either starting from the starting terminal and concluding at the ending terminal or vice versa.
- All fleet BEBs have specific schedules for their service times.
- Every BEB in the fleet departs from the depot at the start of the workday and returns to the depot after completing its assigned services.
- Transit route or transit line typically refers to a specific path or track followed by BEBs travelling between terminals. As the distances travelled for departure and return services' paths may vary, they are defined separately, with route length denoted by superscripts 1 (for departure service path) and 2 (for return service path).
- The transit system has one depot for all BEBs to stay overnight. A large fleet-size transit network might have more than one depot. Overnight charging must occur between t_{start} minutes and t_{end} minutes, which is based on the most cost-effective electricity rate.
- All chargers utilized in overnight charging operations have identical power ratings. Furthermore, we set these chargers' maximum output DC power at 175 kW. This assumption is made to streamline the integration of all chargers into a single power rack, thereby simplifying installation and reducing the complexity of cooling and maintenance requirements.
- There is no restriction on the battery capacities of BEBs; they possess sufficient battery capacity to fulfill their assigned activity blocks.

4.4.2.2 Charging Mechanism Overview

The charging mechanism divides the total available charging time into Q sessions. It determines BEB priorities based on their energy requirements and available charging time. Then, it selects N_{ch} (number of chargers) BEBs with the highest priorities for the current charging session. Subsequently, BEB priorities are recalculated based on the updated

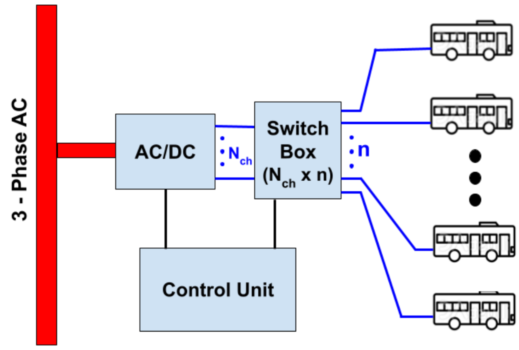

FIGURE 4.3: Overnight charging mechanism overview

BEB deployment, their state of charge (SOC), and the time required for departure. The system selects N_{ch} new BEBs for the next charging session. This process continues until the last session, when all BEBs are expected to be fully charged.

The proposed overnight charging mechanism integrates all chargers into a single unit. Therefore, maintenance, conditioning (cooling), and monitoring can be performed for one unit instead of several charging boxes spread out of the depot. As shown in Figure 4.3, a controllable switch connects the N_{ch} available DC chargers to (N_{ch}) BEBs from the n available BEBs in a depot. (n) is the total number of working BEBs in the transit system that stay at a depot overnight. There are three main units:

- The AC/DC unit encompasses the minimum number of chargers (N_{ch}) required to charge all BEBs in the transit system within a specific time frame. Every charger is connected to the switch box and is controlled and monitored by the control unit.
- The switch box connects the output of (N_{ch}) chargers to (N_{ch}) out of the (n) BEBs with higher priorities in each charging session. It is controlled and monitored by the control unit.
- The control unit calculates the priorities of BEBs for every charging session based on BEBs' SOCs, monitors the AC/DC unit to ensure proper functioning and commands the switch box to connect the (N_{ch}) chargers to BEBs in each charging session.

4.4.2.3 Energy Consumption and Power Analysis

Each BEB must complete a block defined in activity blocks set **BL**. Therefore, each BEB must have energy equal to the worst-case energy requirements in Equation (5.1). BEBs' departure times from and arrival times to the transit network depot are presented by $\mathbf{T^d} = \{t^d_{bl_1}, t^d_{bl_2}, \ldots, t^d_{bl_n}\}$ and $\mathbf{T^a} = \{t^a_{bl_1}, t^a_{bl_2}, \ldots, t^a_{bl_n}\}$ respectively.

According to assumption 4.4.2.1, each BEB performs one activity block. Therefore, the energy required by a BEB to perform the activity block equals the calculated energy for the assigned block.

$$\mathbf{E^b} = \{\mathrm{e_{b_1}}, \mathrm{e_{b_2}}, \ldots, \mathrm{e_{b_n}}\}, \quad \forall \mathrm{b_n} \in \mathbf{B} \tag{4.18}$$

$$\mathrm{e_{b_n}} = \mathrm{e_{bl_n}}, \quad \forall \mathrm{b_n} \in \mathbf{B}, \quad \forall \mathrm{bl_n} \in \mathbf{BL} \tag{4.19}$$

Based on our assumption, the charging time for BEBs occurs between $\mathrm{t_{start}}$ and $\mathrm{t_{end}}$. Therefore, the minimum power required to charge each BEB is given by:

$$\mathbf{P^{bl}} = \{\mathrm{p_{bl_1}}, \mathrm{p_{bl_2}}, \ldots, \mathrm{p_{bl_n}}\}, \quad \forall \mathrm{bl_n} \in \mathbf{BL} \tag{4.20}$$

$$\mathrm{p_{bl_n}} = \frac{\mathrm{e_{bl_n}}}{|\mathrm{t_{start}} - \mathrm{t_{end}}|} \tag{4.21}$$

We also assumed that all applied charger powers $\mathrm{p_{ch}}$ are the same. To this end, it is required to select a charger power at least equal to the maximum power in $\mathbf{P^b}$ as defined in Equation (4.20). It is the primary chargers' power constraint that we must consider:

$$\mathrm{p_{ch}} \geq \max\{\mathrm{p_{bl_1}}, \mathrm{p_{bl_2}}, \ldots, \mathrm{p_{bl_n}}\}, \quad \forall \mathrm{bl_n} \in \mathbf{BL} \tag{4.22}$$

The second charger power constraint is established by a power electronics designer responsible for designing and integrating the AC/DC chargers within the power rack. Typical power for overnight charging ranges from $\mathrm{P_{min}}$ to $\mathrm{P_{max}}$ kW.

$$\mathrm{P_{min}}\ \mathrm{kW} \leq \mathrm{P_{ch}} \leq \mathrm{P_{max}}\ \mathrm{kW} \tag{4.23}$$

We must choose the maximum allowed power to minimize the number of applied chargers. The total required energy consumption by the transit system is calculated by summing the energy requirements of all activity blocks in (5.1), given by:

$$\mathrm{E_{network}} = \sum_{i=1}^{n} \mathrm{e_{bl_i}} \tag{4.24}$$

The total energy E_{network} must be stored through overnight charging. Therefore, the total required power $\mathrm{P_{network}}$ is given by:

$$\mathrm{P_{network}} = \frac{\mathrm{E_{network}}}{|t_{\mathrm{start}} - t_{\mathrm{end}}|} \tag{4.25}$$

Then, by choosing the chargers' power $\mathrm{P_{ch}}$ by complying with two constraints (4.22) and (4.23), the number of required chargers $\mathrm{N_{ch}}$ is calculated by:

$$\mathrm{N_{ch}} = \frac{\mathrm{P_{network}}}{\mathrm{P_{ch}}} \tag{4.26}$$

Now that we have the number of required chargers $\mathrm{N_{ch}}$ and their power $\mathrm{P_{ch}}$, it is plausible to introduce the transit system's BEBs overnight charging mechanism.

4.4.2.4 Overnight Charging Algorithm Design

The proposed overnight charging method divides the available charging time into sessions $\mathbf{N_s}$ in which each charging session time is given by:

$$\mathrm{T_{se}} = \frac{|t_{\mathrm{start}} - t_{\mathrm{end}}|}{\mathbf{N_s}} \tag{4.27}$$

BEBs are then charged during each session based on their charging priorities. The priority-based charging concept assigns the charging priority to all BEBs defined by:

$$\mathrm{pr_n} = \frac{\mathrm{e_{bl_n}}}{\mathrm{T_{se}}} \tag{4.28}$$

$$\mathbf{PR} = \{\mathrm{pr_1}, \mathrm{pr_2}, \ldots, \mathrm{pr_n}\} \tag{4.29}$$

The approach consists of two main parts: the scheduler and the charging unit. The scheduler tracks the departures and arrivals of BEBs, their priorities, and the order in which they need to be charged. The charging unit simulates all charging sessions. The number of charging sessions, denoted as $\mathbf{N_s}$, is an algorithm hyperparameter manually tuned to ensure that all BEBs are charged in the minimum number of sessions possible.

Algorithm 1 (Scheduler): The algorithm takes as input the set of BEBs required rnergy $\mathbf{E^b}$ (5.3), the sets of blocks starting and ending times $\mathbf{T^d}$ and $\mathbf{T^a}$, the set of BEBs $\mathbf{B}$, the set of BEBs' priorities $\mathbf{PR}$, overnight charging start time t_{start}, overnight charging stop timet_{end}. At the Beginning from lines 1-14, the algorithm determines the priority of BEBs by considering their energy requirements and the time available to charge them from the charger. (Each indexed element in the set of priorities PR represented by equation (4.29) corresponds to the priority of the BEB with the same index in the set of BEBs ($\mathbf{B}$). Line 15 stores the number of BEBs in the transit system, and line 16 initializes the sorting indicator. From line 17 to 29, the algorithm sorts the set of priorities of BEBs $\mathbf{PR}$, the set of BEBs $\mathbf{B}$, the set of required energy $\mathbf{E^b}$, and the departure and arrival time sets denoted by $\mathbf{T^d}$ and $\mathbf{T^a}$, respectively, based on priorities from high to low.

Algorithm 2 (Charging Unit): The algorithm takes as input the set of BEBs required energy $\mathbf{E^b}$, the number of charging sessions $\mathbf{N_s}$, the charging session time $\mathbf{T_{se}}$, chargers' power $\mathbf{P_{ch}}$. At the beginning, line 1 declares the Charge set, which keeps track of the

Algorithm 4 Scheduler

Require: Set of BEBs Required Energy ($\mathbf{E^b}$), Set of BEBs (B) Sets of blocks starting and ending times $\mathbf{T^d}$ and $\mathbf{T^a}$, Charging start time t_{start}, Charging stop time t_{end}, Set of BEBs' priorities **PR**

Ensure: Sorted Sets B (BEBs) in descending order, PR (BEBs' Priorities), $\mathbf{E^b}$ (BEBs' Required energy)

1: **for all** $\mathrm{b_i} \in \mathbf{B}$ **do** ▷ Update the BEBs' priorities
2:     **if** $\mathrm{t^a_{bl_i}} < t_{\text{start}}$ & $\mathrm{t^d_{bl_i}} > t_{\text{end}}$ **then**
3:         $\mathrm{pr_i} \leftarrow \frac{\mathrm{e_{b_i}}}{|t_{\text{start}} - t_{\text{end}}|}$
4:     **else if** $\mathrm{t^a_{bl_i}} > t_{\text{start}}$ & $\mathrm{t^d_{bl_i}} < t_{\text{end}}$ **then**
5:
6:         $\mathrm{pr_i} \leftarrow \frac{\mathrm{e_{b_i}}}{\left|\mathrm{t^d_{bl_i}} - \mathrm{t^a_{bl_i}}\right|}$
7:     **else if** $\mathrm{t^a_{bl_i}} > t_{\text{start}}$ & $\mathrm{t^d_{bl_i}} > t_{\text{end}}$ **then**
8:
9:         $\mathrm{pr_i} \leftarrow \frac{\mathrm{e_{b_i}}}{\left|t_{\text{end}} - \mathrm{t^a_{bl_i}}\right|}$
10:     **else**
11:
12:         $\mathrm{pr_i} \leftarrow \frac{\mathrm{e_{b_i}}}{\left|\mathrm{t^d_{bl_i}} - t_{\text{start}}\right|}$
13:     **end if**
14: **end for**
15: $n \leftarrow |\mathbf{B}|$
16: sorted ← false
17: **while** not sorted **do**
18:     sorted ← true
19:     **for** $i = 1$ **to** n **do**
20:         **if** $\mathrm{pr_i} < \mathrm{pr_{i+1}}$ **then**
21:             Swap $\mathrm{pr_i}$ and $\mathrm{pr_{i+1}}$
22:             Swap $\mathrm{b_i}$ and $\mathrm{b_{i+1}}$
23:             Swap $\mathrm{e_{b_i}}$ and $\mathrm{e_{b_{i+1}}}$
24:             Swap $\mathrm{t^a_{bl_i}}$ and $\mathrm{t^a_{bl_{i+1}}}$
25:             Swap $\mathrm{t^d_{bl_i}}$ and $\mathrm{t^d_{bl_{i+1}}}$
26:             sorted ← false
27:         **end if**
28:     **end for**
29: **end while**

BEBs scheduled to charge in the current charging session. Line 2 declares an indicator that determines whether all charging sessions are completed, indicating whether all BEBs are fully charged. Line 3-12, the algorithm receives the $\mathbf{N_{ch}}$ number of BEBs with the highest priorities by calling the algorithm one, simulates the charging sessions, updates the charged BEBs required energy set after every charging session.

Algorithm 5 Charging Unit

Require: BEBs Required Energy $\mathbf{E^b}$, Number of Charging sessions $\mathbf{N_s}$, Charging Session Time $\mathbf{T_{se}}$, Chargers' Power $\mathbf{P_{ch}}$
Ensure: End of charging indicator **CHARGED**

```
Charge ← {}
CHARGED ← False
for j = 1 to N_s do
    Call Algorithm 1
    for j = 1 to N_ch do
        Charge ← Charge ∪ {b_j}
    end for
    Wait for T_se
    for j = 1 to N_ch do
        e_{b_j} ← e_{b_j} − [T_se × P_ch]
    end for
end for
CHARGED ← True
```

4.4.3 MODEL EVALUATION

We initiated the process by computing the necessary energy for executing the Thunder Bay transit system's activity blocks, as outlined in chapter 3. The Thunder Bay transit network comprises seventeen routes (lines) with fourteen terminals. Thirty-three BEBs are allocated to fulfill the designated services outlined in the operational timetable blocks.

4.4.4 Energy Requirement Analyse

We estimated the worst-case energy consumption for all Thunder Bay transit system activity blocks in chapter 3. In the worst-case scenario, 17,612 kWh is required to meet the energy needs of all BEBs to fulfill all activity blocks throughout the working day. Figure 3.3 depicts the daily worst-case energy requirements for activity blocks.

4.4.5 Charger Specifications Calculation

We investigated the best time interval for achieving the Thunder Bay transit system's daily energy requirement. Thunder Bay's electricity rate adheres to the regulations set by the Ontario province regarding cost, consequently, in relation to the daily energy consumption of the transit system. The pricing structure follows an industrial tariff plan, which operates hourly. The price for each hour is determined by the maximum demand power recorded during that hour. Given the characteristic minimum demand for electricity during overnight hours, we anticipate a similar pattern within Thunder Bay City. As depicted in Figure 4.4, all BEBs remain stationed at the depot from 11 p.m.

to 5:30 a.m., coinciding with the period of minimum electricity prices observed over the 24-hour cycle (Orange-color bars). According to equation (4.22), the minimum power

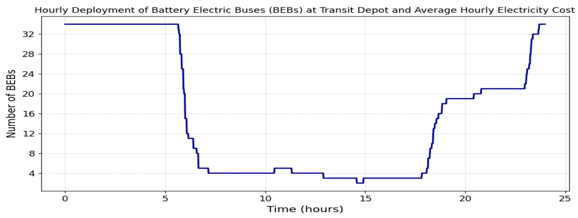

FIGURE 4.4: City of Thunder Bay BEBs deployment at the depot.

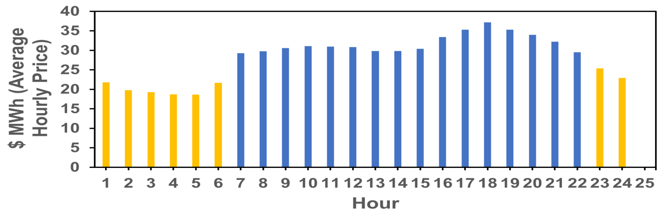

FIGURE 4.5: Hourly Ontario Energy Price

constraint is determined to be 123.64 kW. This constraint is associated with activity block 701, as Figure 3.3 illustrates. In this activity block, the assigned BEB requires 779 kWh of energy to complete the task, which is the maximum activity block energy requirement among all blocks. Based on the assumption, the maximum power constraint (4.23) is 175 kW. Table 4.6 displays the obtained results for the number of chargers corresponding to various charger power levels ranging from 123.64 to 175 kW, as determined by constraints established in the preceding step.

TABLE 4.6: Number of Required Chargers according to charger power

Charger Power (kW)	Number of Chargers
175	15
150	17
125	20

4.4.5.1 Priority Charging Mechanism

The PCM is executed to model the charging of BEBs as they perform activity blocks, as depicted in Figure 3.3. We utilize the block number to identify the BEB assigned to fulfill each block. Charger power is set to 175 kW to utilize the minimum number of chargers. Considering maximum BEBs' availability at the depot and minimizing electricity costs, charging time spans from 11 p.m. to 5:30 a.m. (390 minutes). The charging session duration is set to 13 minutes by manual tuning to maximize charging time utilization.

Thus, we have 30 charging sessions. Figure 4.6 shows the number of charging sessions each BEB in the transit system participates in.

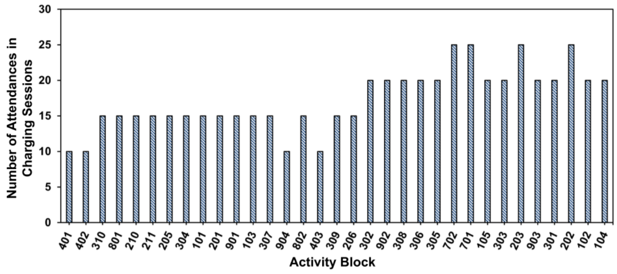

Figure 4.6: Number of charging sessions each BEB in the transit system participates in

In summary, we have outlined an intelligent overnight charging strategy by analyzing the transit system's daily energy needs and considering electricity pricing plans. This strategy includes determining the system's daily worst-case energy requirements, establishing the start and end times for overnight charging, determining the minimum number of chargers needed to minimize infrastructure costs, and specifying the minimum power capacity for each charger (all with identical specifications). PCM facilitates the simultaneous charging of all BEBs while considering their energy requirements and depot availability. By rotating BEBs across chargers during charging sessions, PCM improves resilience to charger failures and distributes potential disruptions across the network, minimizing the effects of failure on a BEB.

4.5 Optimal Number of BEBs for Off-Service Charging

In previous sections, we established the locations of off-service charging sites and devised an algorithm to charge BEBs efficiently. However, given that diesel buses typically cover longer distances than BEBs, the deployment of BEBs necessitates more BEBs to adequately service the transit system. Hence, we need to determine the minimum required number of BEBs and develop an efficient approach to allocating these additional BEBs to the various activity blocks within the transit system.

This section introduces a planning methodology to determine the minimum number of BEBs required within a transit system by sharing them among its activity blocks. It also emphasizes the efficient allocation of BEBs to transit system activity blocks by the CACA, aiming to minimize the distances travelled by shared BEBs between activity blocks. The model is assessed using actual transit system data from the City of Thunder Bay.

4.5.1 Introduction

The studies highlight a significant gap in addressing the off-service charging problem without determining the minimum number of BEBs and allocation strategy to fulfill the transit system's daily activity blocks. This section aims to minimize the number of BEBs required for off-service charging. To achieve this goal, we introduce a planning algorithm that considers various factors, including the energy requirements of BEBs and the similarities between the transit system's activity blocks. The algorithm aims to find the best configuration for the number of BEBs while simultaneously minimizing their energy consumption to fulfill activity blocks. While optimization offers a powerful solution, it often needs to be improved in terms of intuitive comprehension for planners. Each modification to the transit system requires planners to re-optimize, potentially resulting in entirely new solutions compared to previous iterations. Developing reliable off-service charging planning can mitigate the impacts of potential malfunctions in BEBs' operations and uncertainties arising from unpredictable service schedule delays during the charging process. However, determining the minimum number of BEBs and the allocation strategy for performing the transit system's activity blocks presents a significant challenge, requiring innovative algorithms to minimize infrastructure costs by reducing the required BEBs and minimizing their energy consumption through minimized travel distances.

4.5.2 SYSTEM MODEL

This section introduces a planning algorithm to determine the number of BEBs and their allocation to transit system activity blocks within a fully electric Thunder Bay City transit system. The proposed planning approach relies on the worst-case energy consumption scenario for all assigned BEBs. This worst-case energy consumption is the foundation for planning the transition from diesel-powered to off-service charging electric-powered transit systems, as detailed in Chapter 3. Notations introduced in Chapter 3 are utilized for consistency and clarity.

The Off-service charging plan aims to determine the minimum number of BEBs required to perform daily services, assigning them to activity blocks. To achieve this objective, we divide each activity block's energy requirements in the first step, as given by (5.1), by BEB battery capacity α kWh. Equation (4.30) represents the number of BEBs needed for that particular activity block.

$$\mathrm{NoB}_{\mathrm{bl_n}} = \lfloor \mathrm{e}_{\mathrm{bl_n}} / \alpha \rfloor \tag{4.30}$$

The remainder energy, calculated by Equation (4.31), becomes the input for the Clustering step.

$$\mathrm{e}^{\mathrm{r}}_{\mathrm{bl_n}} = \mathrm{e}_{\mathrm{bl_n}} \mod \alpha \tag{4.31}$$

We define a new set of activity blocks' energy as Equation (4.32).

$$\mathbf{E}^{\mathbf{bl}}_{\mathbf{R}} = \{\mathrm{e}^{\mathrm{r}}_{\mathrm{bl_1}}, \mathrm{e}^{\mathrm{r}}_{\mathrm{bl_2}}, \dots, \mathrm{e}^{\mathrm{r}}_{\mathrm{bl_n}}\}, \quad \forall \mathrm{bl_n} \in \mathbf{BL} \tag{4.32}$$

In the next step, we add extra BEBs to fulfill the activity blocks' services to compensate for the remaining energy. However, adding extra BEBs incurs significant costs to the transit system, so it should be done one by one. Additionally, the added BEBs should be utilized for the activity blocks with paths that have the minimum distances. This ensures that the BEBs' energy to change their paths is minimized. We can efficiently manage the transit system's energy consumption and operational costs by optimizing the assignment of extra BEBs to activity blocks with minimal distance paths. Then CACA clusters activity blocks whose paths are close to each other and ensures that the sum of their remainder required energies does not exceed the battery capacity α of a single BEB. Consequently, the number of clusters added to the sum of quotients, given by (4.30), determines the minimum number of BEBs required for the operation.

4.5.2.1 Similarity Matrix

Each activity block encompasses two dimensions of data: temporal and spatial data. The temporal dimension illustrates the service timing within a daily work schedule, while the spatial dimension delineates the path that BEB must traverse during working hours. To simplify the representation, we focus solely on the spatial dimension, condensing it into a graph path within the transit network graph. Consequently, we obtain several paths representing an activity block within the transit network graph shown in Fig. 4.7.

To measure the distance between two paths in a graph, we can utilize the Jaccard index [27], which measures the similarity between the paths and can quantify their similarity or dissimilarity. In the context of paths in a graph, we can represent each path as a set of nodes or edges. Then, the Jaccard index between two paths can be calculated as the ratio of common nodes to the total number of unique nodes across both paths.

We define a Similarity Matrix (**SM**) as a matrix in which the rows and columns represent the activity blocks in the set **BL**. **SM** elements range from zero to one, representing the similarity between two activity blocks' paths (sub-graphs), where zero denotes no

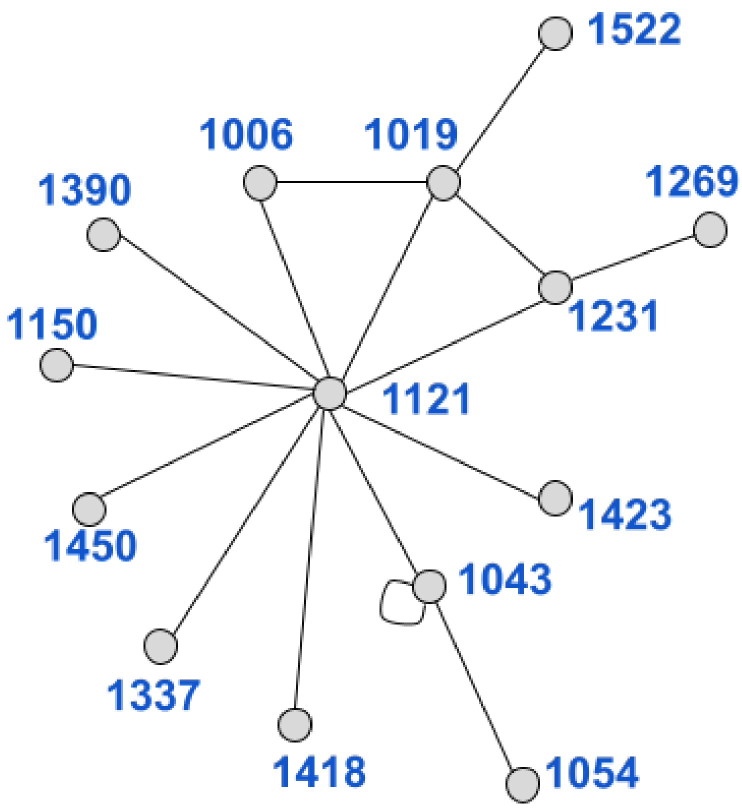

FIGURE 4.7: Thunder Bay transit network graph

similarity, and one indicates identical paths (sub-graphs).

$$\mathrm{SM} = \begin{bmatrix} s_{11} & s_{12} & \cdots & s_{1n} \\ s_{21} & s_{22} & \cdots & s_{2n} \\ \vdots & \vdots & \ddots & \vdots \\ s_{n1} & s_{n2} & \cdots & s_{nn} \end{bmatrix} \tag{4.33}$$

In this matrix, s_{ij} represents the similarity between the activity block j path (sub-graph) and the activity block i path (sub-graph). Each activity block includes several transit network's terminals. We define the set of nodes representing these terminals within the activity blocks, as shown below

$$\mathbf{PN_n} = \{\mathrm{t}_1, \mathrm{t}_2, \ldots, \mathrm{t_t}\}, \quad \forall \mathrm{t_t} \in \mathbf{T}, \quad \forall \mathrm{n} \in \mathbf{BL} \tag{4.34}$$

The Jaccard similarity score measures the similarity between two activity blocks by comparing the sets of nodes within the blocks, denoted as $\mathbf{PN_{bl_j}}$ and $\mathbf{PN_{bl_i}}$.

$$S_{ij} = \frac{|\mathbf{PN_{bl_j}} \cap \mathbf{PN_{bl_i}}|}{|\mathbf{PN_{bl_j}} \cup \mathbf{PN_{bl_i}}|} \tag{4.35}$$

4.5.2.2 Constraint Affinity Clustering Algorithm

The CACA is designed to cluster the paths of activity blocks based on their similarity while ensuring that the sum of their energy requirements does not exceed the battery capacity α kWh of the BEB. The CACA identifies the activity block with the maximum energy consumption from the new activity blocks' energy consumption set (4.32). Next, it aims to find an activity block with maximum similarities to this initial block. Suppose the total energy consumption of the grouped activity blocks falls below the battery threshold, which is α kWh battery capacity. In that case, these activity blocks are grouped, and their energies are summed. This process continues iteratively until the cumulative energy consumption reaches or exceeds the battery threshold. As a result, the algorithm generates clusters of activity blocks that can be served by a single BEB, ensuring efficient resource utilization and optimizing energy allocation for transportation purposes. Algorithm 6 outlines the procedural steps of the CACA algorithm, offering a clear and concise overview of its functionality.

Algorithm 6 Constraint Affinity Clustering Algorithm

Require: Activity Blocks' Energy consumption $\mathbf{E_R^{bl}}$, Activity Blocks Set **BL** Similarity Martix **SM**, BEB battery capacity α

Ensure: The set of Clusters of Activity Blocks (**C**)

while BL is Empty **do**
  $\mathrm{C} \leftarrow \{\}$
  Let *merged* be **true**
  while *merged* is **true do**
    merged $\leftarrow$ **false**
    Let $i = \mathrm{argmax}\{\mathbf{E_R^{bl}}\}$
    Let R_i be the ith row of Similarity Martix SM
    $j \leftarrow \mathrm{argmax}\{R_i\}$
    if $\mathrm{e^r_{bl_i}} + \mathrm{e^r_{bl_j}} \leq \alpha$ **then**
      $\mathrm{bl_i} \leftarrow \mathrm{bl_i} \cup \mathrm{bl_j}$
      $\mathbf{BL} \leftarrow \mathbf{BL} \setminus \{\mathrm{bl_j}\}$
      $\mathrm{e^r_{bl_i}} \leftarrow \mathrm{e^r_{bl_i}} + \mathrm{e^r_{bl_j}}$
      $\mathbf{E_R^{bl}} \leftarrow \mathbf{E_R^{bl}} \setminus \{\mathrm{e^r_{bl_j}}\}$
      $\mathbf{SM} \leftarrow \mathbf{SM} \setminus \{\mathrm{column(j)}\}$ ▷ Remove column (j) from similarity matrix
      merged $\leftarrow$ **true**
    end if
  end while
  $\mathrm{C} \leftarrow \mathrm{bl_i}$
  $\mathbf{BL} \leftarrow \mathbf{BL} \setminus \mathrm{bl_i}$
  $\mathbf{BL} \leftarrow \mathbf{E_R^{bl}} \setminus \mathrm{e^r_{bl_i}}$
  $\mathbf{SM} \leftarrow \mathbf{SM} \setminus \{\mathrm{row(i)}\}$ ▷ Remove row (i) from similarity matrix
end while

4.5.3 MODEL EVALUATION

We initiated energy calculations for the city of Thunder Bay transit system's activity blocks. The transit system consists of seventeen routes and fourteen terminals. Thirty-three activity blocks fulfill the scheduled services.

4.5.3.1 Thunder Bay Transit System's Energy Requirement Analysis

We consider a worst-case scenario where all BEBs within the Thunder Bay transit system consume 1.9 kWh per kilometre. Consequently, 17,612 kWh is required to fulfill all activity blocks throughout the working day. BEBs utilize a 600 kWh battery capacity, with 20 percent reserved for State of Charge (SOC) backup, leaving 480 kWh available for consumption. To determine the number of BEBs needed for each activity block (division quotient) and the remaining energy amount for blocks-sharing BEBs, we divide the energy requirements of the activity blocks by 480 kWh. The sum of division quotients for all activity blocks equals 33, indicating that 33 BEBs are required. Figure 5.1 depicts the activity blocks' remainder energy, which extra sharing BEBs should address. This step

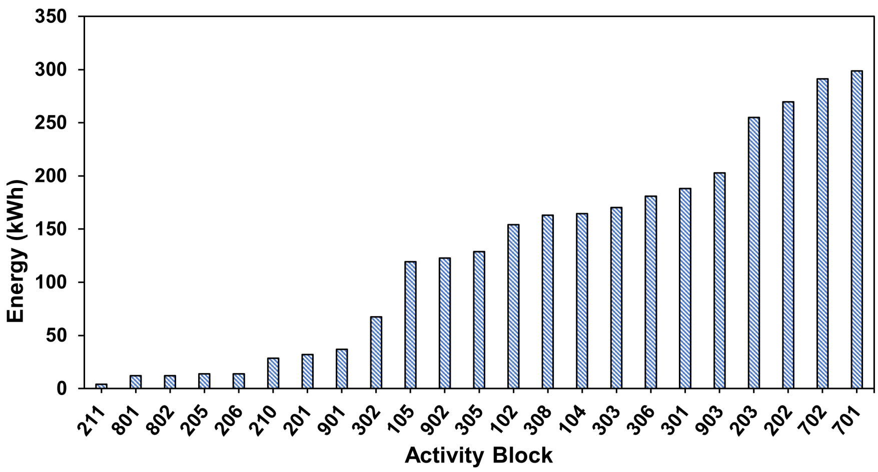

FIGURE 4.8: Activity blocks' remainders energy.

calculated that 33 block-dedicated BEBs are required to perform each activity block, leaving 23 activity blocks needing to be fully covered and needing additional BEBs. The next phase involves determining the number of additional BEBs needed and how they are allocated to these remaining activity blocks.

4.5.3.2 Thunder Bay Transit System's Similarity Martix

As previously mentioned, to determine the groups of activity blocks sharing a BEB to fulfill their remaining services, which cannot be performed with activity block-dedicated BEBs, we pass the activity blocks with remaining energy to the CACA. To apply the CACA, we projected activity blocks onto a spatial dimension. Figure 4.7 shows the graph of the city of Thunder Bay, while Figure 4.9 illustrates the structural similarity between two activity block sub-graphs. The similarity matrix is constructed for activity blocks

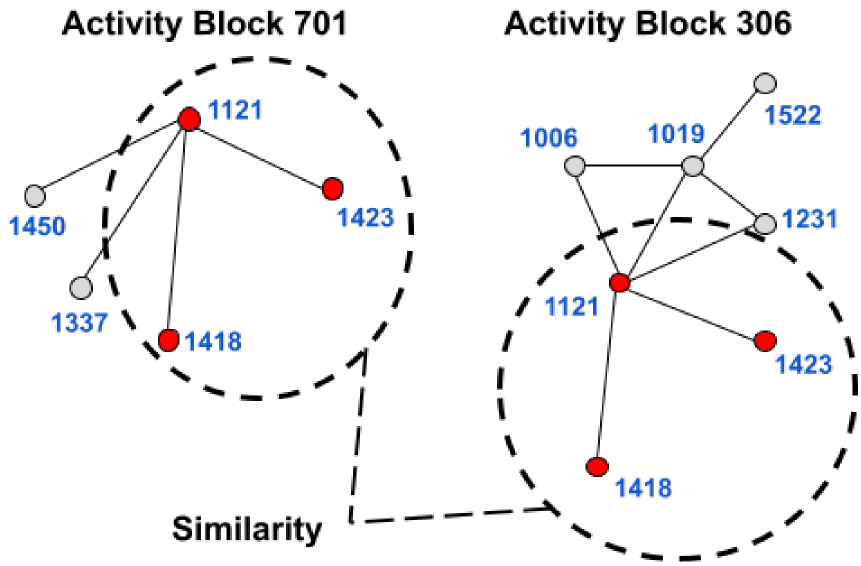

FIGURE 4.9: Activity blocks 701 and 306 graphs similarity

that have energy remains. Table 4.7 shows a sample of the constructed similarity matrix.

TABLE 4.7: Activity Blocks' Similarity Matrix Sample

Activity Block	701	306	202	902	702	203
701	1	0.34	0.14	0.125	1	0.14
306	0.34	1	0.25	0.58	0.34	0.25
202	0.14	0.25	1	0.4	0.14	1
902	0.125	0.58	0.4	1	0.125	0.4
702	1	0.34	0.14	0.125	1	0.14
203	0.14	0.25	1	0.4	0.14	1

4.5.3.3 Constrained Affinity Clustering Algorithm Results

We applied the CACA algorithm to the Thunder Bay Transit system's activity blocks outputs from the previous step. The algorithm aimed to create groupings of the transit system's activity blocks while considering structural similarity and energy constraints, configuring 480 kWh. As indicated in Table 4.8, there are five clusters, each representing a group of activity blocks sharing one BEB to fulfill their services, which could not be fulfilled by the dedicated activity block BEB. The fully electric transit system requires

Table 4.8: Activity Blocks Sharing BEBs

Cluster	Activity Blocks	Sum of Energy (kWh)
1	701, 306	480
2	702, 308, 802, 801	480
3	202, 203, 210, 901	472
4	903, 902, 302, 201,205,206	454
5	301, 104, 105	474

33 activity block-dedicated BEBs plus an additional 5 BEBs shared among the activity blocks, resulting in 38 BEBs to fulfill the transit system's daily services.

In summary, We formulated an off-service charging strategy through a comprehensive analysis of the daily energy requirements of the transit system and careful consideration of the transit system's service timetable. This strategy includes assessing the transit system's daily worst-case energy needs and determining the minimum required BEBs to minimize infrastructure costs. Additionally, we developed the clustering algorithm (CACA) to ensure an effective solution for grouping activity blocks for shared BEB usage. This algorithm minimizes travelling distances while considering energy balancing among the shared BEBs within the transit system.

Chapter 5

Planning for Opportunity Charging

This chapter presents a three-step planning approach to determine the minimum number of on-route charging terminals needed within a transit system. To effectively model on-route charging, conducting a comprehensive analysis of the transit system's energy consumption is crucial, as detailed in Chapter 3. This analysis yields valuable insights for infrastructure planners, including understanding energy consumption levels within the transit system, determining the minimum number of charging terminals required, and efficiently assigning transit system activity blocks to the charging terminals to balance charging loads. The chapter emphasizes allocating transit system activity blocks to identified chargers to maximize BEBs' charging opportunities and ensure balanced energy consumption between the charging terminals. Furthermore, the chapter proposes an optimization method to adjust the timetables of inherited activity blocks from a diesel-fueled transit system. This method aims to maximize charging opportunities at the allocated terminals while reducing the simultaneous presence of BEBs at these terminals. The model's effectiveness is evaluated using actual transit system data from the Thunder Bay transit system.

5.1 Charging Terminals Identification for Activity Blocks

5.1.1 Introduction

The literature review underscores a significant gap in addressing the on-route charging problem without offering guidance on determining the minimum number of charging terminals and assigning BEBs to them, considering the inherited timetables from the diesel-fuelled transit system. This consideration is particularly favourable for transit planners transitioning from a diesel-powered system to an electric one. We aim to maximize the opportunity for Battery BEBs to charge while minimizing the number of charging terminals and ensuring energy balancing. To achieve these objectives, we propose a planning approach that takes into account several factors, such as the energy requirements for fulfilling the transit system's activity blocks, the accessibility of all transit system activity blocks to charging terminals, the number of stops each activity block has at every charging terminal, and the total energy each charging terminal should provide throughout the working day. The proposed method determines the minimum number of charging terminals and allocates charging terminals to activity blocks for charging BEBs. It aims to maximize the charging opportunities for BEBs while ensuring energy balancing among the charging terminals. Since the activity blocks must be no change when migrating from a diesel-fueled transit system to a fully electric one, we suggest tuning the timing of activity blocks to maximize their charging opportunities.

5.1.2 SYSTEM MODEL

This section introduces an algorithm to determine the minimum number of terminals for on-route charging within a fully electric transit system. The proposed planning approach relies on the BEB worst-case energy consumption scenario. This worst-case energy consumption is the foundation for planning the transition from diesel-powered to on-route charging electric-powered transit systems, as detailed in Chapter 3. Notations introduced in Chapter 3 are utilized for consistency and clarity.

5.1.2.1 Preliminaries

Before introducing the mathematical model, we outline the following assumptions:

- A service refers to a trip along a route, either starting from the starting terminal and concluding at the ending terminal or vice versa.
- All fleet BEBs have specific schedules for their service times.
- Every BEB in the fleet departs from the depot at the start of the workday and returns to the depot after completing its assigned services.
- A transit route or line denotes the path BEBs take between terminals. Departure and return service paths are delineated separately with superscripts 1 (for departure) and 2 (for return), reflecting potential variations in distance travelled.
- The worst-case energy consumption (caused by weather conditions, HVAC on and driving habits) is α kWh per kilometre.

- All chargers utilized in on-route charging operations have identical power ratings.
- One BEB serves one activity block in the transit system and can charge at only one charging terminal.

The set $\mathbf{T} = \{\mathrm{t}_1^1, \mathrm{t}_2^1, \ldots, \mathrm{t}_{1|2}^{\mathrm{r}}\}$ represents all starting and ending routes' terminals in the transit system, where $\forall \mathrm{r} \in \mathbf{R}$. Subscripts one or two define the starting terminal or ending terminal. $\mathbf{L} = \{\mathrm{l}_1^1, \mathrm{l}_1^2, \mathrm{l}_2^1, \mathrm{l}_2^2 \ldots, \mathrm{l}_\mathrm{r}^1, \mathrm{l}_\mathrm{r}^2\}, \quad \forall \mathrm{r} \in \mathrm{R}$ be Set of all distances from the transit network routes' initial terminals to their ending terminals (superscript 1) or from the transit network routes' ending terminals to their initial terminals (superscript 2).

As stated, each BEB must complete a single activity block defined in the activity blocks set **BL**. Therefore, each BEB must have energy equal to the total energy requirement to perform the assigned activity block's services, as represented in Equation (5.1).

$$\mathbf{E^{bl}} = \{\mathrm{e_{bl_1}}, \mathrm{e_{bl_2}}, \ldots, \mathrm{e_{bl_n}}\}, \quad \forall \mathrm{bl_n} \in \mathbf{BL} \tag{5.1}$$

$$\mathrm{e_{bl_n}} = \mathrm{e^s_{s_i}} + \ldots + \mathrm{e^s_{s_j}}, \quad \forall \mathrm{e^s_{s_j}}, \ldots, \mathrm{e^s_{s_j}} \in \mathbf{E^s} \tag{5.2}$$

According to our assumption 5.1.2.1, each BEB performs one activity block. Therefore, the energy required by a BEB to perform the activity block equals the calculated energy for the assigned activity block.

$$\mathbf{E^b} = \{\mathrm{e_{b_1}}, \mathrm{e_{b_2}}, \ldots, \mathrm{e_{b_n}}\}, \quad \forall \mathrm{b_n} \in \mathbf{B} \tag{5.3}$$

$$\mathrm{e_{b_n}} = \mathrm{e_{bl_n}}, \quad \forall \mathrm{b_n} \in \mathbf{B}, \quad \forall \mathrm{bl_n} \in \mathbf{BL} \tag{5.4}$$

5.1.2.2 Opportunity Matrix

Each activity block consists of services related to various transit routes. Each route has starting and ending terminals defined in the set **T**. Therefore, a BEB assigned to perform the activity block will have stops at those terminals. These stops serve as opportunities for BEB charging as the BEB completes service in the activity block and prepares to start a new service defined within the activity block.

We define an opportunity matrix (**OM**) in which the rows represent the activity blocks in the set **BL**, and the columns represent all terminals defined in the set **T**. Each value in the matrix is a non-negative integer indicating how many daily stops the activity block has at the terminal, with zero indicating that the activity block has no stop.

$$\mathbf{OM} = \begin{bmatrix} o_{11} & o_{12} & \cdots & o_{1m} \\ o_{21} & o_{22} & \cdots & o_{2m} \\ \vdots & \vdots & \ddots & \vdots \\ o_{n1} & o_{n2} & \cdots & o_{nm} \end{bmatrix} \tag{5.5}$$

In this matrix, o_{ij} represents the number of daily stops at the terminal terminal j in the activityblock i.

5.1.2.3 On-Route Charging Planing

An algorithm is proposed to find the on-route charging terminals within the set $\mathbf{T}$, determine the number of chargers at each location, and specify which BEBs should be charged at each terminal to balance the charging load among the charging terminals. The algorithm consists of two main steps: identifying candidate terminals for on-route charging and determining which terminals should serve which BEBs.

- **Determining Charging Terminals:** We define the set of transit system terminals' service indexes, which indicate how many activity blocks have the terminal as a stop:

  $$\mathbf{SI} = \{\mathrm{si}_1, \mathrm{si}_2, \ldots, \mathrm{si}_\mathrm{t}\}, \quad \forall \mathrm{t} \in \mathbf{T} \tag{5.6}$$

  The terminal service index is given by:

  $$\mathrm{si}_\mathrm{t} = \sum_{i=1}^{n} o_{it}, \quad \text{where } i \text{ denotes the rows in the } \mathbf{OM} \text{ (5.5)} \tag{5.7}$$

  The approach starts by determining the minimum number of terminals as on-route charging terminals by Algorithm 7. It ensures the minimum infrastructure cost for on-route chargers accessible by all BEBs performing the transit system's activity blocks.

  Algorithm 7 (Determining Charging Terminal(s)): The algorithm takes as input the set of transit system terminals $\mathbf{T}$, the set of transit system terminals' service indexes $\mathbf{SI}$, transit system activity blocks set $\mathbf{BL}$, and the transit system $\mathbf{OM}$. The algorithm output is the set of terminals utilized for BEBs on-route charging:

  $$\mathbf{T_{ch}} = \{\mathrm{t}_1^{\mathrm{ch}}, \mathrm{t}_2^{\mathrm{ch}}, \ldots, \mathrm{t}_\mathrm{n}^{\mathrm{ch}}\}, \quad \text{where } n \leq |\mathbf{T}| \tag{5.8}$$

  From lines 1 to 13, the algorithm initially sorts the set of transit network terminals $\mathbf{T}$ and their corresponding service indexes $\mathbf{SI}$ based on service index values in descending order. From lines 14 to 25, the algorithm checks the accessibility of blocks to the terminal with the maximum index number, removes the blocks with access to the terminal, and adds the terminal to the set of charging terminals. It then checks the next terminal with the maximum index number until no more blocks are in the set **BL**.

Algorithm 7 Determining Charging Terminal(s)

Require: The set of transit system terminals (**T**), the set of transit system terminals' service indexes (**SI**), the set of transit system activity blocks (**BL**), the transit system opportunity matrix (**OM**)

Ensure: The set of the minimum number of terminals for on-route charging ($\mathbf{T_{ch}}$) that all activity blocks access them during their activities

```
T_ch ← {}
n ← |T|
sorted ← false
while not sorted do
    sorted ← true
    for i = 1 to n do
        if SI_i < SI_{i+1} then                          ▷ In descending order
            Swap SI_i and SI_{i+1}
            Swap T_i and T_{i+1}
            sorted ← false
        end if
    end for
end while
T_access ← {T}
j = 1
while BL ≠ {} do
    j = j + 1
    T_ch ← T_ch ∪ {T_access[j]}
    for i = 1 to m do
        if OM[i][j] ≠ 0 then                   ▷ block i has stop at the terminal j
            BL ← BL \ {BL[j]}
        end if
    end for
end while
```

- **Allocating Charging Terminals to the Activity blocks:** The charging terminals are identified to cover all activity blocks in the transit system. We must determine which charging terminal is responsible for charging each activity block. This determination consists of three steps: identifying activity blocks with access to only one charging terminal, identifying activity blocks with access to multiple charging terminals with different opportunity indexes, and assigning activity blocks with access to multiple charging terminals with equal opportunities using energy balancing. The first two steps are implemented by Algorithm 8, and the optimization approach achieves the third step.

Algorithm 8 (Charging Terminal(s) Allocations): From lines 1 to 4, the algorithm creates some empty sets to keep the grouped activity blocks assigned to the charging terminals in the set $\mathbf{T_{ch}}$.

From lines 8 to 16, the algorithm iterates through the terminals, checks the opportunity indexes, and keeps the indexes that are not zero for further assignment purposes.

Allocating charging terminals to activity blocks with access to only one charging terminal: In the first step, as shown in algorithm 8, Line 17 checks the opportunity index o_{ij} corresponding to each activity block(i) and all charging terminals in set $\mathbf{T_{ch}}$. If there is only one charging terminal with a non-zero opportunity index, lines 19-20, assign the activity block to that charging terminal with a non-zero opportunity index, and then the assigned activity block is removed from the set of activity blocks ($\mathbf{BL}$).

Allocating charging terminals to activity blocks with access to multiple charging terminals: In the second step, we identify the activity blocks with access to two or more terminals. From lines 22 to 29, the algorithm checks if the activity block has access to multiple charging terminals in $\mathbf{T_{ch}}$; if so, the block is assigned to the terminal with the maximum opportunity index, and then the assigned activity block is removed from the activity blocks set. This step has no activity block assignment if the maximum opportunity index occurs more than once. Such activity blocks are assigned in the third step using the energy-balancing method.

Allocating charging terminals to remaining activity blocks by energy balancing: The remaining activity blocks are assigned to the charging terminals to minimize the variance of energy provided by chargers, $\mathrm{E_t}$ is the amount of total provided energy by charging terminal (t):

$$\begin{aligned} &\text{Minimize} \quad \frac{1}{\mathrm{N}}\sum_{t=1}^{\mathrm{N}}(\mathrm{E_t^a}-\bar{\mathrm{E}})^2, \mathrm{N}=|\mathbf{T_{ch}}| \\ &\bar{\mathrm{E}}=\frac{1}{\mathrm{N}}\sum_{t=1}^{\mathrm{N}}\mathrm{E_t^a} \end{aligned} \tag{5.9}$$

The amount of energy that each charging terminal should provide to assigned blocks is given by:

$$\begin{aligned} &\mathrm{E_t^a}=\mathrm{e_{bl_m^a}}+\mathrm{e_{bl_n^a}}+\cdots+\mathrm{e_{bl_k^a}} \\ &\mathrm{t}\in\{1,2,\ldots,|\mathbf{T_{ch}}|\} \\ &\mathrm{bl_m},\mathrm{bl_n},\mathrm{bl_k}\in\mathbf{BL} \end{aligned} \tag{5.10}$$

Algorithm 8 Charging Terminal(s) Allocations

Require: The set of transit system's charging terminals $\mathbf{T_{ch}}$, transit system terminals' service indexes (**SI**), the set of transit system activity blocks **BL**, the set of transit system activity blocks worst-case energy consumption $\mathbf{E^{bl}}$, Opportunity Matrix (OM)
Ensure: the sets of activity blocks assigned to all charging terminals for on-route charging $\mathbf{T_{ch}}$

for $i \leftarrow 1$ to $|\mathbf{T_{ch}}|$ **do**
  $\mathbf{BL^a_i} \leftarrow \{\}$
end for
$\mathbf{Temp} \leftarrow \{\}$
$\mathbf{OMindex} \leftarrow \{\}$
for $i \leftarrow 1$ to $|\mathbf{BL}|$ **do** ▷ Loop through each row in OM
  $nonZeElInRow \leftarrow 0$
  for $j \leftarrow 1$ to $|\mathbf{T}|$ **do** ▷ Loop through each element in the row
    if $o[i][j] \neq 0$ **then** ▷ o[i][j] element row i and column j in matrix OM
      if T[j] in $\mathbf{T_{ch}}$ **then**
        $nonZeElInRow \leftarrow nonZeElInRow + 1$
        $\mathbf{Temp} \leftarrow \mathbf{Temp} \cup j$
        $\mathbf{OMindex} \leftarrow \mathbf{OMindex} \cup \mathrm{o[i][j]}$
      end if
    end if
  end for
  if $|\mathbf{Temp}| = 1$ **then**
    find index *index* in $\mathbf{T_{ch}}$ such that $\mathbf{T_{ch}}[index] = \mathbf{T}[Temp]$
    $\mathbf{BL^a_{index}} \leftarrow \mathbf{BL}[i]$
    $\mathbf{BL} \leftarrow \mathbf{BL} - \mathbf{BL}[i]$
  end if
  if $|\mathbf{Temp}| > 1$ **then**
    $i_{max} \leftarrow argmax(\mathbf{OMindex})$
    if Mode($\mathbf{OMindex}[i_{max}]$) > 1 **then**
      find index *index* in $\mathbf{T_{ch}}$ such that $\mathbf{T_{ch}}[index] = \mathbf{T}[i_{max}]$
      $\mathbf{BL^a_{index}} \leftarrow \mathbf{BL}[i]$
      $\mathbf{BL} \leftarrow \mathbf{BL} - \mathbf{BL}[i]$
    end if
  end if
end for

5.1.3 MODEL EVALUATION

We began by calculating the required energy for operating the activity blocks of the Thunder Bay transit system.

5.1.3.1 Energy Requirement Analysis

We considered a worst-case scenario where all BEBs within the Thunder Bay transit system consume 1.9 kWh per kilometer. Consequently, 17,612 kWh is required to fulfill all activity blocks throughout the working day. Figure 5.1 illustrates the worst-case daily energy requirements for the activity blocks.

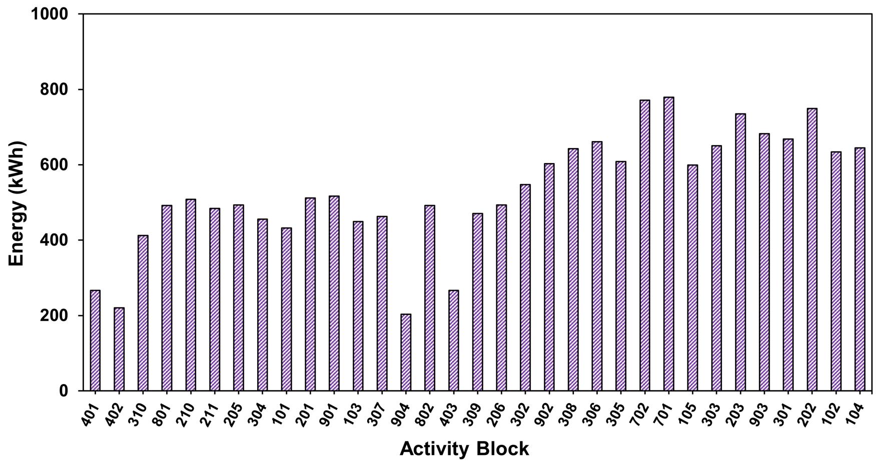

FIGURE 5.1: Thunder Bay transit system activity blocks worst-case energy requirements

5.1.3.2 Identifying Charging Terminals for Thunder Bay Transit System

The on-route charging terminals candidates for the Thunder Bay transit system are routes' starting and ending terminals. **OM** (see Equation 5.5) was then constructed. The Service Indexes for these terminals are calculated by summing the matrix elements column-wise in all columns representing the charging terminal candidates shown in Figure 5.2. As shown in Figure 5.2, the Waterfront terminal (1121) has the highest Service Index among all terminals, which is 28. Therefore, it should be the first choice for a charging terminal. However, some activity blocks do not stop at the Waterfront terminal (1121). In such cases, we must identify the charging terminal where those activity blocks have stops. This terminal should have the highest service index after the Waterfront Terminal (1121). According to Figure 5.2, two candidates after the Waterfront terminal, City Hall terminal (1019) and Confederation College terminal (1231), have the same Service Index of 23, the next highest index, following the Waterfront terminal Index. We selected the City Hall terminal because it has a higher correlation with the Waterfront terminal[1], This gives us greater flexibility in assigning activity blocks to charging terminals, thereby achieving more efficient energy balancing among the charging terminals.

5.1.3.3 Activity Blocks Assignment to Charging Terminals

Before assigning activity blocks to charge at the charging terminals, we remove the activity blocks 401, 402, 403, and 904 that need low energy. We expect BEBs can complete those

[1]They have more shared activity blocks that stop at both terminals.

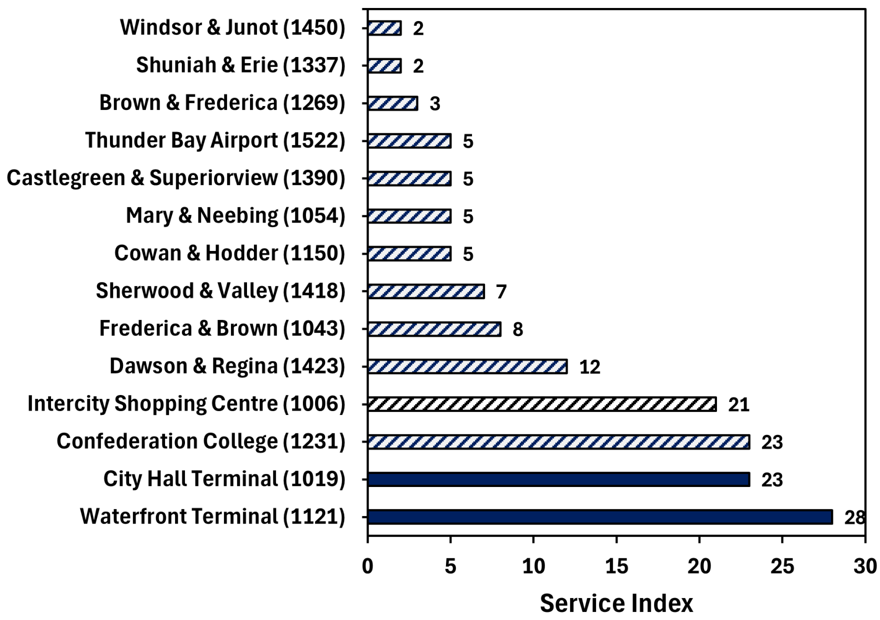

FIGURE 5.2: Thunder Bay transit system On-Route charging terminal candidates' Service Indexes

activity blocks with no need to charge along the way. The assignment of activity blocks to utilize charging terminals begins by assigning activity blocks with access to only one of the charging terminals. The results are displayed in Table 5.1. In the second step, we

TABLE 5.1: First Step of Activity Blocks Assignments to the Charging Terminals

Terminal	Activity Blocks
Waterfront Terminal (1121)	210, 211, 201, 702, 701, 203, 202
City Hall Terminal (1019)	205, 206

investigated the activity blocks with access to multiple charging terminals to determine how many stops they have in each terminal (see Figure 5.3). Then, we assigned blocks to terminals with more stops, giving them more opportunities to receive charges. As shown in Figure 5.3, activity blocks 801, 802, 901, 306, and 308 have more stops at the City Hall terminal; therefore, their charging is assigned to the City Hall terminal, while activity blocks 902 and 903 have more stops at the Waterfront terminal, so their charging is assigned to the Waterfront terminal.

TABLE 5.2: Second Step of Activity Blocks Assignments to the Charging Terminals

Terminal	Activity Block(s)
Waterfront Terminal (1121)	210, 211, 201, 702, 701, 203, 202, 902, 903
City Hall Terminal (1019)	205, 206, 801, 802, 901, 306, 308

In the third step, we assign the remaining activity blocks considering energy balancing as defined in Equation 5.9. To solve this optimization problem, we utilized the 'minimize'

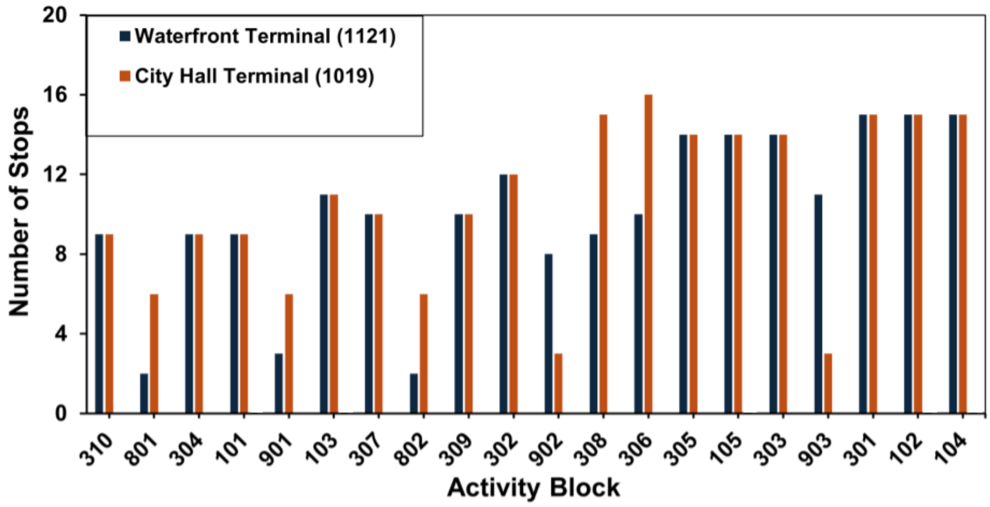

FIGURE 5.3: The number of stops activity blocks with access to Waterfront and City Hall terminals

function from the 'scipy.optimize' package in Python. We experimented with various solver methods, including SLSQP, L-BFGS-B, Nelder-Mead, Powell, TNC, and Trust-constr. Among these, the Powell method yielded the best results. According to the optimized results shown in Table 5.3, activity blocks 101, 301, 302, 303, 304, 305, 307, 309, and 310 are assigned to the City Hall terminal for charging, whereas activity blocks 102, 103, 104, and 105 are assigned to the Waterfront terminal for charging.

TABLE 5.3: Third Step of Activity Blocks Assignments to the Charging Terminals

Terminal	Activity Block(s)
Waterfront Terminal (1121)	210, 211, 201, 702, 701, 203, 202, 902, 903, 102, 103, 104, 105
City Hall Terminal (1019)	205, 206, 801, 802, 901, 306, 308, 101, 301, 302, 303, 304, 305, 307, 309, 310

5.2 Activity Blocks Tuning

This section introduces a systematic approach to optimize and adjust the transit system's timetable. The goal is to maximize opportunities for BEBs to meet their energy needs through on-route charging during working hours while ensuring that the travel demands of the transit system are fully addressed and not adversely affected. Adjusting an existing timetable instead of designing a new one from scratch offers several advantages. It ensures minimal disruption to passengers' routines, avoiding confusion and inconvenience. Additionally, this approach is more straightforward and quicker to implement than a complete overhaul, allowing for a smoother transition. Moreover, adjusting an existing timetable is less expensive than creating a new one from scratch, requiring fewer resources for planning and implementation. Minimal adjustments also mean that staff need less retraining than learning an entirely new schedule.

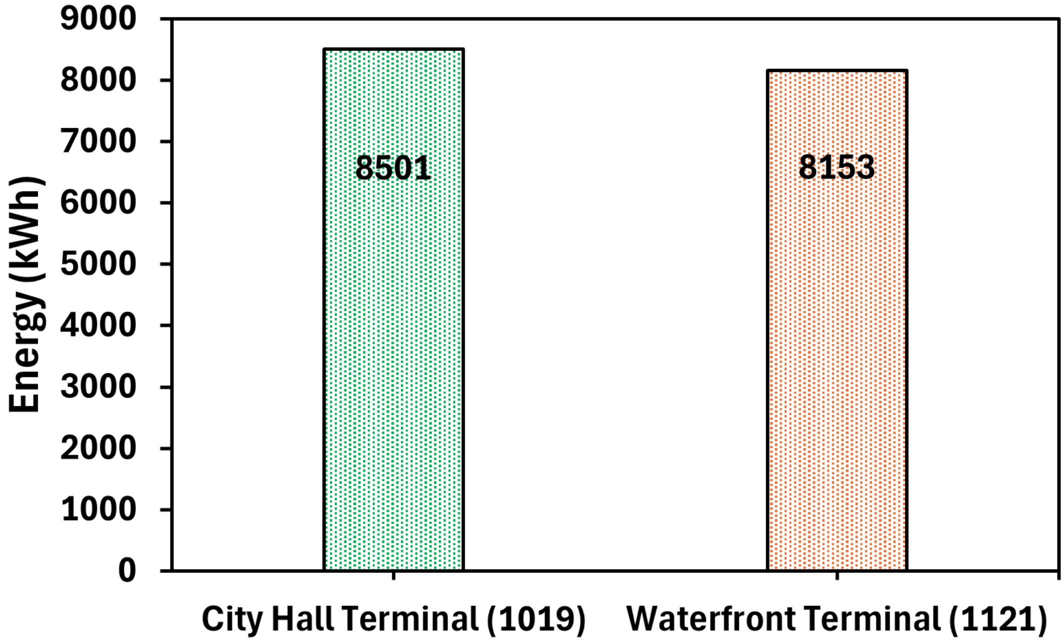

FIGURE 5.4: Balanced energy provided by charging terminals to charge BEBs

This adaptive approach can optimize the use of existing charging infrastructure without requiring additional investments. Changes can be made incrementally based on real-world data and feedback, allowing for gradual and sustainable optimization. Moreover, adjustments are grounded in historical data and operational insights, ensuring they are informed by actual performance rather than hypothetical scenarios. Because the existing timetable has been tested and validated, adjusting tends to yield more predictable and manageable outcomes than designing a completely new timetable. This predictability can help transit agencies implement changes with greater confidence and efficiency.

Minor adjustments to an existing timetable typically require less regulatory approval than creating an entirely new schedule, saving time and administrative effort for transit authorities. Furthermore, adjusting a timetable tends to be more acceptable to stakeholders, including passengers, employees, and funding agencies, fostering support and cooperation within the transit system. This scalability enables transit systems to adapt dynamically to changing conditions and demands as they integrate electric buses, making adjustments a practical, cost-effective, and less disruptive method to improve on-route BEB charging opportunities. It uses existing infrastructure and data while maintaining continuity, making it a more feasible and sustainable strategy for transit agencies.

Effective on-route charging is crucial to maximize the utility and efficiency of BEBs. One promising approach to enhance on-route charging opportunities is through the temporal dispersion of BEBs schedules. By tuning the departure and arrival times of buses, it is possible to optimize the availability and utilization of charging infrastructure, extending the operational range of BEBs and minimizing service disruptions. This study explores the potential of temporal dispersion in inherited transit system timetables to maximize on-route BEB charging opportunities. We examine how adjusting the timing of BEBs operations can alleviate the pressure on charging stations and ensure a more consistent and efficient use of charging resources. Our research aims to provide actionable insights for transit agencies seeking to enhance the sustainability and reliability of their BEB fleets.

In the proposed model, we assumed that the charging terminals are defined (5.8), the activity block allocations to the charging terminals are specified (5.11), and they are fixed, which means all BEBs performing transit activity blocks always charge at specific charging terminals. We define the set of charging terminals.

$$\mathbf{BL_i^{ch}} = \{\mathrm{bl_1}, \mathrm{bl_2}, \ldots, \mathrm{bl_n}\}, \quad \forall \mathrm{bl_n} \in \mathbf{BL} \quad \mathrm{i} \in \mathbf{T_{ch}}, \text{where } n \leq |\mathbf{BL}| \tag{5.11}$$

Considering the diesel-fueled transit system's timetable and activity blocks, the BEBs are supposed to stop at the allocated charging terminal at certain times, defined in a set which is given by equation (5.12) and depicted in Figure 5.5.

$$\mathbf{ST_{ch_i}^{bl_j}} = \{\mathrm{st_{ch_{i1}}^{bl_j}}, \mathrm{st_{ch_{i2}}^{bl_j}}, \ldots, \mathrm{st_{ch_{is}}^{bl_j}}\}, \text{where (s) is the total number of activity block j daily stop times at charging terminal i} \tag{5.12}$$

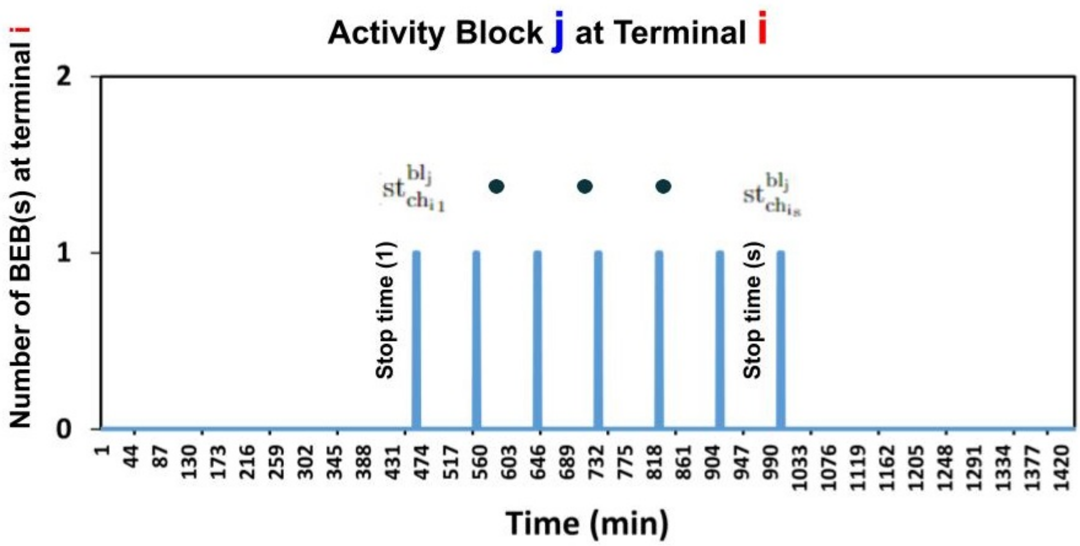

FIGURE 5.5: Activity block (j) stop times at charging terminal (i)

Then, we define a set which includes all activity blocks' daily stop times at allocated charging terminals which is given by equation (5.13) and depicted in Figure 5.6.

$$\mathbf{ST_{ch_i}} = \{\mathrm{st_{ch_{i1}}}, \mathrm{st_{ch_{i2}}}, \ldots, \mathrm{st_{ch_{ia}}}\}, \text{where (a) is the total number of all activity blocks stop times at charging terminal i} \tag{5.13}$$

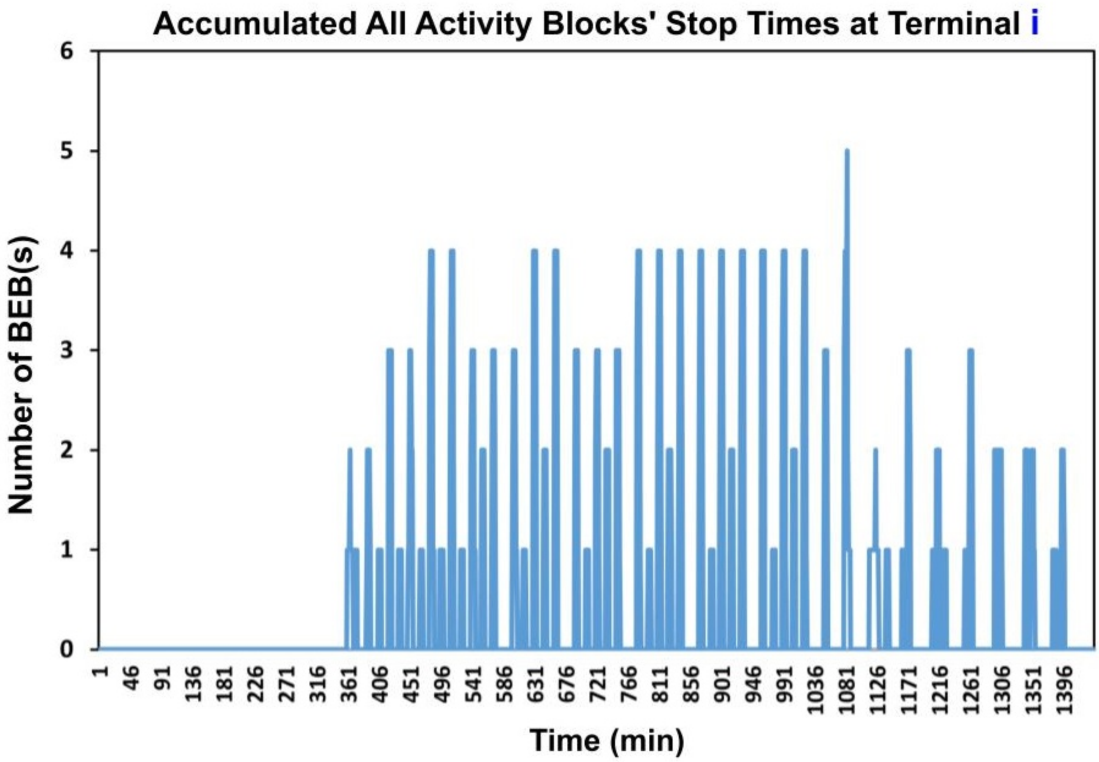

FIGURE 5.6: All activity blocks' stop times (accumulated) at charging terminal (i)

5.2.1 Activity Block Sinusoidal Model

The activity block stop times at the charging terminal have fixed time intervals 5.18. Therefore, we can represent the stop times with a sinusoidal function (5.17) with a specific frequency, phase shift, and activity starting and ending times, depicted in Figure 5.7. Each block $\mathrm{bl_n}$ in **BL** comprises the daily services assigned to one BEB. The BEBs' departure times from and arrival times to the transit network depot are presented by $\mathbf{T^d} = \{\mathrm{t^d_{bl_1}}, \mathrm{t^d_{bl_2}}, \ldots, \mathrm{t^d_{bl_n}}\}$ and $\mathbf{T^a} = \{\mathrm{t^a_{bl_1}}, \mathrm{t^a_{bl_2}}, \ldots, \mathrm{t^a_{bl_n}}\}$ respectively. Thus, Equation (5.16) gives the phase of representing sinusoidal function.

$$\mathrm{TI^{bl_j}_{ch_i}} = \left|\mathrm{st^{bl_j}_{ch_{i2}}} - \mathrm{st^{bl_j}_{ch_{i1}}}\right| = \left|\mathrm{st^{bl_j}_{ch_{i3}}} - \mathrm{st^{bl_j}_{ch_{i2}}}\right| \tag{5.14}$$

$$\mathrm{f^{bl_j}_{ch_i}} = \frac{2\pi}{\mathrm{TI^{bl_j}_{ch_i}}} \tag{5.15}$$

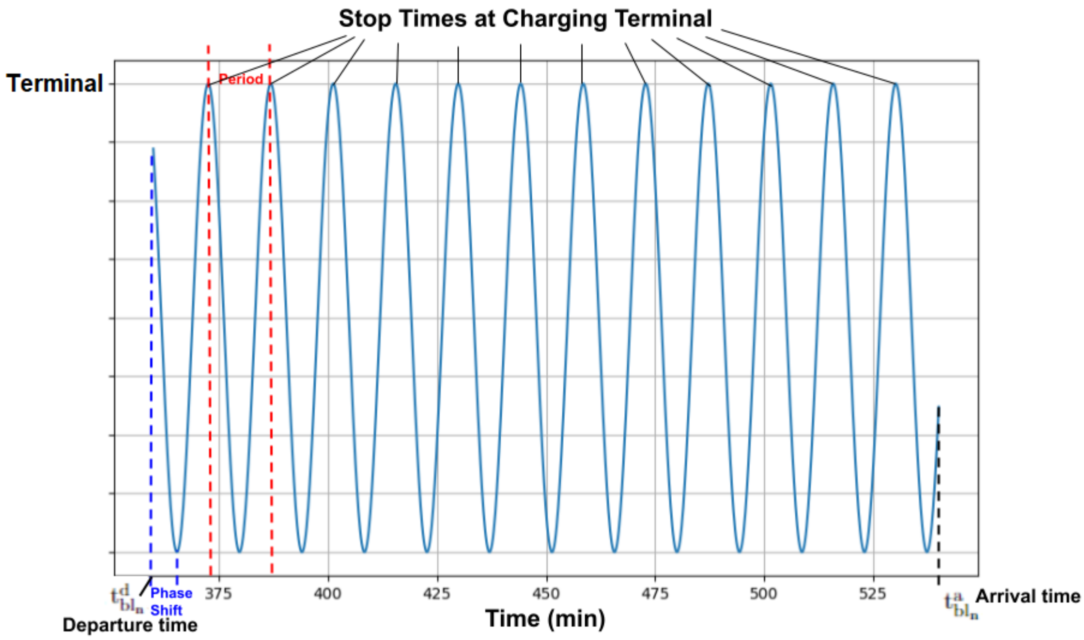

FIGURE 5.7: A sinusoidal-modelled activity block

$$\varphi_{\mathrm{ch_i}}^{\mathrm{bl_j}} = \frac{\pi}{2} - \frac{2 \cdot \pi \cdot \mathrm{t}_{\mathrm{bl_j}}^{\mathrm{d}}}{\mathrm{TI}_{\mathrm{ch_i}}^{\mathrm{bl_j}}} \tag{5.16}$$

$$\mathrm{bl_j(t)} = \mathrm{A}(\sin\left(2\pi \mathrm{f}_{\mathrm{ch_i}}^{\mathrm{bl_j}} \mathrm{t} + \varphi_{\mathrm{ch_i}}^{\mathrm{bl_j}}\right) + 1) \text{ ,Where A is the maximum distance (km) - distance to charging terminal} \tag{5.17}$$

5.2.2 Optimization Model

We charge the activity blocks' BEBs at the stop times (sinusoidal maxima). These stop times are BEBs' opportunity to charge at the charging terminal. Therefore, to maximize these opportunities, we should ensure that the activity blocks' stop times are dispersed along the time axis, minimizing stop times synchronicities without changing the service frequency related to travel demand and the transit system response. As we modelled the activity blocks' timing and distance for charging terminals, we can determine the optimal values of sinusoidal phase shifts while keeping the frequency unchanged. This approach will enable us to achieve the best charging opportunities with minimal overlap by tuning the timetable without altering service frequencies. For instance, Figure 5.8 illustrates the synchronicity between two activity blocks, while Figure 5.9 demonstrates the process of shifting phases to eliminate this synchronicity. We must mathematically define the objective and constraints to formulate an optimization problem for sinusoidal phase shifts such that their maxima are evenly distributed along the time axis.

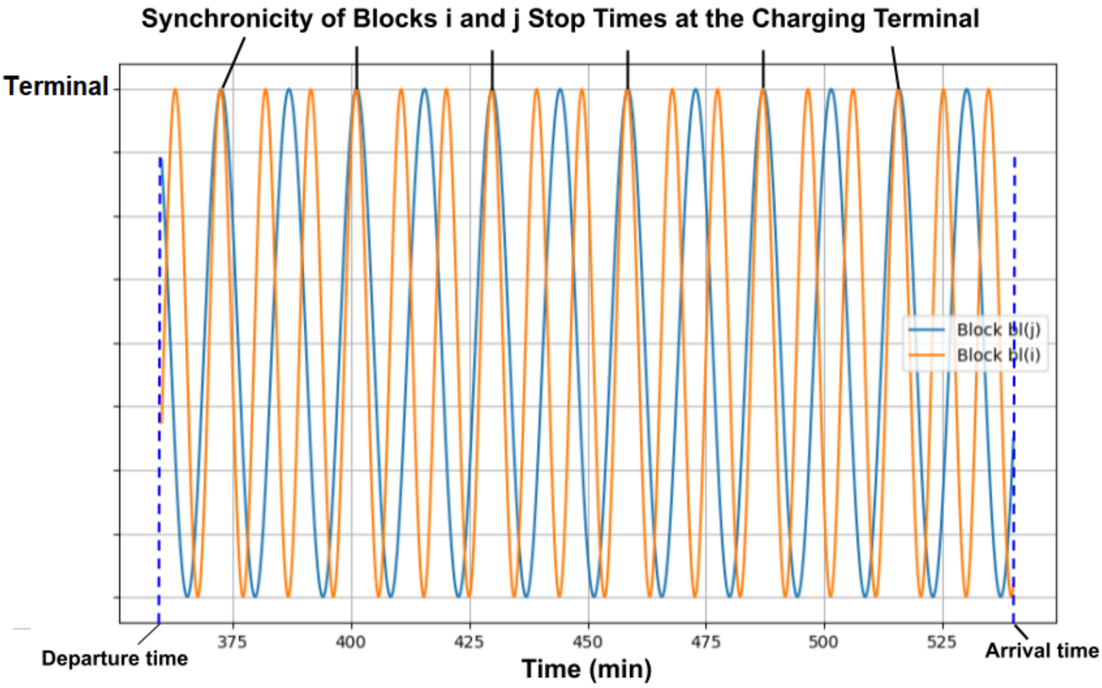

FIGURE 5.8: Synchronicity of activity blocks i and j stop times at the charging terminal

Let's assume we have n sinusoidal functions in the activity blocks set belonging to the specific charging terminal (5.11) given by (5.17).

The objective is optimizing the phase shifts $\varphi_{\mathrm{ch_i}}^{\mathrm{bl_j}}$ such that the maximum points of these functions are evenly distributed along the specified time interval (working hours) $[T_1, T_2]$ on the time axis.

Determining the Number of Maxima: The number of maxima for each function $\mathrm{bl_j}(t)$ within the interval $[T_1, T_2]$ is given by:

$$T = |T_2 - T_1| \tag{5.18}$$

$$m_j = \left\lfloor \frac{T \cdot f_{\mathrm{ch_i}}^{\mathrm{bl_j}}}{2\pi} \right\rfloor \tag{5.19}$$

The maxima of $\mathrm{bl_j}(t)$ occur at:

$$t_{j,k} = \frac{\frac{\pi}{2} + 2k\pi - \varphi_{\mathrm{ch_i}}^{\mathrm{bl_j}}}{2\pi f_{\mathrm{ch_i}}^{\mathrm{bl_j}}}, \quad k \in \{0, 1, \ldots, m_j - 1\} \tag{5.20}$$

Objective Function: Minimize the total deviation of the time instances $t_{j,k}$ from evenly spaced intervals within the specified interval $[T_1, T_2]$.

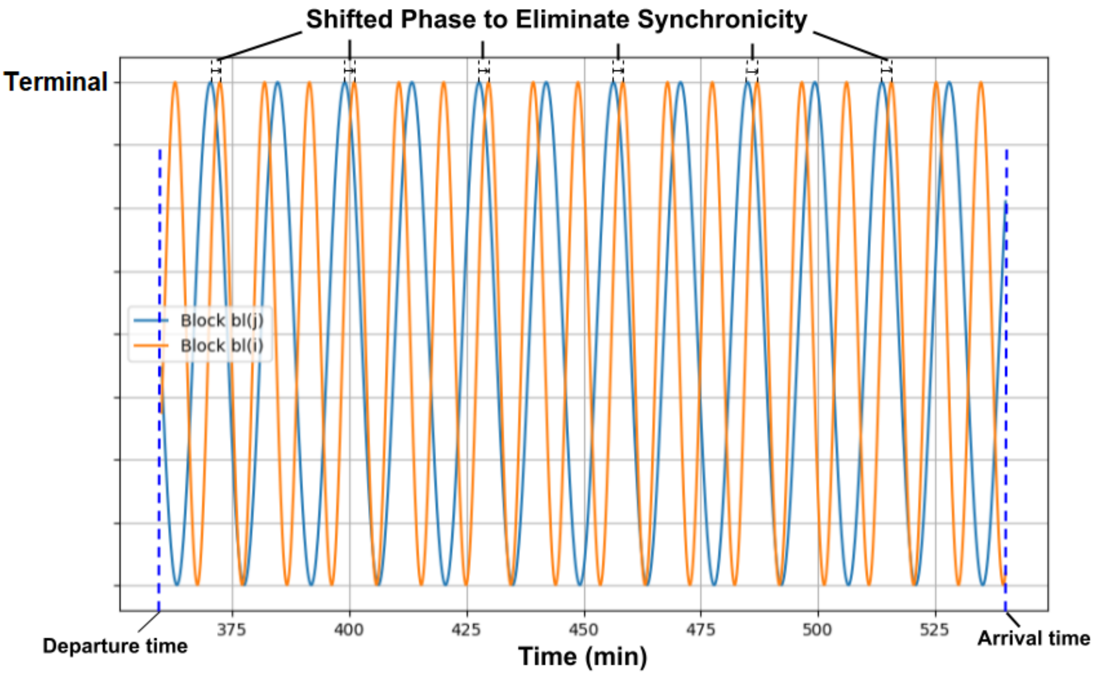

FIGURE 5.9: Phase shifting to eliminate the synchronicity of stop times

The objective function is formulated as:

$$\text{Minimize} \sum_{j=0}^{M-1} \left| t_j - \left(j \frac{T}{M} \right) \right| \tag{5.21}$$

where M is the total number of maxima from all functions:

$$M = \sum_{i=1}^{n} m_i \tag{5.22}$$

and t_j are the sorted maxima of all functions.

The optimization problem is formulated as follows:

$$
\begin{aligned}
&\text{Minimize} \quad \sum_{j=0}^{M-1} \left| t_j - \left(j\frac{T}{M} \right) \right| \\
&\text{Minimize} \quad \sum_{j=0}^{M-1} \left| \frac{\frac{\pi}{2} + 2k\pi - \varphi_{ch_i}^{bl_j}}{2\pi f_{ch_i}^{bl_j}} - \left(j\frac{T}{M} \right) \right| \\
&\text{subject to} \\
&t_{j,k} = \frac{\frac{\pi}{2} + 2k\pi - \varphi_{ch_i}^{bl_j}}{2\pi f_{ch_i}^{bl_j}}, \quad k \in \{0, 1, \ldots, m_j - 1\} \\
&\quad \varphi_{ch_i}^{bl_j} \in [0, 2\pi], \quad i = 1, 2, \ldots, n
\end{aligned}
\tag{5.23}
$$

This formulation aims to find the phase shifts $\varphi_{ch_i}^{bl_j}$ that minimize the deviation of the maxima positions from their expected evenly spaced positions within the interval $[T_1, T_2]$.

5.2.3 Optimization Model Transformation

The type of optimization described in Equation (5.23) is a constrained nonlinear optimization problem. It involves minimizing an objective function subject to constraints on the variables. The objective function aims to reduce the deviation of the maxima positions from evenly spaced intervals, and the constraints ensure that the phase shifts $\varphi_{ch_i}^{bl_j}$ are within the range $[0, 2\pi]$. In this section, we aim to transform the optimization problem defined in Equation (5.23) to a more straightforward optimization problem to solve.

Activity blocks' timing and distance for charging at terminals are modelled as sinusoidal functions, as shown in Equation (5.17). We aim to simplify the optimization problem in two steps: first, by reducing the time interval without affecting the final result, and second, by redefining the objective function.

Reducing the interval: The original optimization problem, as defined in Equation 5.23, aims to find the activity blocks phase shifts to evenly distribute the sinusoidal maxima within the working interval (T), which is specified in Equation 5.18. Despite numerical techniques being employed to solve the defined objective function, reducing the interval can decrease the required time and resources to solve the problem. Since the block activities have fixed frequencies over the working time, their maximum points' relative positions to each other follow a repetitive pattern. The repetition frequency is the least common multiple (LCM) of the activity block frequencies. Therefore, if we solve the optimization problem for a period of LCM frequency, the result for the remaining total time interval replicates the achieved result in a period of LCM frequency. Let F_{LCM} be the LCM of the activity block frequencies $\{f_{ch_i}^{bl_1}, \ldots, f_{ch_i}^{bl_n}\}$. The new optimization period is given by:

$$\begin{aligned} F_{LCM} &= LCM(f_{ch_i}^{bl_1}, \ldots, f_{ch_i}^{bl_n}) \\ T_{LCM} &= \frac{1}{F_{LCM}} \end{aligned} \tag{5.24}$$

M_{LCM} is the total number of maxima from all functions within time interval T_{LCM} :

$$M_{LCM} = \sum_{i=1}^{n} m_i^{LCM} \tag{5.25}$$

The updated definition of the optimization problem is as follows:

$$\begin{aligned} &\text{Minimize} \quad \sum_{j=0}^{M_{LCM}-1} \left| \frac{\frac{\pi}{2} + 2k\pi - \varphi_{ch_i}^{bl_j}}{2\pi f_{ch_i}^{bl_j}} - \left(j \frac{T_{LCM}}{M_{LCM}} \right) \right| \\ &\text{subject to} \\ &t_{j,k} = \frac{\frac{\pi}{2} + 2k\pi - \varphi_{ch_i}^{bl_j}}{2\pi f_{ch_i}^{bl_j}}, \quad k \in \{0, 1, \ldots, m_j - 1\} \\ &\quad \varphi_{ch_i}^{bl_j} \in [0, 2\pi], \quad i = 1, 2, \ldots, n \end{aligned} \tag{5.26}$$

Figure 5.10 depicts the new time interval and its replicas along the total time interval.

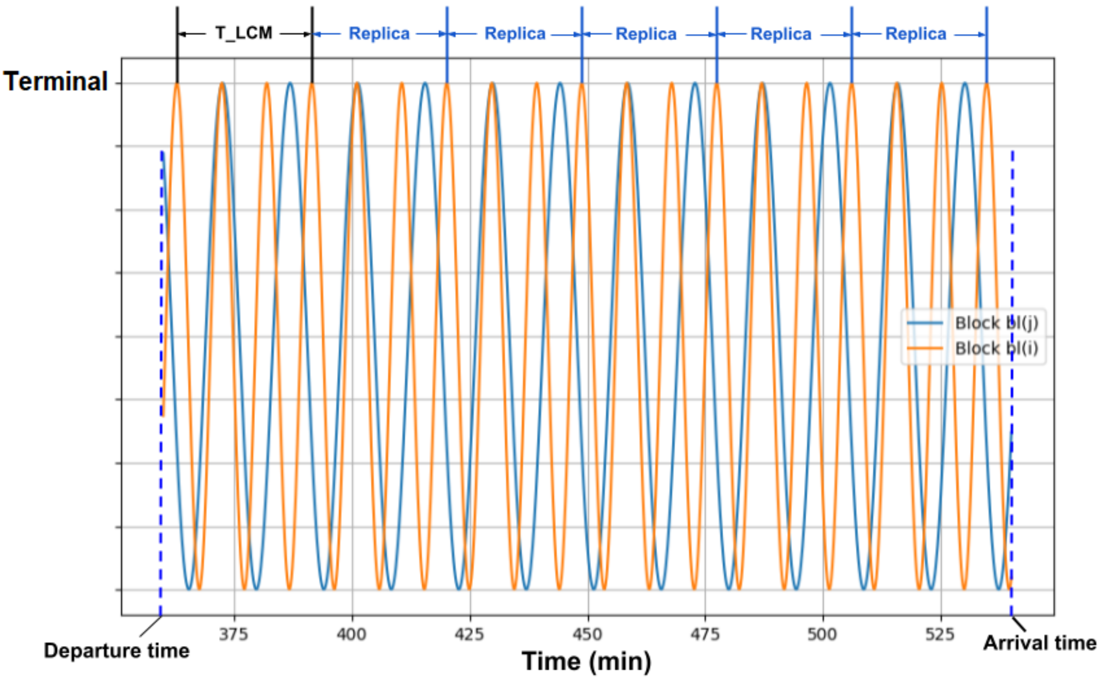

FIGURE 5.10: The new time interval and its replicas along the total time interval

Redefining the objective function: To redefine a more straightforward objective function, we utilize that evenly distributing the maxima along the time axis minimizes overlapping sinusoidal functions and maximizes the area under the maximum function of the sinusoidal functions. To mathematically prove that evenly distributing the maximum points of the sinusoidal functions by phase shifting leads to an increased area under the resulting maximum function, we analyze the overlap and distribution of the maxima.

Let us consider n sinusoidal functions given by:

$$\mathrm{f_i(t) = A_i \sin(\omega_i t + \phi_i), \quad i = 1, 2, \ldots, n} \tag{5.27}$$

where $\mathrm{A_i}$ is the amplitude, ω_i is the angular frequency, and ϕ_i is the phase shift of the i-th sinusoidal function.

The resulting maximum function is defined as:

$$\mathrm{M(t) = \max_i \{f_i(t)\}} \tag{5.28}$$

The area under M(t) over a period T is given by:

$$\mathrm{Area(M) = \int_0^T M(t)\, dt} \tag{5.29}$$

When the maxima of the functions $\mathrm{f_i(t)}$ are not evenly distributed, there are intervals where multiple functions contribute to M(t), causing more overlaps and leading to a lower overall value of M(t).

If the maxima are evenly distributed, the contributions to M(t) are spread out, minimizing the overlaps. This results in more intervals where a single function dominates, increasing the values of M(t).

Each sinusoidal function $\mathrm{f_i(t)}$ has a period $\mathrm{T_i} = \frac{2\pi}{\omega_\mathrm{i}}$. If we align the maxima of these functions such that they are evenly distributed within a common period T (e.g., the least common multiple of the individual periods), we can write:

$$\phi_\mathrm{i} = \frac{2\mathrm{k}\pi}{\mathrm{n}}, \quad \mathrm{k = 0, 1, \ldots, n-1} \tag{5.30}$$

where k is adjusted to distribute the maxima evenly.

The maximum function M(t) will have contributions from different functions at different intervals, leading to:

$$\mathrm{M(t) = \max_i \{A_i \sin(\omega_i t + \phi_i)\}} \tag{5.31}$$

We aim to show:

$$\int_0^T \mathrm{M}(t)\, dt \tag{5.32}$$

is maximized when the maxima are evenly distributed. By symmetry and periodicity:

$$\int_0^T \max_i \{A_i \sin(\omega_i t + \phi_i)\}\, dt \tag{5.33}$$

is maximized due to less overlap and more continuous contributions from individual functions. For overlapping regions where multiple $f_i(t)$ contribute similarly, the integral value is lower than for non-overlapping regions:

$$\int_a^b \max\{f_i(t), f_j(t)\}\, dt < \int_a^b f_i(t)\, dt + \int_a^b f_j(t)\, dt \tag{5.34}$$

Evenly distributing the maxima ensures minimal overlap, thus:

$$\mathrm{Area}(\mathrm{M}) = \int_0^T \mathrm{M}(t)\, dt \tag{5.35}$$

is maximized due to optimal phase shifts. By aligning phase shifts to evenly distribute the maxima of $f_i(t)$, the area under $\mathrm{M}(t)$ increases. This is because the overlap between different sinusoidal functions is minimized, and the intervals where individual functions dominate are maximized.

Figures 5.11 (a), 5.11 (b), and 5.11 (c) depict three sets of phase shifts ($\pi/4 \leftarrow \pi/8$), ($\pi/2 \leftarrow \pi/8$), and ($\pi \leftarrow \pi/8$) for two sinusoidal functions, along with their constructed maximum functions and the area under the absolute difference of their maximum functions. It is clear that evenly distributing the maximum points of the sinusoidal functions by phase shifting leads to an increased area under the resulting maximum function.

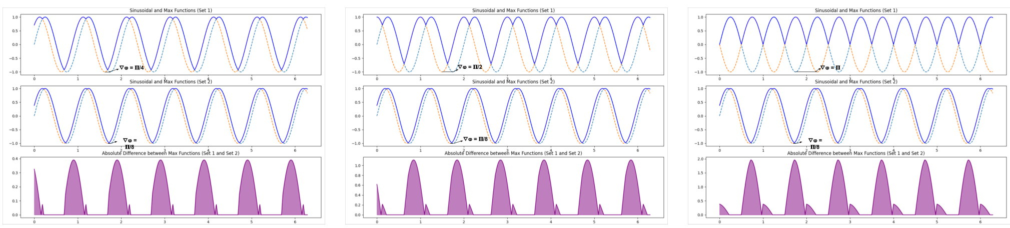

(a) Phase shift $\pi/4 \leftarrow \pi/8$ (b) Phase shift $\pi/2 \leftarrow \pi/8$ (c) Phase shift $\pi \leftarrow \pi/8$

FIGURE 5.11: Three phase shifts maximum, functions and the area under the maximum functions

Considering the fact of evenly distributing the sinusoidal functions and the area under the constructed maximum function from them, We define a new function that, for each point on the time axis, selects the maximum value among the sinusoidal functions as the function value. the new function $M_i(t)$ that selects the maximum value among these activity blocks sinusoidal functions in Equation (5.17) at time t is defined as:

$$M_i(t) = \max\{bl_1(t), bl_2(t), \ldots, bl_n(t)\} \quad \forall bl_n(t) \in \mathbf{BL_i^{ch}} \tag{5.36}$$

For a visual representation, Figure 5.8 illustrates the new function constructed from two activity blocks in Figure 5.12.

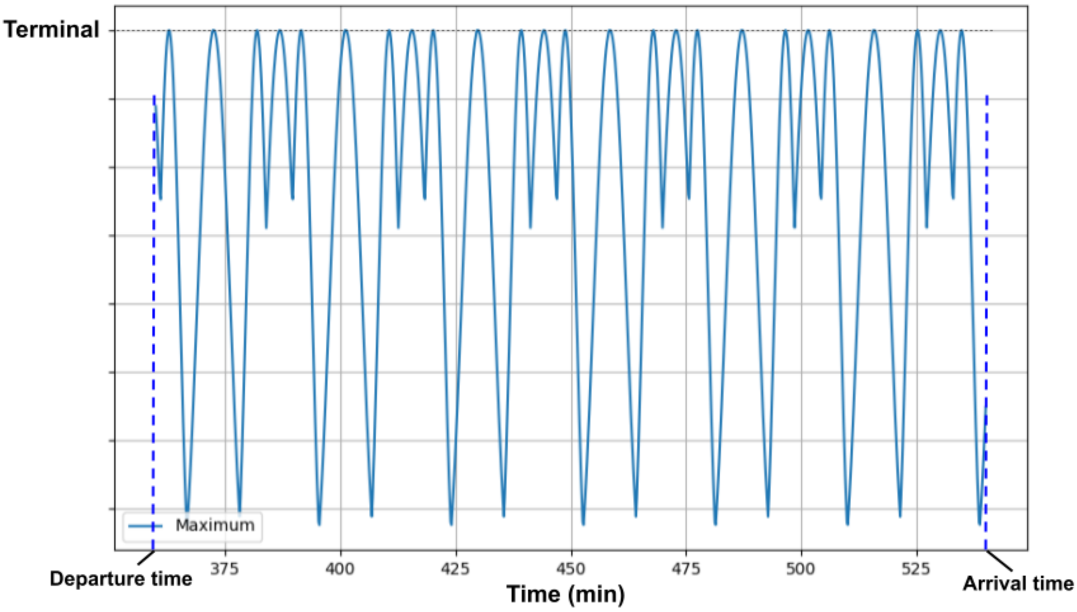

FIGURE 5.12: Illustration of the constructed maximum function from two activity blocks

Therefore, the optimization problem redefinition to find the optimal phase shifts aims to maximize the area under the $M_i(t)$ is given by:

$$\begin{aligned}
&\text{Maximize Area}(M) = \text{Maximize} \int_0^{T_{LCM}} M(t)\,dt \\
&\text{subject to} \\
&t_{j,k} = \frac{\frac{\pi}{2} + 2k\pi - \varphi_{ch_i}^{bl_j}}{2\pi f_{ch_i}^{bl_j}}, \quad k \in \{0, 1, \ldots, m_{LCM_j} - 1\} \\
&\quad \varphi_{ch_i}^{bl_j} \in [0, 2\pi], \quad i = 1, 2, \ldots, n
\end{aligned} \tag{5.37}$$

As a result we have optimized phase shifts ${\varphi_{\mathrm{ch_i}}^{\mathrm{bl_j}}}^*$ in Equation (5.38) and the maximum area A^* in Equation (5.39).

$$ {\varphi_{\mathrm{ch_i}}^{\mathrm{bl_j}}}^* = \arg\max_{\varphi_{\mathrm{ch_i}}^{\mathrm{bl_j}}} \left(\int_0^{\frac{1}{\mathrm{F_{LCM}}}} \max_{\mathrm{i}} \left(\sin\left(2\pi \mathrm{f}_{\mathrm{ch_i}}^{\mathrm{bl_j}} \mathrm{t} + \varphi_{\mathrm{ch_i}}^{\mathrm{bl_j}} \right) \right) \mathrm{dt} \right) \quad \forall \mathrm{bl_j} \in \mathbf{BL} \tag{5.38} $$

$$ \mathrm{A}^* = \int_0^{\frac{1}{\mathrm{F_{LCM}}}} \max_{\mathrm{i}} \left(\sin\left(2\pi \mathrm{f}_{\mathrm{ch_i}}^{\mathrm{bl_j}} + {\varphi_{\mathrm{ch_i}}^{\mathrm{bl_j}}}^* \right) \right) \mathrm{dt} \quad \forall \mathrm{bl_j} \in \mathbf{BL} \tag{5.39} $$

At the end we calculate the new activity blocks timetable with respect to optimized phase shifts given by:

$$ \mathrm{t_{j,k}} = \frac{\frac{\pi}{2} + 2\mathrm{k}\pi - {\varphi_{\mathrm{ch_i}}^{\mathrm{bl_j}}}^*}{2\pi \mathrm{f}_{\mathrm{ch_i}}^{\mathrm{bl_j}}}, \quad \text{Where} \quad \mathrm{t_{j,k}} \in \mathrm{T} \tag{5.40} $$

5.2.4 Optimization Solver Methods

According to Equation (5.37), the functions are sinusoidal, involve constraints, and have some variables (activity blocks' sinusoidal modells phase shifts). Therefore, we need an optimization solver that can effectively handle both the smooth nature of sinusoidal functions and the constraints. Gradient-based methods are generally efficient for smooth and differentiable functions, and there are several solvers that can handle constraints. These are brief descriptions of the solver methods utilized in this thesis.

- Nelder-Mead: The Nelder-Mead method, also known as the simplex method, is a widely-used heuristic optimization technique for nonlinear optimization problems without derivative information. Introduced by John Nelder and Roger Mead in 1965, this method is particularly effective for minimizing or maximizing a function in a multidimensional space [50]. The algorithm operates by constructing a simplex—a geometric figure consisting of n+1 vertices for an n-dimensional problem—and improving the simplex to converge toward the best solution. Its robustness and simplicity make it a valuable tool for solving real-world optimization problems where the objective function may be noisy or discontinuous. According to "Numerical Recipes: The Art of Scientific Computing", the Nelder-Mead method remains a fundamental algorithm in numerical optimization due to its ease of implementation and ability to handle complex, multimodal landscapes [54]. Despite its heuristic nature, the Nelder-Mead method has demonstrated remarkable efficacy in various applications, including engineering design, economics, and machine learning.

- BFGS (Broyden-Fletcher-Goldfarb-Shanno): The BFGS algorithm is a popular iterative method for solving unconstrained nonlinear optimization problems. The BFGS algorithm belongs to the family of quasi-Newton methods, designed to approximate the Newton-Raphson method but with improved computational efficiency by avoiding the direct computation of the Hessian matrix. Instead, BFGS updates an estimate of the Hessian matrix using gradient information from successive iterations [8].

  In the BFGS method, at each iteration k, an update to the position vector $\mathrm{x_k}$ is calculated using:

  $$\mathrm{x_{k+1} = x_k - \alpha_k H_k^{-1} \nabla f(x_k)} \tag{5.41}$$

  where α_k is the step size determined by a line search, $\mathrm{H_k}$ is the current approximation to the Hessian matrix, and $\nabla\mathrm{f(x_k)}$ is the gradient of the objective function at $\mathrm{x_k}$.

  The Hessian approximation $\mathrm{H_k}$ is updated using:

  $$\mathrm{H_{k+1} = H_k + \frac{y_k y_k^T}{y_k^T s_k} - \frac{H_k s_k s_k^T H_k}{s_k^T H_k s_k}} \tag{5.42}$$

  where $\mathrm{s_k = x_{k+1} - x_k}$ and $\mathrm{y_k = \nabla f(x_{k+1}) - \nabla f(x_k)}$.

  This method balances Newton's method's fast convergence rates and the simplicity of gradient descent.

- TNC (Truncated Newton): The TNC method is a popular iterative optimization algorithm for solving unconstrained nonlinear optimization problems. It combines the efficiency of Newton's method in determining search directions with a trust-region approach to manage step sizes and ensure convergence. The TNC is particularly effective in scenarios where the Hessian matrix of second derivatives may be expensive or impractical to compute directly. The algorithm approximates the Hessian matrix using limited-memory techniques and adjusts step sizes dynamically based on the objective function's curvature and gradients. The steps of the TNC method can be summarized as follows [49]:

1. Compute gradient and approximate Hessian:

   $\nabla \mathrm{f}(\mathrm{x_k})$ (gradient at current iterate $\mathrm{x_k}$)

   $B_k \approx \nabla^2 f(x_k)$ (approximate Hessian)

2. Solve the trust-region subproblem:

   $\min_{\mathrm{p}} \mathrm{f}(\mathrm{x_k} + \mathrm{p}) \quad \text{subject to} \quad \|\mathrm{p}\|_{\mathrm{B}} \leq \Delta_{\mathrm{k}}$

   where $\|\mathrm{p}\|_{\mathrm{B}} = \sqrt{\mathrm{p}^\top \mathrm{B_k} \mathrm{p}}$ (trust-region radius Δ_{k})

3. Update parameters:

   $\mathrm{x_{k+1}} = \mathrm{x_k} + \mathrm{p_k}$

   Adjust the parameters based on the step $\mathrm{p_k}$ taken.

4. Convergence check:

   Check for convergence based on predefined criteria.

- COBYLA (Constrained Optimization BY Linear Approximations): COBYLA is a widely used derivative-free optimization method for solving nonlinear constrained optimization problems. Unlike traditional methods that rely on gradients or Hessians, COBYLA approximates the objective function and constraints using linear approximations within each iteration [53]. This approach suits it, particularly for scenarios where computing gradients could be more practical and costly. The algorithm iteratively adjusts the solution by exploring the feasible region using linear constraints and updating the approximation based on function evaluations. Mathematically, COBYLA seeks to minimize an objective function f(x) subject to nonlinear inequality constraints $\mathrm{h_i}(\mathrm{x}) \leq 0$ and equality constraints $\mathrm{g_j}(\mathrm{x}) = 0$. The main idea is to generate a sequence of iterates that improves the objective function value while satisfying the constraints using linear approximations.

$$\text{Minimize } \mathrm{f}(\mathrm{x}) \quad \text{subject to } \mathrm{h_i}(\mathrm{x}) \leq 0 \quad \text{and } \mathrm{g_j}(\mathrm{x}) = 0 \tag{5.43}$$

- SLSQP (Sequential Least Squares Programming): SLSQP is a popular optimization algorithm for solving constrained nonlinear optimization problems. It combines the advantages of least squares techniques with sequential quadratic programming methods to efficiently handle equality and inequality constraints. The algorithm iteratively approximates the objective function and constraints using quadratic models, adjusting iteratively to minimize the objective function while satisfying the constraints [37].

- Powell: Powell's method, introduced by M. J. D. Powell in 1964 [52], is a numerical optimization algorithm designed to find the minimum of a function without requiring derivatives. It belongs to the class of conjugate direction methods and is particularly effective for optimizing functions of several variables where direct computation of gradients may be impractical or costly. The method iteratively explores directions in the parameter space, adjusting its search based on the function evaluations to efficiently converge toward the best solution.

- Trust-region constrained (trust-constr): Trust-constr optimization is a powerful technique for solving nonlinear optimization problems subject to constraints. This method is particularly effective when dealing with complex objective functions and constraints that can be difficult to handle using traditional optimization methods. The trust-constr approach iteratively refines a model of the objective function within a trust region, a subset of the feasible region where the model is assumed to be an accurate approximation of the objective function. This method balances the exploration of the feasible space and the accuracy of the approximation, leading to more robust solutions. Mathematically, the trust-region sub-problem can be formulated as follows:

$$\min_{\mathbf{p}} \quad \mathrm{m_k}(\mathbf{p}) = \mathrm{f}(\mathbf{x}_\mathrm{k}) + \nabla \mathrm{f}(\mathbf{x}_\mathrm{k})^\mathrm{T}\mathbf{p} + \frac{1}{2}\mathbf{p}^\mathrm{T}\mathbf{B}_\mathrm{k}\mathbf{p} \quad \text{subject to} \quad \|\mathbf{p}\| \leq \Delta_\mathrm{k} \qquad (5.44)$$

  Here, $\mathrm{m_k}(\mathbf{p})$ is the quadratic model of the objective function f around the current iterate $\mathbf{x}_\mathrm{k}$, $\nabla \mathrm{f}(\mathbf{x}_\mathrm{k})$ is the gradient of the objective function, $\mathbf{B}_\mathrm{k}$ is the Hessian approximation, and Δ_k is the radius of the trust region. The trust-region method adjusts Δ_k dynamically based on the agreement between the model $\mathrm{m_k}$ and the actual objective function f. Trust-region methods have shown significant advantages over line-search methods, particularly in their ability to handle ill-conditioned problems and to converge more reliably to a solution [75].

5.2.5 Evaluation Metrics

To evaluate the performance of the optimization, we measure the synchronicity and temporal dispersion. By looking at the maximum of the histogram bar graph of the times of BEBs presences at the charging terminal, we find the number of BEBs present at the charging terminal at specific times. The maximum number points to the worst-case scenario, representing the need for more chargers and power for charging the BEBs. For instance, Figure 5.15 depicts a maximum of four, which means that at that time, we have four BEBs at the Waterfront terminal.

We propose the Temporal Presence Dispersion Index (TPDI) to quantify the variability in distances between consecutive points along a time axis. It is designed to measure how evenly these points (BEBs precences at the charging terminal) are distributed over time by examining the differences between consecutive distances. TPDI quantifies the spread of presences of BEBs at the charging terminal, indicates how much they are spread out from previous and after BEBs' presences at the charging terminal. More excellent dispersion gives the BEBs more time (opportunities) for charging.

According to Equation (5.20), we define a set in Equation (5.45) that includes the maxima of all activity blocks' sinusoidal functions, which are considered as BEBs presence at the charging terminal.

$$\begin{aligned} \boldsymbol{\mathcal{T}} = \Big\{ \mathrm{t_{j,k}} \mid \mathrm{t_{j,k}} = \frac{\frac{\pi}{2} + 2\mathrm{k}\pi - \varphi^{\mathrm{bl_j}}_{\mathrm{ch_i}}}{2\pi \mathrm{f}^{\mathrm{bl_j}}_{\mathrm{ch_i}}}, \\ \mathrm{k} \in \{0, 1, \ldots, \mathrm{m_j} - 1\}, \quad \mathrm{j} \in \{1, 2, \ldots, |\mathrm{BL}^{\mathrm{ch}}_{i}|\}, \quad \mathrm{t_{j,k}} \in \mathrm{T} \Big\} \end{aligned} \tag{5.45}$$

The set $\mathbf{D}$ encompasses the distances between consecutive BEBs presence times, given by:

$$\begin{aligned} &\mathbf{D} = \{\mathrm{d_2}, \mathrm{d_3}, \ldots, \mathrm{d_i}\} \\ &\mathrm{d_i} = \mathrm{t_{i+1}} - \mathrm{t_i} \quad \text{for} \quad \mathrm{t_i} \in \mathcal{T} \end{aligned} \tag{5.46}$$

Equation (5.47) calculates the differences between consecutive distances.

$$\Delta \mathrm{d_i} = \mathrm{d_{i+1}} - \mathrm{d_i} \quad \text{for} \quad \mathrm{i} = 1, 2, \ldots, |\mathcal{T}| - 2 \tag{5.47}$$

Equation (5.48) calculates the mean of the differences between consecutive distances.

$$\overline{\Delta \mathrm{d}} = \frac{1}{\mathrm{n} - 2} \sum_{\mathrm{i}=1}^{\mathrm{n}-2} \Delta \mathrm{d_i} \tag{5.48}$$

Equation (5.49) calculates the variance of the differences between consecutive distances.

$$\sigma^2_{\Delta \mathrm{d}} = \frac{1}{\mathrm{n} - 1} \sum_{\mathrm{i}=1}^{\mathrm{n}-1} (\mathrm{d_i} - \overline{\Delta \mathrm{d}})^2 \tag{5.49}$$

Therefore, TPDI is given by:

$$\mathrm{TPDI} = \frac{\sigma^2_{\Delta \mathrm{d}}}{\overline{\Delta \mathrm{d}}} \tag{5.50}$$

A TPDI value close to 0 indicates a highly regular or evenly distributed pattern of BEBs' presences at charging terminal over the working time, and higher TPDI values indicate greater variability or clustering of BEBs' presences at charging terminal over the working time.

5.2.6 Model Evaluation

Referring to Table 5.3, we implemented the optimization model for the Waterfront charging terminal. The BEBs fulfilling 13 activity blocks charge at the waterfront terminal. Figures 1 through 3 show the details of Thunder Bay City activity blocks, while Figure 6 depicts the piece-wise sinusoidal-modeled activity blocks charging at the Waterfront terminal.

Figure 5.13 depicts the Thunder Bay City sinusoidal-modelled activity blocks charge at the Waterfront terminal.

After modelling the activity blocks as piece-wise sinusoidal functions, we calculated the LCM of the activity blocks' periods and used that as a time interval in the optimization process. LCM is 180 minutes. Therefore, we selected a 180-minute interval starting at 450 minutes and ending at 630 minutes, representing the active time for all activity blocks.

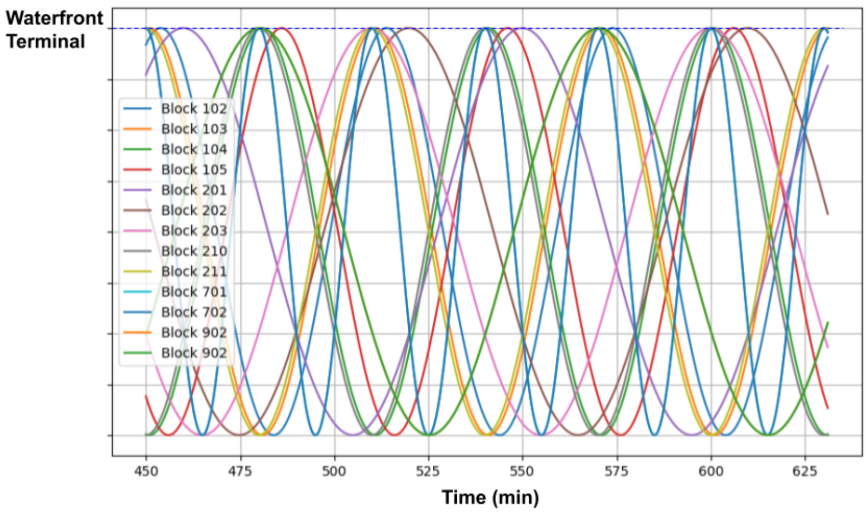

FIGURE 5.13: Sinusoidal-modelled Activity blocks charging at Waterfront terminal within the 180-minute interval before the optimization

Figure 5.14 depicts BEBs' presences at Waterfront terminal and maximum function defined by Equation (5.36) within 180-minute interval before the optimization.

Figure 5.15 illustrates the synchronicity of activity blocks, showing the simultaneous presences of BEBs fulfilling these activity blocks at the Waterfront charging terminal. The maximum number of BEBs arriving at the Waterfront charging terminal together is four,

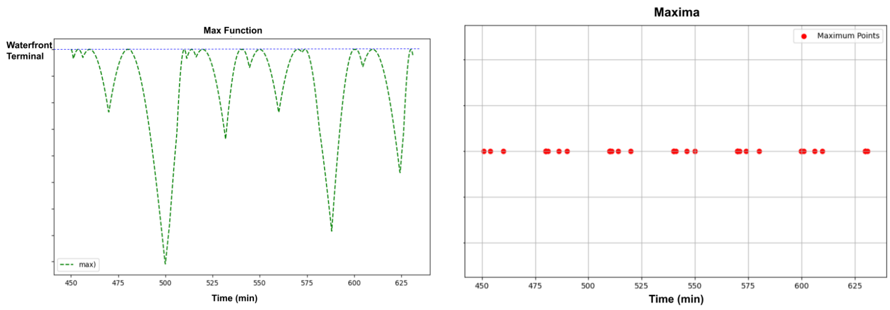

(a) Maximum function (b) Maxima

FIGURE 5.14: Sinusoidal-modelled activity blocks maxima and maximum function charging at the Waterfront terminal before the optimization

which poses a challenge for on-route charging. We will skip some charging opportunities if we utilize fewer than four chargers. Skipping these opportunities might extend the required charging time, which is undesirable for transit planners. Installing four on-route chargers to accommodate all BEBs simultaneously would lead to high infrastructure costs. Additionally, the power demand spikes when four BEBs charge simultaneously, which can significantly increase electricity costs, especially during peak times.

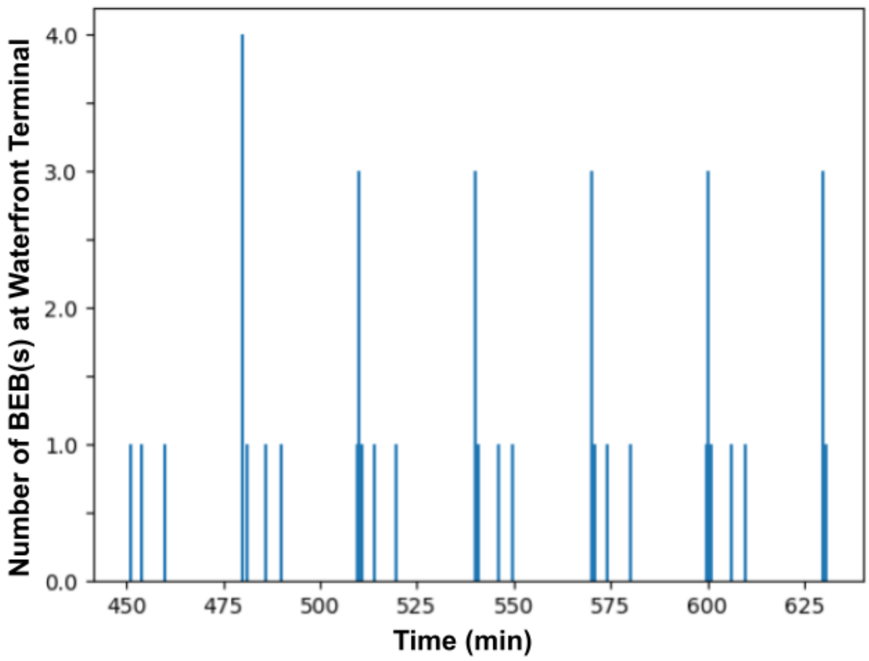

FIGURE 5.15: Number of BEBs at the Waterfront charging terminal before the optimization

According to Equation (5.37), the functions are sinusoidal, involve constraints, and have some variables (activity blocks' sinusoidal modelled phase shifts). Therefore, we need an optimization solver that can effectively handle both the smooth nature of sinusoidal functions and the constraints. Gradient-based methods are generally efficient for smooth and differentiable functions, and there are several solvers that can handle constraints. We selected Python as the programming language for implementing the optimization experiments. The **minimize** function in the **scipy.optimize** package provides several solver methods for optimization problems. We experimented with some the available methods. Table 5.4 demonstrates the results of different solver methods. Based on the results for TPDI scores, **Trust-constr** outperforms the others with an index of 0.65, as shown by the red background in Table 5.4. The maximum number of simultaneous BEBs at the Waterfront terminal during working hours reached the achievable minimum, which is one BEB.

TABLE 5.4: Scheduling Optimization Results with Different Solver Methods for Activity Blocks Charging at the Waterfront Terminal

Solver Method	Mean Differences of Neighbour Distances	std of Differences of Neighbour Distances	TPDI After Opt	Max No. of BEBs Before Opt	Max No. of BEBs After Opt
Nelder-Mead	1.44	1.40	1.36	4	1
Powell	3.88	3.43	3.04	4	2
BFGS	3.17	2.04	1.32	4	2
COBYLA	1.35	1.51	1.7	4	2
TNC	3.12	2.66	2.28	4	2
L-BFGS-B	2.16	1.74	1.40	4	2
SLSQP	2.65	2.22	1.87	4	2
Trust-constr	1.30	0.92	0.65	4	1

Figure 5.16 depicts all activity blocks charging at Waterfront terminal modelled as sinusoidal functions after optimization using the Trust-constr method, which achieved the best result among the other methods. Figure 5.17 depicts the maxima and maximum function within 180-minute interval after the optimization.

Figure 5.18 illustrates the synchronicity of activity blocks, showing the simultaneous presences of BEBs fulfilling these activity blocks at the Waterfront charging terminal after the optimization. The maximum number of BEBs arriving at the Waterfront charging terminal together is one, a decrease from four before the optimization. We can charge all BEBs at every opportunity without skipping any by installing one fast charger. Compared to before the optimization, which required four fast chargers to avoid skipping charging

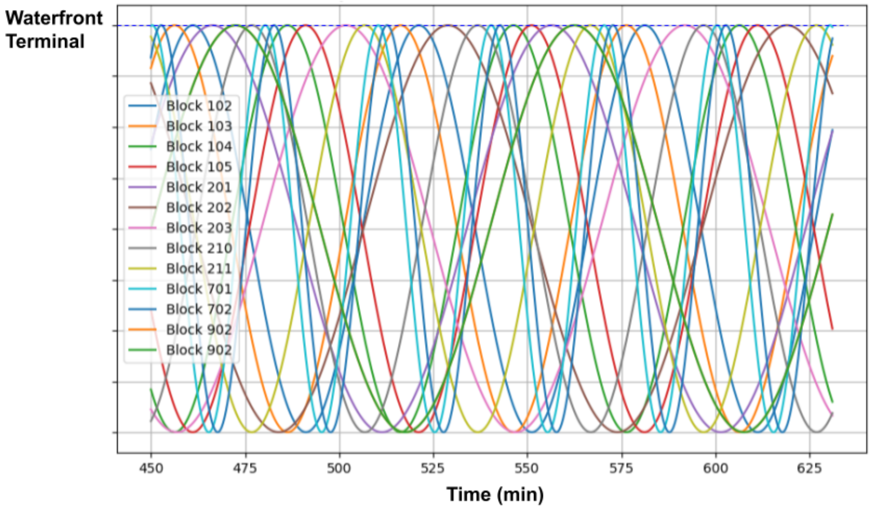

FIGURE 5.16: Sinusoidal-modelled Activity blocks charging at Waterfront terminal within the 180-minute interval after the optimization

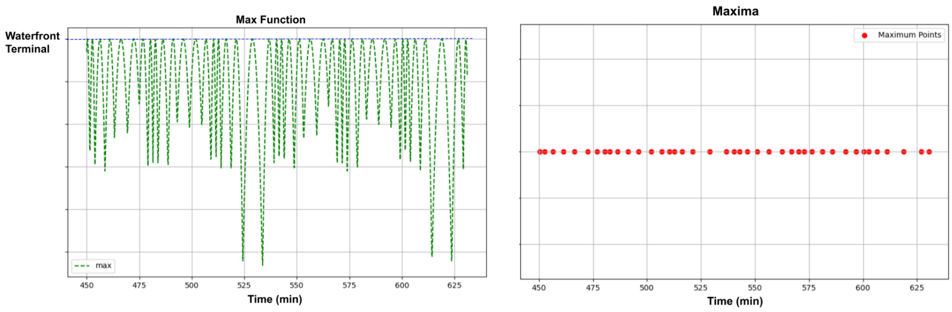

(a) Maximum function (b) Maxima

FIGURE 5.17: Sinusoidal-modelled activity blocks maxima and maximum function charging at the Waterfront terminal after the optimization

opportunities, the capital cost (CAPEX) and operating cost (OPEX) have decreased considerably. Table 5.5 presents the time shifting required in each activity block to tune the transit system's timetable, considering the optimization results. The new tuned timetable ensures that every BEB has maximum charging opportunity without changing its service rate.

Referring to Table 5.3, we ran the optimization model for the City Hall charging terminal, where BEBs fulfill 16 activity blocks charge. Figures 1 through 3 show the details of Thunder Bay City activity blocks, while Figure 7 depicts the piece-wise sinusoidal-modeled activity blocks charging at the City Hall terminal.

LCM of the City Hall charging terminal activity blocks' periods is 300 minutes. Thus, we selected a 300-minute interval starting at 500 and ending at 800, representing the active time for all activity blocks as the optimization interval. Figure 5.19 shows all

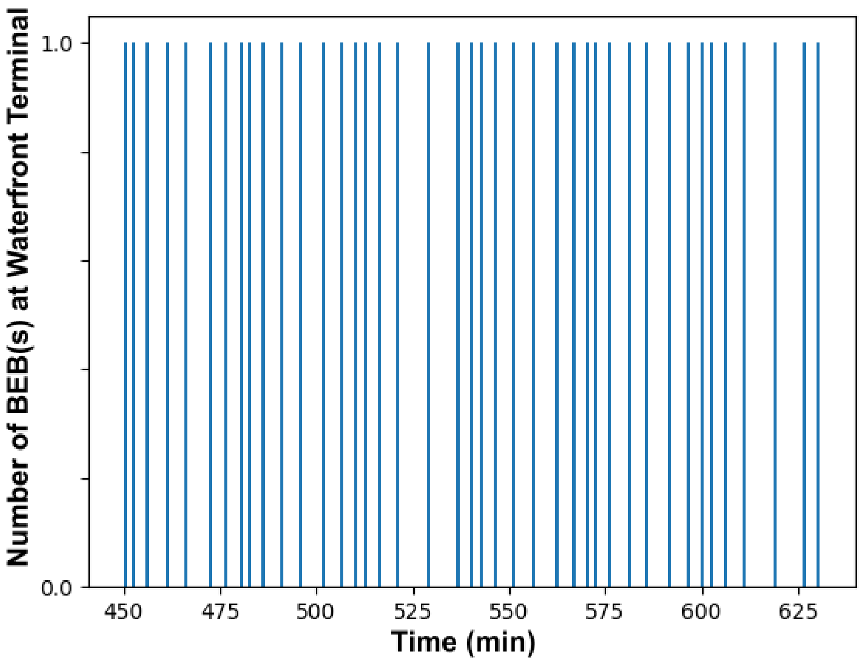

FIGURE 5.18: Number of BEBs at waterfront charging terminal after the optimization

sinusoidal-modelled activity blocks charging at the City Hall terminal modelled before the optimization.

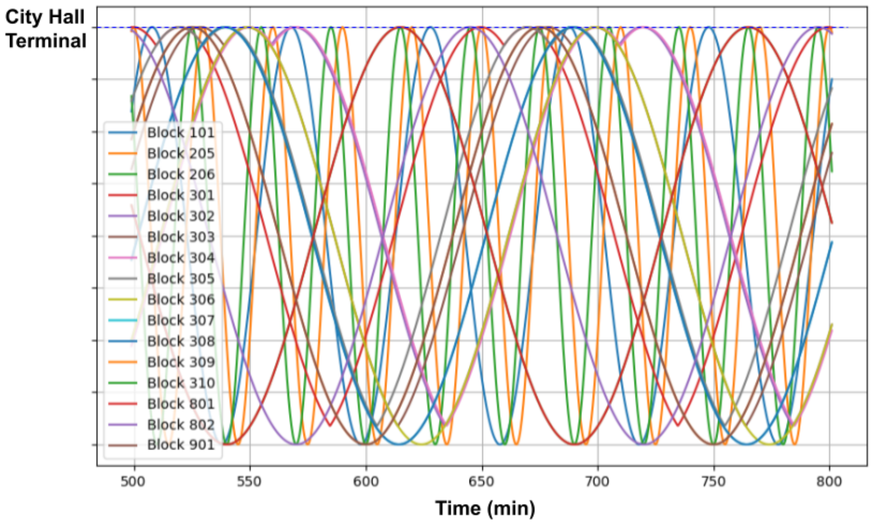

FIGURE 5.19: Sinusoidal-modelled activity blocks charging at City Hall terminal within the 300-minute interval before the optimization

Figure 5.20 depicts the distribution of BEBs' presences at the City Hall terminal over 300-minute interval (maxima) and the maximum function, as defined by Equation (5.36), before the optimization.

TABLE 5.5: Tuned Activity Blocks Charging at Waterfront Terminal

Activity block	Time shifting (min)	Updated Start Time (min)	Updated End Time (min)
201	+ 7	367	1111
702	+ 3	343	1729
701	+ 1	346	1393
203	- 8	377	1389
202	+ 9	369	1412
902	- 8	377	1240
903	+ 6	356	1404
210	- 4	396	1085
211	- 4	426	1085
102	+ 8	350	1428
103	+ 6	366	1111
104	+ 6	363	1428
105	+ 5	370	1400

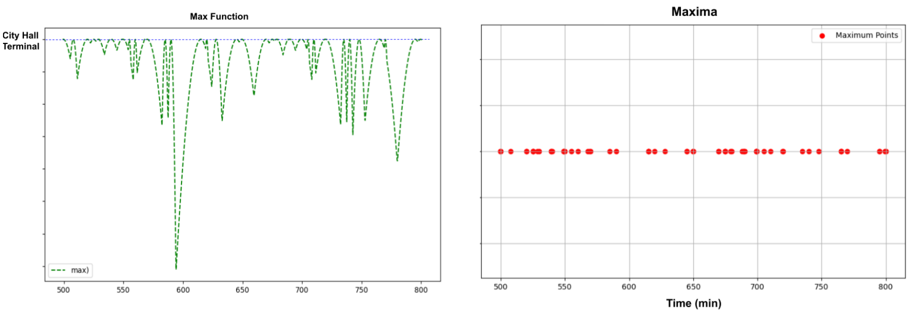

(a) Maximum function (b) Maxima

FIGURE 5.20: Sinusoidal-modelled activity blocks maxima and maximum function charging at City Hall terminal before the optimization

Figure 5.21 illustrates the synchronicity of activity blocks, showing the simultaneous presences of BEBs fulfilling these activity blocks at the City Hall charging terminal. The maximum number of BEBs arriving at the City Hall charging terminal together is three, which poses a challenge for on-route charging. We will skip some charging opportunities if we utilize fewer than three chargers. Skipping these opportunities might extend the required charging time, which is undesirable for transit planners. Installing three on-route chargers to accommodate all BEBs simultaneously would lead to high infrastructure costs. Additionally, the power demand spikes when three BEBs charge simultaneously, which can significantly increase electricity costs, especially during peak times.

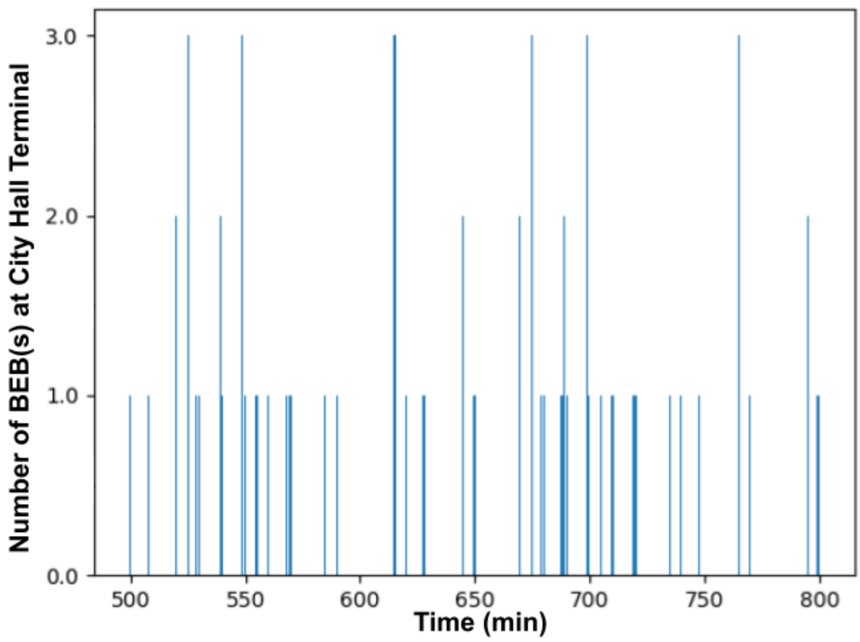

FIGURE 5.21: Number of BEBs at the City Hall charging terminal before the optimization

Table 5.6 demonstrates the results of different solver methods. Based on the results for TPDIs, Nelder-Mead outperforms the others with an index of 1.78, as shown by the red background in Table 5.6. The maximum number of simultaneous BEBs at City Hall terminal during the working hours reached the achievable minimum, which is one BEB.

Figure 5.22 depicts all activity blocks charging at City Hall terminal modelled as sinusoidal functions after optimization using Nelder-Mead method, which achieved the best result among the other methods. Figure 5.23 depicts the maxima and maximum function within 300-minute interval after the optimization.

Figure 5.24 illustrates the synchronicity of activity blocks charging at City Hall terminal, showing the simultaneous presences of BEBs fulfilling these activity blocks at the City Hall terminal after the optimization. The maximum number of BEB(s) arriving at the City Hall charging terminal together is one, a decrease from three before the optimization. We can charge all BEBs at every opportunity without skipping any by installing one fast charger. Compared to before the optimization, which required three fast chargers to avoid skipping charging opportunities, the capital cost (CAPEX) and operating cost (OPEX) have decreased considerably.

TABLE 5.6: Scheduling Optimization Results with Different Solver Methods for Activity Blocks Charging at the City Hall Terminal

Solver Method	Mean Differences of Neighbour Distances	std of Differences of Neighbour Distances	TPDI After Opt	Max No. of BEBs Before Opt	Max No. of BEBs After Opt
Nelder-Mead	2.30	2.02	1.78	3	1
Powell	3.72	3.12	2.61	3	2
BFGS	4.48	3.71	3.07	3	2
COBYLA	3.16	2.65	2.22	3	2
TNC	4.32	3.60	3.00	3	2
L-BFGS-B	4.79	3.92	3.2	3	2
SLSQP	4.53	3.18	2.23	3	2
Trust-constr	3.29	3.07	2.86	3	1

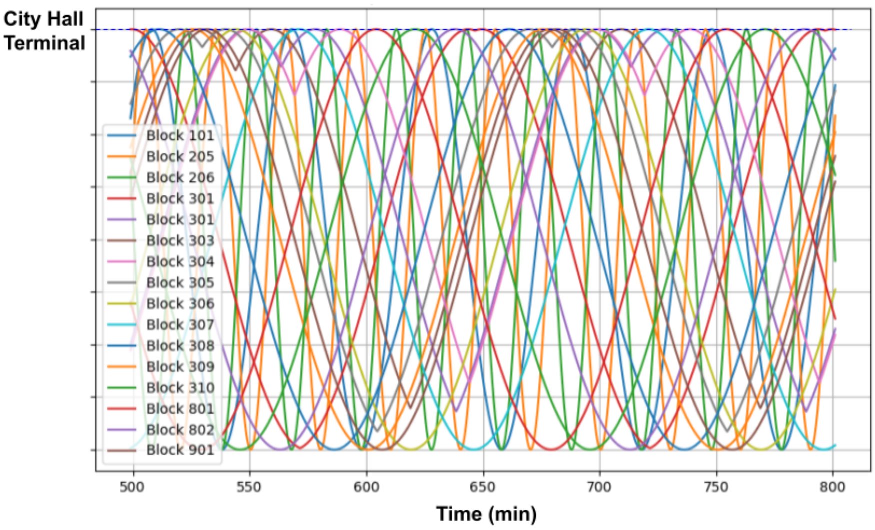

FIGURE 5.22: Sinusoidal-modelled activity blocks charging at City Hall terminal within the 300-minute interval after the optimization

Table 5.7 presents the time shifting required in each activity block charging at City Hall to tune the transit system's timetable, considering the optimization results. The new adjusted timetable ensures that every BEB has maximum charging opportunity without changing its service rate.

In summary, we have formulated an effective on-route charging strategy through a

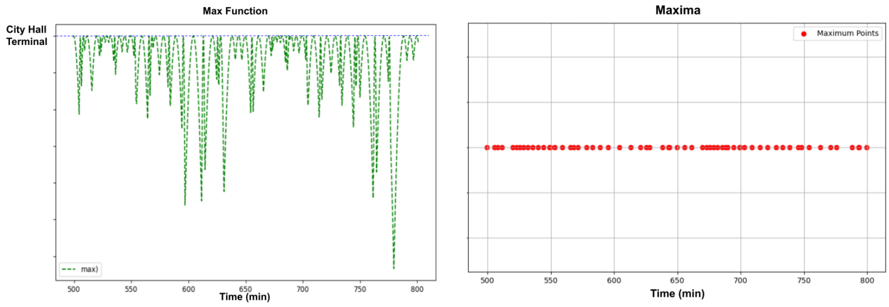

(a) Maximum function (b) Maxima

FIGURE 5.23: Sinusoidal-modelled activity blocks maxima and maximum function charging at City Hall terminal after the optimization

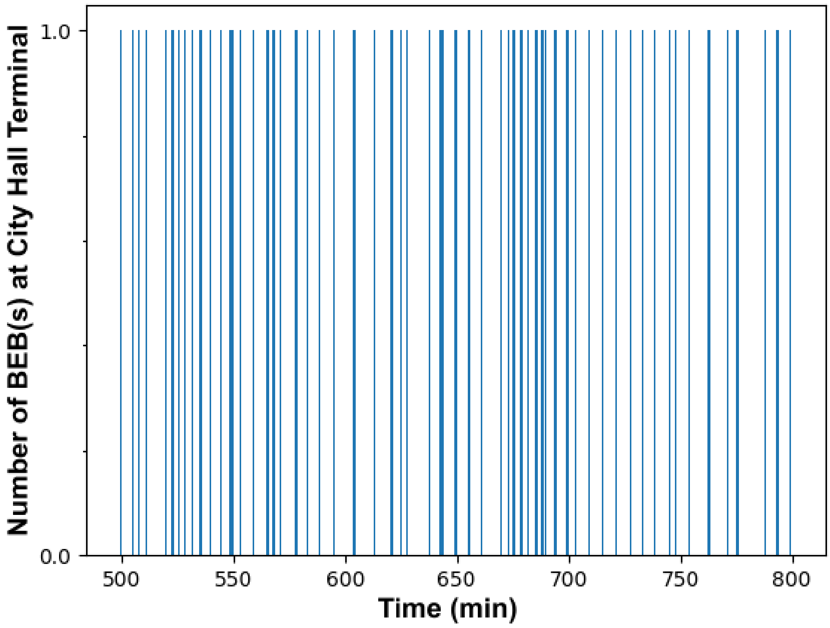

FIGURE 5.24: Number of BEB(s) at City Hall charging terminal after the optimization

comprehensive analysis of the daily energy requirements of the transit system and careful consideration of the transit system's timetable. This strategy includes assessing the transit system's daily worst-case energy needs, determining the minimum number of required charging terminals to minimize infrastructure costs and assigning service activity blocks to charge terminals to maximize the opportunities for BEBs charging. Additionally, we have implemented energy balancing between charging terminals, ensuring a strategic solution for the power grid and transit system planners. Since the transit system activity blocks are periodic time functions, we modelled them as sinusoidal functions, with their maxima representing the times when BEBs are at the charging terminals.

To maximize the charging opportunities for each BEB, they need to be at the charging terminal at intervals that maximize the temporal separation from the presence of other

TABLE 5.7: Tuned Activity Blocks Charging at City Hall Terminal

Activity block	Time shifting (min)	Updated Start Time (min)	Updated End Time (min)
205	+ 6	361	1100
206	- 2	353	1142
801	- 11	359	1074
802	- 7	393	1113
901	+ 7	362	1111
306	- 5	340	1378
308	- 28	332	1351
303	+ 11	376	1406
101	+ 1	351	1101
305	- 1	399	1383
301	- 26	319	1373
302	+ 9	354	1235
304	+ 19	374	1114
307	+ 32	382	1141
310	+ 6	401	1076

BEBs at the same terminal. We proposed an optimization method to achieve maximum temporal dispersion, minimizing synchronicity. Therefore, without altering the activity blocks' service rate, we maximize their charging opportunities by slightly shifting the timing of these activity blocks forward or backward. We evaluated the proposed method using the Thunder Bay City transit system. The results show a considerable improvement in the temporal dispersion of BEBs presences at the Waterfront and City Hall charging terminals with only slight shifts in the activity blocks' times.

Chapter 6

Conclusion and Research Directions

6.1 Conclusions

As many municipalities begin to migrate from diesel buses to fully battery electric bus transit systems, transit planners need to understand the charging process, approaches, and the advantages and shortcomings of each approach. They also need methods to adapt the existing transit system for fully electric sustainable transportation without making extensive changes that could negatively impact the current transportation demand. Considering the two main BEB charging strategies—on-route and off-service charging—the thesis predominantly focuses on practical deterministic optimization for BEB charging facility planning specific to each strategy, assuming known input parameters and constraints with certainty from diesel-fueled transit systems. The thesis addresses some problems associated with each strategy.

we utilized the BEB energy consumption estimator, developed through a data-driven approach, to determine the worst-case energy consumption rate for transit system lines (routes). Using this rate, along with the lengths of each route and their corresponding service schedules (activity blocks), we estimated the daily worst-case energy consumption for the entire transit system. The total estimated daily worst-case required energy is 17,612 kWh.

Regarding off-service charging planning, this thesis addresses three key challenges faced by transit planners in the migration of transit systems from diesel-fueled to fully electric transit systems:

- The placement of charging sites.
- The BEBs charging mechanism.

- Determining the minimum number of BEBs required to fulfill daily transit system services.

Effectively placing off-service charging sites improves overall system performance. The proposed charging site placement method, CGC, is a flexible hierarchical clustering technique that can consider any constraint at each merging step. This flexibility benefits transit system planners, allowing them to define and apply localized constraints specific to particular areas. Load distribution is a pivotal constraint imposed by the power grid. The results indicate that enhancing clustering characteristics aids in optimizing the transit system's charging load balancing among the charging sites. Comparing CGC and K-means, clustering showed that a slight compromise between their clustering performance could create an effective charging load balance. The uniformity in clusters' loads aligns with our specific requirements for power grid constraints, aiding in achieving consistent resource distribution.

It is worth mentioning that when selecting the location for the charging site and the planner decides to utilize the current infrastructures, the proximity to charging site placements is a crucial factor. Choosing a depot or garage as a charging site, which is close to identified charging site placements, is advantageous as it eliminates the need to construct new buildings. Therefore, the nearest depot or garage to the location of the charging site placement is considered the best choice to minimize additional construction efforts.

The outlined overnight charging strategy includes:

- Determining the transit system's daily worst-case energy requirements.
- Establishing the start and end times for overnight charging.
- Determining the minimum number of chargers needed to minimize infrastructure costs.
- Calculating the minimum power capacity.

The proposed mechanism, PCM, facilitates the simultaneous charging of all BEBs while considering their energy requirements and depot availability. By rotating BEBs across chargers during charging sessions, PCM improves resilience to charger failures. It distributes potential disruptions across the chargers, minimizing the effects of any single charger failure on a BEB.

We proposed the clustering method, CACA, to ensure an effective solution for grouping activity blocks for shared BEBs usage. This algorithm minimizes travelling distances while considering energy balancing among the shared BEBs within the transit system.

Regarding on-route charging planning, this thesis addresses three existing problems concerning transit planners in the migration of transit systems from diesel-fueled to fully electric ones:

- Identifying suitable charging terminals among the existing infrastructure.
- Optimal allocating BEBs to the identified charging terminals.
- Adjusting the current transit system timetable to maximize BEBs' charging opportunities and minimize the synchronicity of BEBs' presence at charging terminals.

We proposed the transit system opportunity matrix to determine the minimum number of required charging terminals that all activity blocks can use. Using a three-step method -accessibility, number of stops, and energy balancing between charging terminals- we efficiently assigned activity blocks to charging terminals to maximize opportunities for BEB charging, which is a suitable solution for power grid and transit system planners.

To migrate from a diesel-fueled transit system to a fully electric one, maintaining the inherited bus activity blocks facilitates the process. It can reduce the overhead cost of rescheduling services. To that end, we modelled the transit system activity blocks inherited from the diesel-fueled system as piece-wise sinusoidal functions, where the BEBs' presences at charging terminals correspond to the sinusoidal-modelled activity blocks' maxima. In the on-route charging strategy, BEBs' presence is considered one of the BEBs' charging opportunities. To maximize the charging opportunities for each BEB, it needs to be at the charging terminal at intervals that maximize the temporal separation from the presence of other BEBs at the same terminal. We proposed an optimization method to achieve maximum temporal dispersion, minimizing synchronicity. Therefore, without altering the activity blocks' service rates, we maximize their charging opportunities by slightly shifting the timing of these activity blocks forward or backward. Temporal dispersion helps mitigate the concentration of BEBs at charging terminals, reducing the demand for fast chargers at any given time. By spreading out the charging times, fewer BEBs require charging simultaneously, which decreases the likelihood of congestion and ensures that each BEB can access a charger when needed. This approach minimizes the risk of missed charging opportunities and optimizes the utilization of available charging infrastructure. Consequently, the system can operate more efficiently with fewer fast chargers while maintaining effective and timely charging for all BEBs.

We evaluated the proposed method using Thunder Bay's transit system. The results show a considerable improvement in the temporal dispersion of the BEBs' presence at the Waterfront and City Hall charging terminals with only slight time-shifting of the activity blocks.

6.2 Research Directions

The expectation for BEB transit systems to utilize a combination of various charging technologies arises from several factors. Different regions or transit systems may possess diverse infrastructure capabilities and constraints. Incorporating a mix of charging technologies provides flexibility to adapt to existing infrastructure and accommodate future expansions. Operational efficiency is paramount in BEB transit systems. Different charging technologies offer varying charging speeds, costs, and energy efficiency. By integrating these technologies, BEB transit systems can optimize charging processes to minimize operational costs and maximize efficiency. BEBs may operate on routes with varying distances and schedules, necessitating different charging solutions to meet their range requirements. Utilizing a combination of charging technologies allows greater flexibility in addressing range limitations and optimizing charging schedules. Despite these anticipated benefits, only a few studies have explored integrating different charging technologies in BEB transit systems. This could be attributed to factors such as the complexity of coordinating multiple technologies, limited availability of data on their performance and interoperability, and the relative novelty of BEB technology in many regions. Hence, further research is needed to investigate how to effectively coordinate and integrate diverse charging technologies in BEB transit systems to realize their full potential.

As transit system planners consider multiple criteria such as geographical location, traffic patterns, passenger demand fluctuations throughout the day, and existing infrastructure capacities in their planning processes, one promising avenue for future research is to incorporate localized constraints rather than applying a single general power constraint, as done in our work, during the hierarchical clustering merging process. Additionally, exploring fuzzy clustering techniques could enhance the ability to accommodate varying constraints and uncertainties in transit system optimization. Since delays are an inseparable part of transit systems, they introduce uncertainty into our timetable. Conducting future research on on-route charging scheduling that takes into account uncertainties in the real world is a practical and significant endeavour.

Future research could explore incorporating stochastic elements into the timing of activity blocks, accounting for variations such as delays that might differ for each activity block. By modelling these uncertainties, researchers can develop more robust scheduling algorithms that better reflect real-world conditions. This approach would enable transit systems to adapt to unpredictable events and maintain the practical charging opportunities. Investigating the impact of stochastic delays on the temporal dispersion of BEBs at charging terminals could also help improve the resilience and efficiency of fully electric transit systems. Additionally, future studies could examine how stochastic modelling influences the transit system's overall performance and infrastructure requirements.

We plan to build comprehensive algorithms to assess the proposed models for larger public transit systems where interlining routes and services are more complex than in the City of Thunder Bay.

Bibliography

[1] Understanding demand charges part 1: What are they and why they need to change, Mar 2022.

[2] Hatem Abdelaty, Abdullah Al-Obaidi, Moataz Mohamed, and Hany E.Z. Farag. Machine learning prediction models for battery-electric bus energy consumption in transit. *Transportation Research Part D: Transport and Environment*, 96:102868, 2021.

[3] Matías Alvo, Gustavo Angulo, and Mathias A. Klapp. An exact solution approach for an electric bus dispatch problem. *Transportation Research Part E: Logistics and Transportation Review*, 156:102528, 2021.

[4] Syed Muhammad Arif, Tek Tjing Lie, Boon Chong Seet, Syed Muhammad Ahsan, and Hassan Abbas Khan. Plug-in electric bus depot charging with pv and ess and their impact on lv feeder. *Energies*, 13(9), 2020.

[5] Hussein Basma, Charbel Mansour, Maroun Nemer, Marc Haddad, and Pascal Stabat. Optimization of battery electric bus charging under varying operating conditions. In *2020 IEEE Vehicle Power and Propulsion Conference (VPPC)*, pages 1–6, 2020.

[6] Yiming Bie, Jinhua Ji, Xiangyu Wang, and Xiaobo Qu. Optimization of electric bus scheduling considering stochastic volatilities in trip travel time and energy consumption. *Computer-Aided Civil and Infrastructure Engineering*, 36(12):1530–1548, 2021.

[7] Nico Brinkel, Marle Zijlstra, Ronald van Bezu, Tim van Twuijver, Ioannis Lampropoulos, and Wilfried van Sark. A comparative analysis of charging strategies for battery electric buses in wholesale electricity and ancillary services markets. *Transportation Research Part E: Logistics and Transportation Review*, 172:103085, 2023.

[8] C. G. BROYDEN. The Convergence of a Class of Double-rank Minimization Algorithms 1. General Considerations. *IMA Journal of Applied Mathematics*, 6(1):76–90, 03 1970.

[9] Robert Cervero and Kara Kockelman. Travel demand and the 3ds: Density, diversity, and design. *Transportation Research Part D: Transport and Environment*, 2(3):199–219, 1997.

[10] Arun Chatterjee, Frederick Wegmann, Nicholas Fortey, and Jerry Everett. Incorporating safety and security issues in urban transportation planning. *Transportation Research Record*, 1777:75–83, 01 2001.

[11] Uk-Don Choi, Ho-Kwon Jeong, and Sun-Kyu Jeong. Commercial operation of ultra low floor electric bus for seoul city route. In *2012 IEEE Vehicle Power and Propulsion Conference*, pages 1128–1133, 2012.

[12] Maria Vittoria Corazza, Umberto Guida, Antonio Musso, and Michele Tozzi. A european vision for more environmentally friendly buses. *Transportation Research Part D: Transport and Environment*, 45:48–63, 2016. Special Issue on Climate Change and Transport.

[13] M. Crippa, D. Guizzardi, E. Solazzo, M. Muntean, E. Schaaf, F. Monforti-Ferrario, M. Banja, J.G.J. Olivier, G. Grassi, S. Rossi, and E. Vignati. Ghg emissions 2021 report. Technical Report EUR30831EN, Publications Office of the European Union, Luxembourg, 2021.

[14] David L. Davies and Donald W. Bouldin. A cluster separation measure. *IEEE Transactions on Pattern Analysis and Machine Intelligence*, PAMI-1(2):224–227, 1979.

[15] Iulia Dolganova, Anne Rödl, Vanessa Bach, Kaltschmitt Martin, and Matthias Finkbeiner. A review of life cycle assessment studies of electric vehicles with a focus on resource use. *Resources*, 9, 03 2020.

[16] Reed T. Doucette and Malcolm D. McCulloch. Modeling the co2 emissions from battery electric vehicles given the power generation mixes of different countries. *Energy Policy*, 39(2):803–811, 2011. Special Section on Offshore wind power planning, economics and environment.

[17] Jiuyu Du, Feiqiang Li, Jianqiu Li, Xiaogang Wu, Ziyou Song, Yunfei Zou, and Minggao Ouyang. Evaluating the technological evolution of battery electric buses: China as a case. *Energy*, 176:309–319, 2019.

[18] Nader A. El-Taweel, Hany E. Z. Farag, Gouri Barai, Hatem Zeineldin, Ahmed Al-Durra, and Ehab F. El-Saadany. A systematic approach for design and analysis of electrified public bus transit fleets. *IEEE Systems Journal*, 16(2):2989–3000, 2022.

[19] Onur Elma and Hossam A. Gabber. Flywheel-based ultra-fast on-route charging system for public e-buses. In *2020 International Conference on Electrical, Communication, and Computer Engineering (ICECCE)*, pages 1–4, 2020.

[20] Leslie Eudy, Robert Prohaska, Kenneth Kelly, and Matthew Post. Foothill transit battery electric bus demonstration results. Technical Report NREL/TP-5400-65274, National Renewable Energy Laboratory, January 2016.

[21] Marc Gallet, Tobias Massier, and Thomas Hamacher. Estimation of the energy demand of electric buses based on real-world data for large-scale public transport networks. *Applied Energy*, 230:344–356, 2018.

[22] Jean-Baptiste Gallo, Ted Bloch-Rubin, and Jasna Tomić. Peak demand charges and electric transit buses. *US Department of Transportation, Tech. Rep.*, 2014.

[23] K. Gkiotsalitis, C. Iliopoulou, and K. Kepaptsoglou. An exact approach for the multi-depot electric bus scheduling problem with time windows. *European Journal of Operational Research*, 306(1):189–206, 2023.

[24] D. Goehlich, F. Spangenberg, and A. Kunith. Stochastic total cost of ownership forecasting for innovative urban transport systems. In *2013 IEEE International Conference on Industrial Engineering and Engineering Management*, pages 838–842, 2013.

[25] D. Gohlich, A. Kunith, and T. Ly. Technology assessment of an electric urban bus system for berlin. *Urban Transport XX*, pages 138–137, 2014.

[26] Lili Gong, Wu Cao, Kangli Liu, and Jianfeng Zhao. Optimal charging strategy for electric vehicles in residential charging station under dynamic spike pricing policy. *Sustainable Cities and Society*, 63:102474, 2020.

[27] John Hancock. *Jaccard Distance (Jaccard Index, Jaccard Similarity Coefficient)*. 10 2004.

[28] Yi He, Zhaocai Liu, and Ziqi Song. Optimal charging scheduling and management for a fast-charging battery electric bus system. *Transportation Research Part E: Logistics and Transportation Review*, 142:102056, 2020.

[29] Yi He, Ziqi Song, and Zhaocai Liu. Fast-charging station deployment for battery electric bus systems considering electricity demand charges. *Sustainable Cities and Society*, 48:101530, 2019.

[30] Yi He, Ziqi Song, and Zhaocai Liu. Fast-charging station deployment for battery electric bus systems considering electricity demand charges. *Sustainable Cities and Society*, 48, 04 2019.

[31] Adnane Houbbadi, Rochdi Trigui, Serge Pelissier, Eduardo Redondo-Iglesias, and Tanguy Bouton. Optimal scheduling to manage an electric bus fleet overnight charging. *Energies*, 12(14), 2019.

[32] Mordor Intelligence. China electric bus market - growth, trends, covid-19 impact, and forecasts (2022-2027). https://www.mordorintelligence.com/industry-reports/china-electric-bus-market, 2022. Accessed June 02, 2022.

[33] Amra Jahic, Mina Eskander, and Detlef Schulz. Charging schedule for load peak minimization on large-scale electric bus depots. *Applied Sciences*, 9(9), 2019.

[34] Mengyan Jiang, Yi Zhang, and Yi Zhang. A branch-and-price algorithm for large-scale multidepot electric bus scheduling. *IEEE Transactions on Intelligent Transportation Systems*, 24(12):15355–15368, 2023.

[35] Ryuichi Kitamura. Panel analysis in transportation planning: An overview. *Transportation Research Part A: General*, 24(6):401–415, 1990.

[36] Mustafa Cagatay Kocer, Ogun Yurdakul, and Sahin Albayrak. Optimal scheduling of battery swapping stations for electric public transportation. In *2021 IEEE PES Innovative Smart Grid Technologies Europe (ISGT Europe)*, pages 1–5, 2021.

[37] D. Kraft. *A Software Package for Sequential Quadratic Programming*. Deutsche Forschungs- und Versuchsanstalt für Luft- und Raumfahrt Köln: Forschungsbericht. Wiss. Berichtswesen d. DFVLR, 1988.

[38] Aigars Laizans, Igors Graurs, Aivars Rubenis, and George Utehin. Economic viability of electric public busses: Regional perspective. *Procedia Engineering*, 134:316–321, 12 2016.

[39] Antti Lajunen. Lifecycle costs and charging requirements of electric buses with different charging methods. *Journal of Cleaner Production*, 172:56–67, 2018.

[40] David Levinson and Kevin Krizek. *Metropolitan transport and land use: Planning for place and plexus, second edition*. 01 2018.

[41] Lu Li, Hong K. Lo, and Feng Xiao. Mixed bus fleet scheduling under range and refueling constraints. *Transportation Research Part C: Emerging Technologies*, 104:443–462, 2019.

[42] Kai Liu, Hong Gao, Zhe Liang, Meng Zhao, and Cheng Li. Optimal charging strategy for large-scale electric buses considering resource constraints. *Transportation Research Part D: Transport and Environment*, 99:103009, 2021.

[43] Tao Liu and Avishai (Avi) Ceder. Battery-electric transit vehicle scheduling with optimal number of stationary chargers. *Transportation Research Part C: Emerging Technologies*, 114:118–139, 2020.

[44] Zhaocai Liu, Ziqi Song, and Yi He. Planning of fast-charging stations for a battery electric bus system under energy consumption uncertainty. *Transportation Research Record*, 2672(8):96–107, 2018.

[45] Mohamed Lotfi, Pedro Pereira, Nikolaos Paterakis, Hossam A.Gabbar, and Joao Catalao. Optimizing charging infrastructures of electric bus routes to minimize total ownership cost. pages 1–6, 06 2020.

[46] Xinyu Lu, Jie Li, Shijing Yuan, Haiming Jin, Chentao Wu, and Zhan Xu. Toward real-time pricing and allocation for surplus resources in electric bus charging stations. *IEEE Transactions on Intelligent Transportation Systems*, pages 1–15, 2023.

[47] Dhendra Marutho, Sunarna Hendra Handaka, Ekaprana Wijaya, and Muljono. The determination of cluster number at k-mean using elbow method and purity evaluation on headline news. In *2018 International Seminar on Application for Technology of Information and Communication*, pages 533–538, 2018.

[48] Moataz Mohamed, Hany Farag, Nader El-Taweel, and Mark Ferguson. Simulation of electric buses on a full transit network: Operational feasibility and grid impact analysis. *Electric Power Systems Research*, 142:163–175, 2017.

[49] Stephen G. Nash. A survey of truncated-newton methods. *Journal of Computational and Applied Mathematics*, 124(1):45–59, 2000. Numerical Analysis 2000. Vol. IV: Optimization and Nonlinear Equations.

[50] J. A. Nelder and R. Mead. A Simplex Method for Function Minimization. *The Computer Journal*, 7(4):308–313, 01 1965.

[51] Jinghui Pan, Xiaomei Wu, Qijin Feng, and Yong Ji. Optimization of electric bus charging station considering energy storage system. In *2020 8th International Conference on Power Electronics Systems and Applications (PESA)*, pages 1–5, 2020.

[52] M. J. D. Powell. An efficient method for finding the minimum of a function of several variables without calculating derivatives. *The Computer Journal*, 7(2):155–162, 01 1964.

[53] M. J. D. Powell. *A Direct Search Optimization Method That Models the Objective and Constraint Functions by Linear Interpolation*, pages 51–67. Springer Netherlands, Dordrecht, 1994.

[54] William H Press, Saul A Teukolsky, William T Vetterling, and Brian P Flannery. *Numerical Recipes: The Art of Scientific Computing.* Cambridge University Press, 2007.

[55] Luca Pugi, Adriano Alessandrini, Riccardo Barbieri, Lorenzo Berzi, Marco Pierini, Fabio Cignini, Antonino Genovese, and Fernando Ortenzi. Design and testing of a supercapacitor storage system for the flash recharge of electric buses. *International Journal of Electric and Hybrid Vehicles*, 13:57, 01 2021.

[56] Nan Qin, Azwirman Gusrialdi, R. Paul Brooker, and Ali T-Raissi. *Transportation Research Part A: Policy and Practice*, 94:386–396, 2016.

[57] S. Rafique, M.S.H. Nizami, U.B. Irshad, M.J. Hossain, and S.C. Mukhopadhyay. A two-stage multi-objective stochastic optimization strategy to minimize cost for electric bus depot operators. *Journal of Cleaner Production*, 332:129856, 2022.

[58] Marco Rinaldi, Erika Picarelli, Andrea D'Ariano, and Francesco Viti. Mixed-fleet single-terminal bus scheduling problem: Modelling, solution scheme and potential applications. *Omega*, 96:102070, 2020.

[59] Matthias Rogge, Sebastian Wollny, and Dirk Uwe Sauer. Fast charging battery buses for the electrification of urban public transport—a feasibility study focusing on charging infrastructure and energy storage requirements. *Energies*, 8(5):4587–4606, 2015.

[60] Peter J. Rousseeuw. Silhouettes: A graphical aid to the interpretation and validation of cluster analysis. *Journal of Computational and Applied Mathematics*, 20:53–65, 1987.

[61] Editorial Staff. 66 per cent growth for us electric bus market in 2022, according to calstart, 2023.

[62] Boud Verbrugge, Mohammed Hasan, Haaris Rasool, Thomas Geury, Mohamed El Baghdadi, and Omar Hegazy. Smart integration of electric buses in cities: A technological review. *Sustainability*, 13:12189, 11 2021.

[63] Boud Verbrugge, Abdul Mannan Rauf, Haaris Rasool, Mohamed Abdel-Monem, Thomas Geury, Mohamed El Baghdadi, and Omar Hegazy. Real-time charging scheduling and optimization of electric buses in a depot. *Energies*, 15(14), 2022.

[64] Vijaya, Shweta Sharma, and Neha Batra. Comparative study of single linkage, complete linkage, and ward method of agglomerative clustering. In *2019 International Conference on Machine Learning, Big Data, Cloud and Parallel Computing (COMITCon)*, pages 568–573, 2019.

[65] Haiwei Wang, Wei Wu, Yunfei Li, Chen Chen, and Xiao Xu. Refined charging strategy for electric buses based on data-driven. In *2020 International Conference on Electrical Engineering and Control Technologies (CEECT)*, pages 1–7, 2020.

[66] Juntao Wang and Xiaolong Su. An improved k-means clustering algorithm. In *2011 IEEE 3rd International Conference on Communication Software and Networks*, pages 44–46, 2011.

[67] Lining Wang, Pralit L. Patel, Sha Yu, Bo Liu, Jeff McLeod, Leon E. Clarke, and Wenying Chen. Win–win strategies to promote air pollutant control policies and non-fossil energy target regulation in china. *Applied Energy*, 163:244–253, 2016.

[68] Yusheng Wang, Yongxi Huang, Jiuping Xu, and Nicole Barclay. Optimal recharging scheduling for urban electric buses: A case study in davis. *Transportation Research Part E: Logistics and Transportation Review*, 100:115–132, 2017.

[69] Yusuke Watanabe, Toshiyuki Nakamura, Jan-Dirk Schmöcker, Nobuhiro Uno, and Takenori Iwamoto. Adjusting bus timetables considering observed delays and passenger numbers. In *2017 IEEE 20th International Conference on Intelligent Transportation Systems (ITSC)*, pages 585–590, 2017.

[70] Justin Whitaker, Greg Droge, Matthew Hansen, Daniel Mortensen, and Jacob Gunther. A network flow approach to battery electric bus scheduling. *IEEE Transactions on Intelligent Transportation Systems*, 24(9):9098–9109, 2023.

[71] Weitiao Wu, Yue Lin, Ronghui Liu, and Wenzhou Jin. The multi-depot electric vehicle scheduling problem with power grid characteristics. *Transportation Research Part B: Methodological*, 155:322–347, 2022.

[72] Dong-Fan Xie, Ya-Peng Yu, Guang-Jing Zhou, Xiao-Mei Zhao, and Yong-Jun Chen. Collaborative optimization of electric bus line scheduling with multiple charging modes. *Transportation Research Part D: Transport and Environment*, 114:103551, 2023.

[73] Tsubasa Yamaguchi, Mansur A.S., and Tsunenori Mine. Prediction of bus delay over intervals on various kinds of routes using bus probe data. In *2018 IEEE/ACM 5th International Conference on Big Data Computing Applications and Technologies (BDCAT)*, pages 97–106, 2018.

[74] Pengcheng You, Zaiyue Yang, Yongmin Zhang, Steven H Low, and Youxian Sun. Optimal charging schedule for a battery switching station serving electric buses. *IEEE Transactions on Power Systems*, 31(5):3473–3483, 2015.

[75] Ya-xiang Yuan. Trust region algorithms for nonlinear programming. 01 1994.

[76] Boya Zhou, Ye Wu, Bin Zhou, Renjie Wang, Wenwei Ke, Shaojun Zhang, and Jiming Hao. Real-world performance of battery electric buses and their life-cycle benefits with respect to energy consumption and carbon dioxide emissions. *Energy*, 96:603–613, 2016.

[77] Guang-Jing Zhou, Dong-Fan Xie, Xiao-Mei Zhao, and Chaoru Lu. Collaborative optimization of vehicle and charging scheduling for a bus fleet mixed with electric and traditional buses. *IEEE Access*, 8:8056–8072, 2020.

[78] Yu Zhou, Qiang Meng, and Ghim Ping Ong. Electric bus charging scheduling for a single public transport route considering nonlinear charging profile and battery degradation effect. *Transportation Research Part B: Methodological*, 159:49–75, 2022.

[79] Yu Zhou, Ghim Ping Ong, Qiang Meng, and Haipeng Cui. Electric bus charging facility planning with uncertainties: Model formulation and algorithm design. *Transportation Research Part C: Emerging Technologies*, 150:104108, 2023.

[80] Friederike Ziegler and Tim Schwanen. 'i like to go out to be energised by different people': An exploratory analysis of mobility and wellbeing in later life. *Ageing and Society*, 31:758 – 781, 07 2011.

Thunder Bay Transit System Activity Blocks

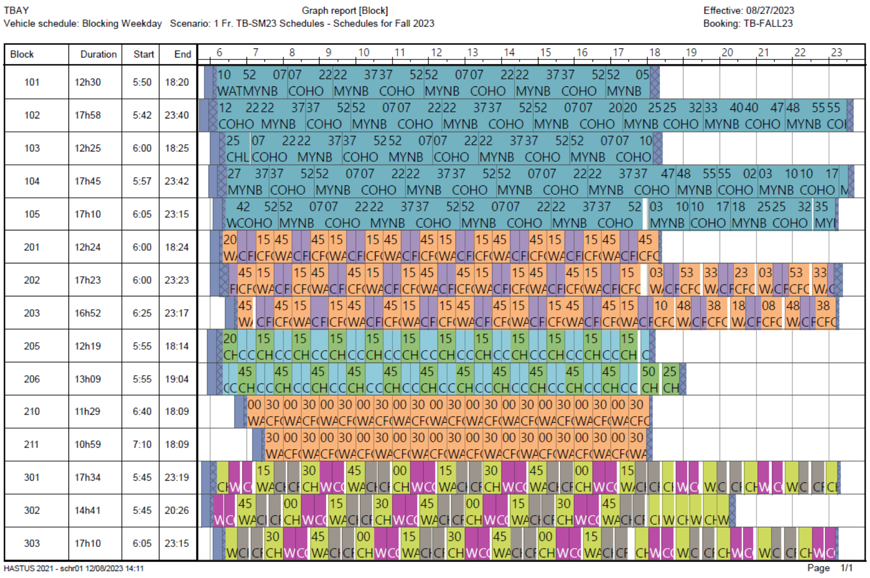

FIGURE 1: Thunder Bay City activity blocks page one

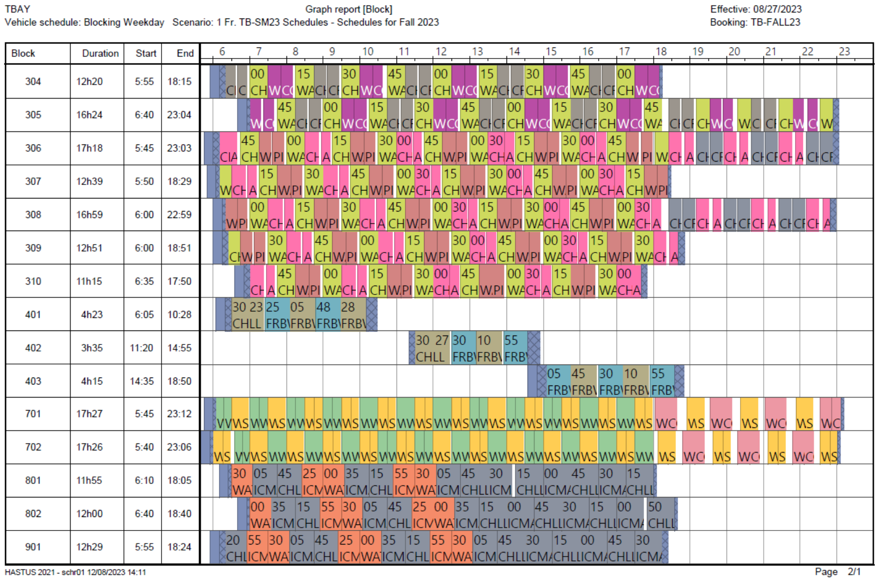

FIGURE 2: Thunder Bay City activity blocks page two

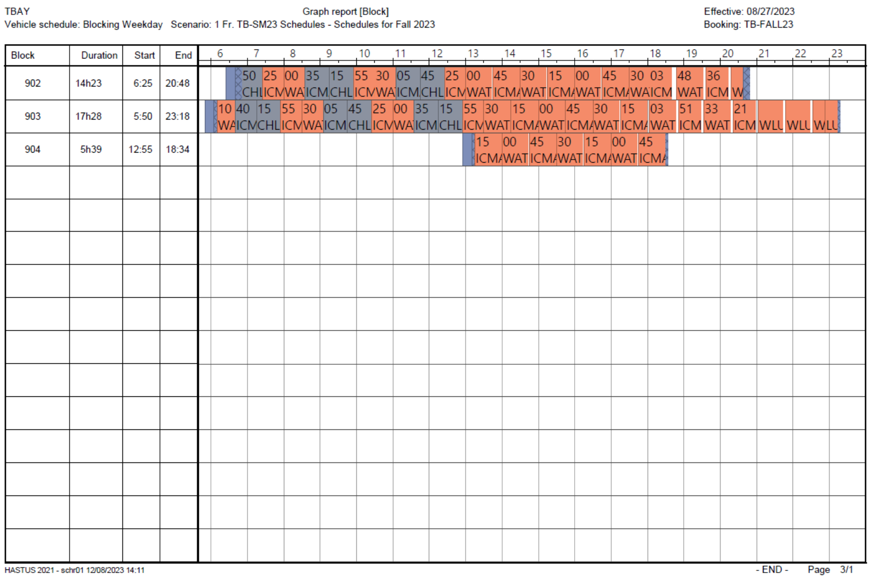

FIGURE 3: Thunder Bay City activity blocks page three

Topology Grade

The Topology Grade % represents the percentage of the route's topographical difficulty relative to its length. It is calculated by dividing the elevation change by the route length and then expressing the result as a percentage. The formula for calculating the Topology Grade % is given by:

$$\text{Topology Grade \%} = \left(\frac{\text{Elevation Change}}{\text{Length}}\right) \times 100 \tag{1}$$

The City of Thunder Bay transit system comprises 17 lines: 1, 2, 3C, 3J, 3M, 4, 5, 6, 7, 8, 9, 10, 11, 12, 13, 14, and 16. Lines 4, 6, and 12 feature a loop shape, meaning the starting and ending terminals are the same. For the remaining lines, the length of routes and the number of stops along the way may vary between the two directions, from starting to ending terminals and vice versa. We calculate the routes' elevation profiles, shown in Figures 4 and 5.

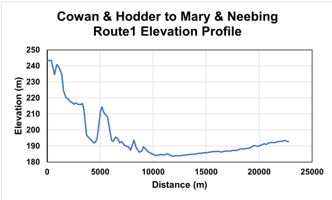

(a) Line 1 Southbnd

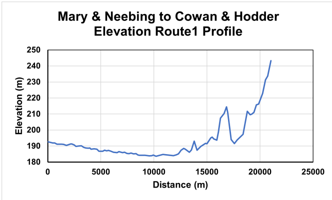

(b) Line 1 Northbnd

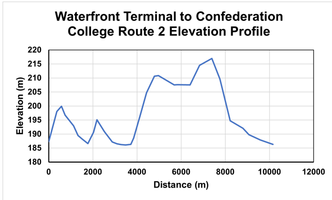

(c) Line 2 Westbnd

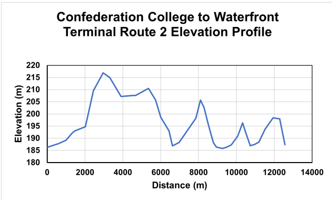

(d) Line 2 Eastbnd

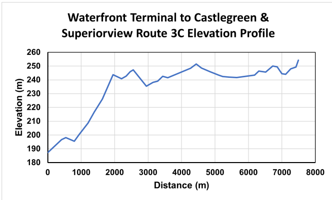

(e) Line 3C Westbnd

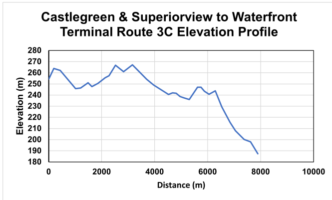

(f) Line 3C Eastbnd

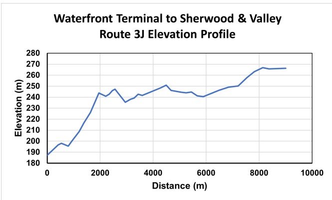

(g) Line 3J Westbnd

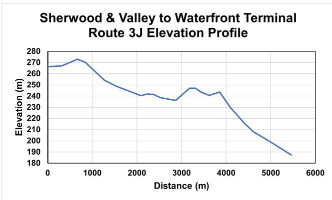

(h) Line 3J Eastbnd

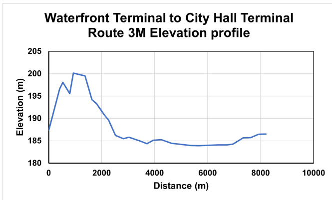

(i) Line 3M Southbnd

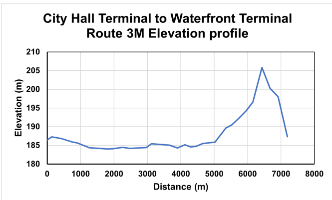

(j) Line 3M Northbnd

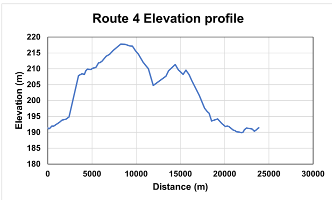

(k) Line 4 Loop

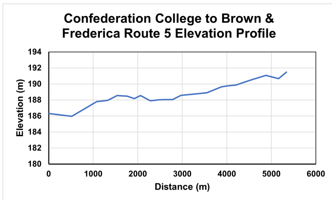

(l) Line 5 Southbnd

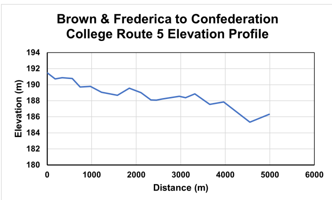

(m) Line 5 Northbnd

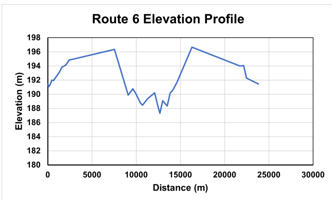

(n) Line 6 Loop

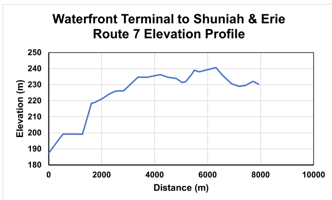

(o) Line 7 Westbnd

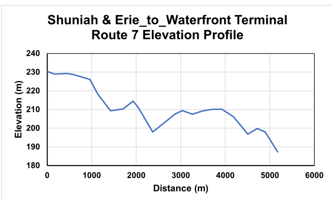

(p) Line 7 Eastbnd

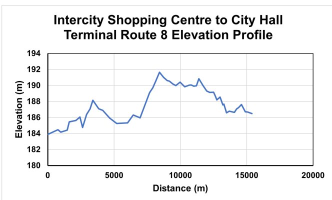

(q) Line 8 Southbnd

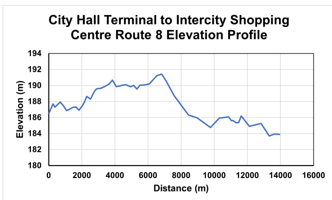

(r) Line 8 Northbnd

FIGURE 4: Lines 1, 2, 3C, 3J, 3M, 4, 5, 6, and 7 elevation profiles.

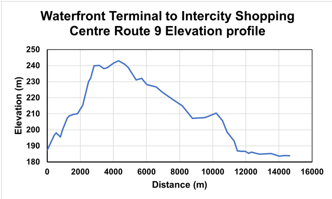

(a) Line 9 Westbnd

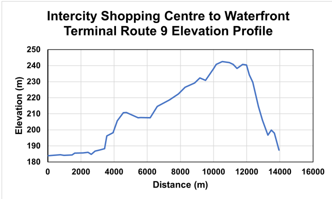

(b) Line 9 Eastbnd

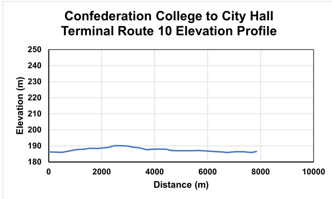

(c) Line 10 Westbnd

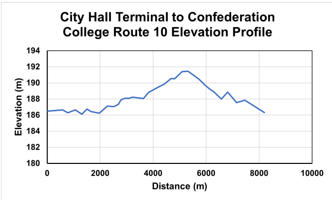

(d) Line 10 Eastbnd

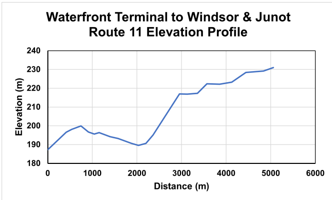

(e) Line 11 Eastbnd

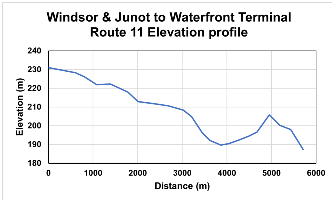

(f) Line 11 Westbnd

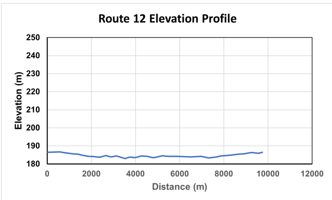

(g) Line 12 Loop

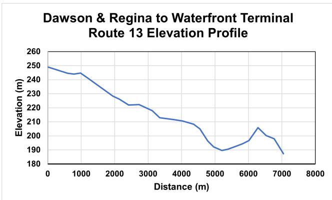

(h) Line 13 Westbnd

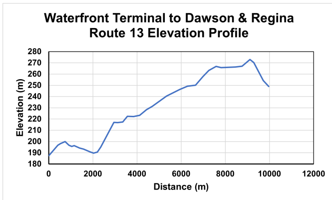

(i) Line 13 Eastbnd

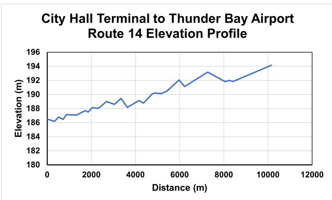

(j) Line 14 Westbnd

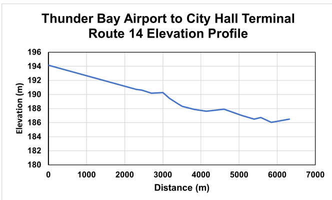

(k) Line 14 Eastbnd

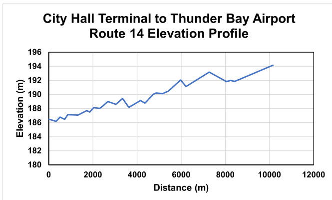

(l) Line 16 Westbnd

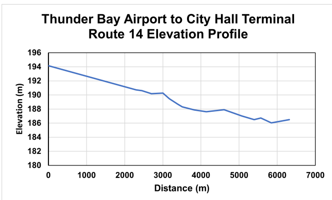

(m) Line 16 Eastbnd

FIGURE 5: Lines 8, 9, 10, 11, 12, 13, 14, and 16 elevation profiles.

Thunder Bay City Transit Activity Blocks' Sinusoidal Models

Table 1 encompasses the details of Thunder Bay City transit's activity blocks charging at the Waterfront terminal.

TABLE 1: Activity Blocks Charging at the Waterfront Terminal

Activity block	Start Time (min)	End Time (min)	Duration (min)	Time Interval (min)	Phase shift (rad)
201	360	1104	744	90	0.28π
702	340	1386	1046	30	0.5π
701	345	1392	1047	30	0.5π
203	385	1397	1012	90	1.17π
202	360	1403	1043	90	0.95π
902	385	1248	863	90	1.83π
903	350	1398	1048	90	1.61π
210	400	1089	689	60	0.5π
211	430	1089	659	60	1.5π
102	342	1420	1078	60	1.37π
103	360	1105	745	60	1.47π
104	357	1422	1065	60	0.47π
105	365	1395	1030	60	0.3π

Figure 6 shows Thunder Bay City Transit's activity blocks piece-wise sinusoidal models charging at the Waterfront terminal.

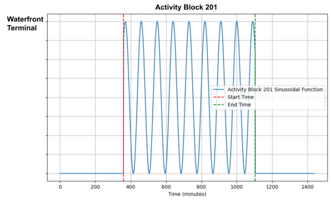

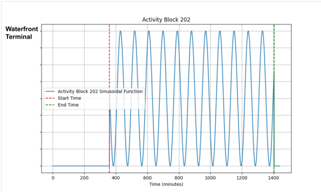

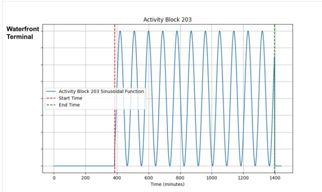

(a) Thunder Bay transit network activity block 201 (b) Thunder Bay transit network activity block 202 (c) Thunder Bay transit network activity block 203

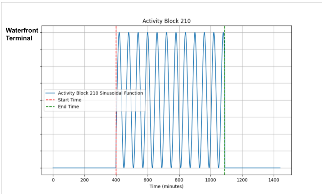

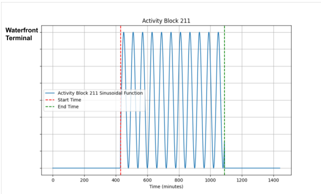

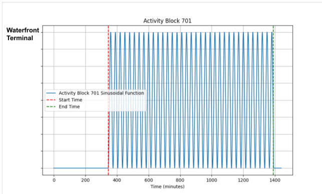

(d) Thunder Bay transit network activity block 210 (e) Thunder Bay transit network activity block 211 (f) Thunder Bay transit network activity block 701

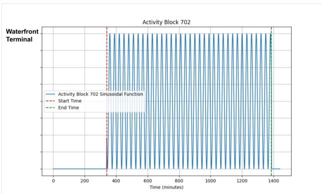

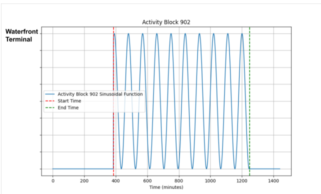

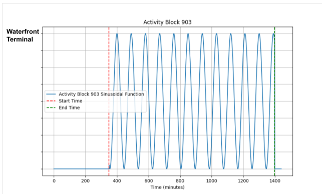

(g) Thunder Bay transit network activity block 702 (h) Thunder Bay transit network activity block 902 (i) Thunder Bay transit network activity block 903

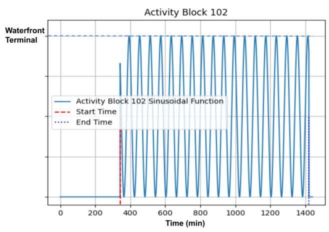

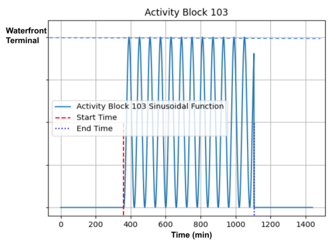

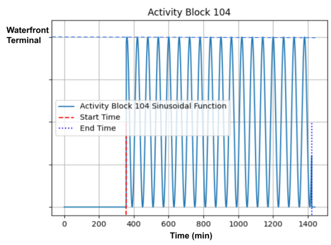

(j) Thunder Bay transit network activity block 102 (k) Thunder Bay transit network activity block 103 (l) Thunder Bay transit network activity block 104

FIGURE 6: City of Thunder Bay transit system piece-wise sinusoidal-modelled activity blocks charging at Waterfront terminal

Table 2 encompasses the details of Thunder Bay City Transit's activity blocks charging at City Hall terminal.

Figure 7 shows Thunder Bay City Transit's activity blocks piece-wise sinusoidal models charging at the City Hall terminal.

Table 2: Activity Blocks Charging at the City Hall Terminal

Activity block	Start Time (min)	End Time (min)	Duration (min)	Time Interval (min)	Phase shift (rad)
205	355	1094	739	30	1.17π
206	355	1144	789	30	1.5π
801	370	1085	715	150	0.3π
802	400	1120	720	150	1.9π
901	355	1104	749	150	1.5π
306	345	1383	1038	150	1.18π
308	360	1379	1019	150	1.31π
303	365	1395	1030	150	1.18π
101	350	1100	750	60	1.57π
305	400	1384	984	150	1.3π
301	345	1399	1054	150	1.57π
302	345	1226	881	150	0.91π
304	355	1095	740	150	0.9π
307	350	1109	759	150	1.31π
309	360	1131	771	150	1.5π
310	395	1070	675	150	0.3π

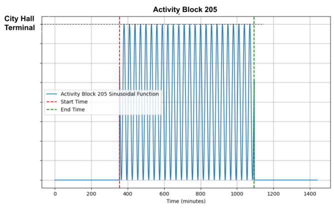

(a) Thunder Bay transit network activity block 205

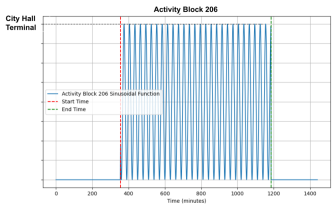

(b) Thunder Bay transit network activity block 206

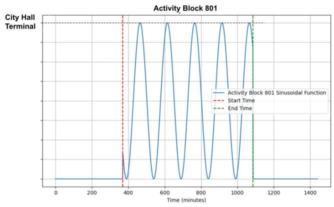

(c) Thunder Bay transit network activity block 801

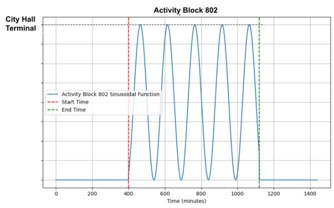

(d) Thunder Bay transit network activity block 802

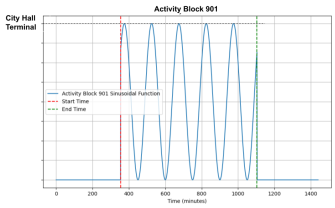

(e) Thunder Bay transit network activity block 901

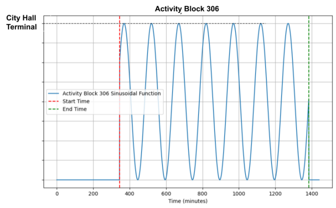

(f) Thunder Bay transit network activity block 306

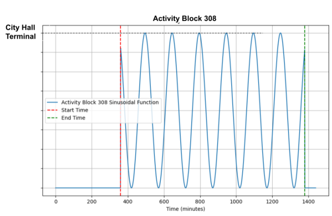

(g) Thunder Bay transit network activity block 308

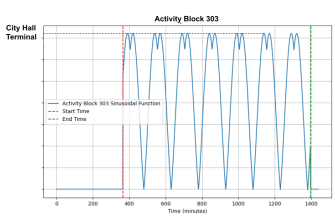

(h) Thunder Bay transit network activity block 303

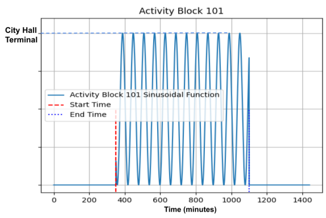

(i) Thunder Bay transit network activity block 101

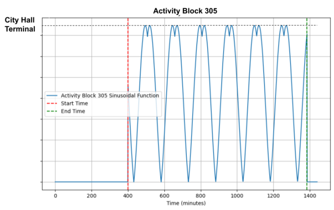

(j) Thunder Bay transit network activity block 305

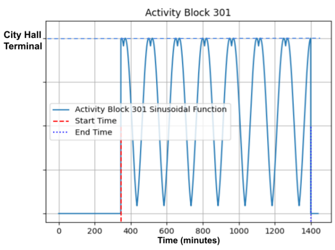

(k) Thunder Bay transit network activity block 301

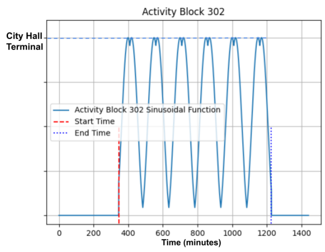

(l) Thunder Bay transit network activity block 302

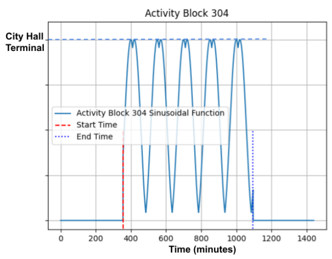

(m) Thunder Bay transit network activity block 304

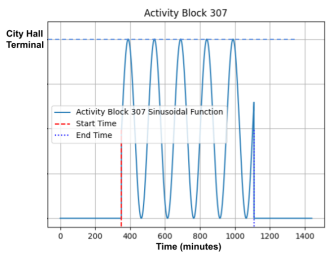

(n) Thunder Bay transit network activity block 307

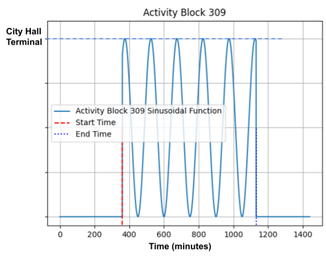

(o) Thunder Bay transit network activity block 309

FIGURE 7: City of Thunder Bay transit system piece-wise sinusoidal-modelled activity blocks charging at the City Hall terminal